DEVELOPMENT OF EXPRESSION SYSTEM FOR THE PRODUCTION OF RECOMBINANT HUMAN ANTIBODY

Witsanu Srila

A Thesis Submitted in Partial Fulfillment of the Requirements for the Degree of Doctor of Philosophy in Biotechnology

Suranaree University of Technology

Academic Year 2019

การพัฒนาระบบการแสดงออกของยีนเพื่อการผลิตแอนติบอดีมนุษย์ปรับแต่งพันธุกรรม

นายวิษณุ ศรีลา

วิทยานิพนธ์นี้เป็นส่วนหนึ่งของการศึกษาตามหลักสูตรปริญญาวิทยาศาสตรดุษฎีบัณฑิต
สาขาวิชาเทคโนโลยีชีวภาพ
มหาวิทยาลัยเทคโนโลยีสุรนารี
ปีการศึกษา 2562

DEVELOPMENT OF EXPRESSION SYSTEM FOR THE PRODUCTION OF RECOMBINANT HUMAN ANTIBODY

Suranaree University of Technology has approved this thesis submitted in partial fulfillment of the requirements for the Degree of Doctor of Philosophy.

Thesis Examining Committee

(Assoc. Prof. Dr. Apichat Boontawan)
Chairperson

(Prof. Dr. Montarop Yamabhai)
Member (Thesis Advisor)

(Prof. Dr. Nicole Borth)
Member

(Prof. Dr. Florian Rüker)
Member

(Prof. Dr. Enrico Mastrobattista)
Member

(Prof. Dr. Trent Munro)
Member

(Prof. Dr. Stephen Mahler)
Member

(Assoc. Prof. Flt. Lt. Dr. Kontorn Chamniprasart)
Vice Rector for Academic Affairs and Internationalization

(Prof. Dr. Neung Teaumroong)
Dean of Institute of Agricultural Technology

วิษณุ ศรีลา : การพัฒนาระบบการแสดงออกของยีนเพื่อการผลิตแอนติบอดีมนุษย์ปรับแต่งพันธุกรรม (DEVELOPMENT OF EXPRESSION SYSTEM FOR THE PRODUCTION OF RECOMBINANT HUMAN ANTIBODY) อาจารย์ที่ปรึกษา : ศาสตราจารย์ ดร. มณฑารพ ยมาภัย, 149 หน้า.

โมโนโคลนอลแอนติบอดีมีส่วนแบ่งทางการตลาดมากที่สุด เนื่องจากมีการใช้ในการวินิจฉัย การป้องกัน และการรักษาโรค และยังมีโมโนโคลนอลแอนติบอดีอีกจำนวนมากที่กำลังจะออกสู่ตลาดในอีกไม่กี่ปีข้างหน้า การเติบโตอย่างเด่นชัดของชีวผลิตภัณฑ์ (Biologics) ส่งผลให้มีความต้องการระบบการแสดงออกที่มีคุณภาพและได้ผลผลิตสูง ผู้วิจัยได้พัฒนาระบบการแสดงออกของชิ้นส่วนแปรผันสายเดี่ยว (single-chain variable fragment, scFv) ที่เชื่อมต่อกับโปรตีนสีเขียวมรกตเรืองแสง (Emerald Green Fluorescent Protein, EmGFP) ที่มีประสิทธิภาพ เหมาะสำหรับการผลิตฟลูโอบอดี้ (fluobodies) ประสิทธิภาพของระบบ scFv-EmGFP ที่พัฒนาขึ้นนี้ถูกแสดงผ่านการประยุกต์ใช้เพื่อการตรวจหาไวรัสพิษสุนัขบ้าและสารพิษจากเชื้อรา จะเห็นได้ว่าระบบนี้มีศักยภาพในการตรวจวิเคราะห์ทั้งเชิงปริมาณและเชิงคุณภาพของสารต่าง ๆ ได้ รวมทั้งสำหรับใช้ในการบันทึกภาพ ของตัวอย่างทางชีวภาพที่เกิดขึ้นจริงในช่วงเวลาต่าง ๆ (real-time bioimaging) ด้วย

วิทยานิพนธ์นี้ยังมีงานวิจัยที่แสดงให้เห็นถึงประโยชน์ของการประยุกต์ใช้เส้นทางปฏิบัติการ (pipeline) ที่รวดเร็วของการทดลองการแสดงออกแบบชั่วคราว (transient expression) ที่ทำซ้ำได้ เพื่อระบุการตั้งค่าที่ดีที่สุดอย่างรวดเร็วก่อนการพัฒนาเซลล์ไลน์แบบเสถียร (stable cell line) ตัวแปรที่อยู่ในเส้นทางปฏิบัติการนี้ ได้แก่ ลำดับยีนที่ปรับรหัสพันธุกรรมให้เหมาะสม (optimized codon) และการเลือกชนิดของเปปไทด์สัญญาณ (signal peptides) ที่เหมาะสม โดยในเส้นทางปฏิบัติการนั้น สิ่งสำคัญที่จะต้องคำนึงถึง คือการกำหนดลักษณะสมบัติของพฤติกรรมเซลล์อย่างระมัดระวัง เช่น อัตราการเติบโตและผลผลิตที่เฉพาะเจาะจง การเลือกแต่ละองค์ประกอบอย่างรวดเร็วในแต่ละกรณี จะเป็นประโยชน์อย่างมากต่อการสร้างโคลนในการผลิตแอนติบอดีเพื่อการรักษาแบบยาชีววัตถุคล้ายคลึง (biosimilar) ที่มีประสิทธิภาพและรวดเร็วขึ้น

ในการทดลองสุดท้ายของวิทยานิพนธ์นี้ เทคโนโลยีการแก้ไขยีนแบบคริสเปอร์ (CRISPR) ได้ถูกนำมาใช้ในการสร้างระบบการแสดงออกของเซลล์ Chinese Hamster Ovary (CHO) โดยได้ทำการลบ ยีนกลูตามีนซินทีเทสออก (glutamine synthetase-knockout) อย่างมีประสิทธิภาพ เพื่อให้เหมาะสมสำหรับการสร้างเซลล์ไลน์แบบเสถียรที่ใช้ผลิตยาชีวผลิตภัณฑ์ เพราะระบบนี้สามารถเร่ง

ความเร็วในการหาโคลนที่มีกำลังการผลิตสูง เนื่องจากกระบวนการคัดเลือกนี้มีความเข้มงวดสูง และลดการสะสมแอมโมเนียในเซลล์

สาขาวิชาเทคโนโลยีชีวภาพ ลายมือชื่อนักศึกษา_____

ปีการศึกษา 2562 ลายมือชื่ออาจารย์ที่ปรึกษา_____

WITSANU SRILA : DEVELOPMENT OF EXPRESSION SYSTEM FOR THE PRODUCTION OF RECOMBINANT HUMAN ANTIBODY : PROF. MONTAROP YAMABHAI, Ph.D., 149 PP.

IMMUNOFLUORESCENCE/CODON OPTIMIZATION/SIGNAL PEPTIDE/ CHINESE HAMSTER OVARY (CHO) CELLS/ /MONOCLONAL ANTIBODY/ KNOCKOUT

Monoclonal antibodies (mAbs) dominate the market with the largest revenue share due to their use in diagnosis, prevention, and treatment of diseases. More mAbs will be on the market in the coming years. The growing significance of biologics has resulted in the demand for high quality and productivity expression systems. In this thesis, an efficient single-chain variable fragment (scFv)-Emerald Green Fluorescent Protein (EmGFP) expression system, suitable for production of fluobodies has been developed. The efficacy of scFv-EmGFP was demonstrated via an application for the detection of rabies virus and mycotoxins. This system has potential to be used for both quantitative and qualitative analysis of various analytes as well as real-time bioimaging of biological samples.

In this research, the benefits of applying a rapid pipeline of reproducible transient expression experiments to quickly identify the best settings before the development of a stable cell line has been demonstrated. The parameters included in this pipeline were codon optimized gene sequences and combinations of different signal peptides. An important aspect of such a pipeline including careful characterization of cell behavior, such as growth rate and specific productivity have been evaluated. This rapid selection

of individual elements on a case by case basis would hugely benefit the efficient and timely generation of production clones for biosimilar therapeutic antibody manufacturing.

Finally, CRISPR-based gene editing technology was employed to create an efficient glutamine synthetase (GS)-knockout Chinese Hamster Ovary (CHO) cell expression system suitable for generation of stable cell line expressing biologics drug. This system could accelerate the identification of high producing clones because of high selection stringency and reduction of ammonia accumulation in the cells.

School of Biotechnology

Academic Year 2019

Student's Signature Witsanu Sriba

Advisor's Signature

ACKNOWLEDGEMENTS

Firstly, I would like to express my sincere gratitude to thesis advisor Prof. Dr. Montarop Yamabhai, the continuous support of my Ph.D study and related research, for her patience, motivation, and immense knowledge. I appreciate her contributions of time, ideas, and funding to make my Ph.D. experience productive and stimulating.

I would like to express my gratitude to Prof. Dr. Nicole Borth who provided me an opportunity to work as intern at BOKU for one and a half years. She guided me, giving a good help by sharing her expertise in the field.

I am also greatly thankful for Dr. Martina Baumann for her guidance on antibody production in CHO cells and CHO cells engineering, giving a good help by sharing her expertise in the field.

I would like to thanks all committees Assoc. Prof. Dr. Apichat Boontawan, Prof. Dr. Nicole Borth, Prof. Dr. Florian Rüker, Prof. Dr. Enrico Mastrobattista, Prof. Dr. Trent Munro and Prof. Dr. Stephen Mahler for their valuable time and patience to read my thesis.

I would also like to thanks the Royal Golden Jubilee PhD program of Thailand (PHD/0191/2557) for their financial support for my study and research experience at Institute of Animal Cell Technology and Systems Biology, Department of Biotechnology, University of Natural Resources and Life Sciences, Vienna (BOKU), Austria for one and a half years.

I would like to thanks MY lab members. I am grateful for their good help and friendship.

I would like to thanks IMICS members at BOKU that have contributed immensely to my personal and professional time at BOKU, Austria. The group has been a source of friendships as well as good advice and collaboration.

Finally, I express my very profound gratitude to my parents and my older sister to for providing me with unfailing support and continuous encouragement throughout my years of study. This accomplishment would not have been possible without them.

Witsanu Srila

CONTENTS

Page

CONTENTS (Continued)

Page

CONTENTS (Continued)

Page

CONTENTS (Continued)

Page

CONTENTS (Continued)

Page

LIST OF TABLES

Table **Page**

LIST OF FIGURES

Figure **Page**

LIST OF FIGURES (Continued)

Figure **Page**

LIST OF FIGURES (Continued)

Figure **Page**

LIST OF FIGURES (Continued)

Figure **Page**

LIST OF ABBREVIATIONS

FLISA	=	Fluorescence-linked immunosorbent assay
scFv	=	Single-chain variable fragment
AFB1	=	Aflatoxin B1
BSA	=	Bovine serum albumin
ZEN	=	Zearalenone
EmGFP	=	Emerald Green Fluorescent Protein
FITC	=	Fluorescein isothiocyanate
FACS	=	Fluorescence-activated cell sorter
IPTG	=	Isopropyl-β-D-thiogalactopyranoside
PMSF	=	Phenylmethylsulfonyl fluoride
PBS	=	Phosphate Buffered Saline
ELISA	=	Enzyme-linked immunosorbent assay
KD	=	Kringle domain
HRP	=	Horseradish peroxidase
CHO	=	Chinese hamster ovary
DNA	=	Deoxyribonucleic acid

LIST OF ABBREVIATIONS (Continued)

SP	=	Signal peptide
LC	=	Light chain
HC	=	Heavy chain
Adali_GA	=	Adalimumab genes were codon-optimized and synthesized from GeneArt
Adali_GS	=	Adalimumab genes were codon-optimized and synthesized from GenSript
mAb	=	Monoclonal antibody
UTR	=	Untranslated region
CMV	=	Cytomegalovirus
CAI	=	Codon adaptation index
ER	=	Endoplasmic reticulum
q_p	=	Cell-specific productivity
V_H	=	Heavy chain variable domain
V_L	=	Light chain variable domain
HC	=	Heavy chain constant domains
CL	=	Light chain constant domain
ORF	=	Open reading frame
VCD	=	Viable cell density
OPD	=	*o*-Phenylenediamine dihydrochloride
OD	=	Optical intensity
RT-qPCR	=	Quantitative reverse transcription PCR

LIST OF ABBREVIATIONS (Continued)

SDS-PAGE	=	Sodium dodecyl sulphate-polyacrylamide gel electrophoresis
TGE	=	Transient gene expression
WPRE	=	Woodchuck posttranscriptional regulatory element
GS	=	Glutamine synthetase
MSX	=	Methionine sulfoxinime
GOI	=	Gene of interest
DHFR	=	Dihydrofolate reductase
MTX	=	Methotrexate
ATP	=	Adenosine triphosphate
gRNA	=	Guide RNA
CRISPR	=	Clustered regularly interspaced palindromic repeats
Cpf1	=	CRISPR from *Prevotella* and *Francisella* 1
DNA	=	Deoxyribonucleic acid
RNA	=	Ribonucleic acid
GAPDH	=	Glyceraldehyde 3-phosphate dehydrogenase
FUT8	=	Alpha-(1,6)-fucosyltransferase
FC	=	Fold change
ZFN	=	Zinc finger nuclease
TALEN	=	Ttranscription activator-like effector nucleases
LOF	=	Loss of function
L-Gln	=	L-glutamine

LIST OF ABBREVIATIONS (Continued)

lnc	=	long noncoding
q_{mAb}	=	specific mAb productivity
µg	=	microgram
kDa	=	(kilo) Dalton
µl	=	microlitre
IU	=	International unit
°C	=	degrees Celsius
g	=	grams
h	=	hours
L	=	litre
M	=	molar
mg	=	milligram
min	=	minute
ml	=	milliliter
rpm	=	Revolution
v/v	=	volume per unit volume
w/v	=	weight per unit volume

CHAPTER I

INTRODUCTION

1.1 Significant of this study

The worldwide biologics market is predicted to reach nearly USD 400 billion by 2025. Besides, the expression vectors market is valued at approximately $317.1 million in 2020 (http://www.grandviewresearch.com). Growing significance of biologics can lead to higher market revenues over the forecast period. More than 650 biologics have been approved till date, and over 1,500 biologics are under clinical development. Monoclonal antibodies (mAbs) dominated the market with biggest revenue share due to increase in usage of mAbs in different therapeutics areas. In 2020, ~70 mAb products will be on the market (Ecker, Jones, & Levine, 2015). The growing significance of biologics has resulted in the development of technologies for different types of high quality and productivity expression systems.

Biologics are medicines derived from living cells for therapeutics and diagnostics. They are also known as biopharmaceuticals. Majority of these are produced using recombinant DNA technology. This technology allows a company to produce customized medicines to treat specific diseases. Alternatives to biologics are biobetters and biosimilars (Dolinar & Reilly, 2013). Biosimilars are biologics manufactured by a different company. Biobetters are recombinant drugs, which are considered the refined versions of biopharmaceuticals. These receive 12 years of market protection as against biosimilars. The current estimated cost of some biosimilars drives prices down by

50 percent compared with originator products, so potential savings in manufacturing costs are attractive Thus, a number of companies have begun investing in these due to the patents of some biologics have been already expired (Nelson & Gallagher, 2014).

Several expression hosts have been utilized for the manufacturing of biologics, two dominant expression systems are bacterial and mammalian cells, in addition to some other expression hosts including yeast, insect, transgenic animals and plant (Frenzel, Hust, & Schirrmann, 2013). Bacterial expression systems are used for simple proteins that do not require complex glycosaccharides for their efficacy or stability. While mammalian expression systems are applied to produce the complex proteins that require the posttranslational modifications. Chinese hamster ovary (CHO) cells are the main expression system for biologic productions (Chusainow et al., 2009; Frenzel et al., 2013). They can be adapted to suspension growth in chemically-defined animal component-free media, they can secrete high levels of recombinant mAbs and provide a human-like glycosylation pattern with few concerns for immunogenic reactions (Jenkins, Meleady, Tyther, & Murphy, 2009; van Beers & Bardor, 2012; Zhu, 2012). CHO cells generate a heterogeneous population of cells by stable transfection with vector-expressing recombinant mAb. Some CHO cells express high levels of a mAb via a combination of integration sites and amplification regions of genomic DNA.

Gene expression levels of CHO cells involve multiple parameters including codon, gene copy number, the chromosomal integration site of gene, transcriptional regulation, mRNA processing and stability, tRNA abundance, translation efficiency and SPs (Feng et al., 1999; Hung et al., 2010; Kanaya, Yamada, Kinouchi, Kudo, & Ikemura, 2001; Ou et al., 2014; You et al., 2018). The design of heterologous gene for recombinant expression

has been identified as a bottleneck at translation of protein and thus recognizes a key issue that necessaries to be solved to achieve high levels of gene expression. The expression vectors are often a key to success in production efficiency. Codon optimization has been widely utilized to improve the heterologous gene expression by using codon preference (codon usage bias) that are optimized in a particular host(Gustafsson, Govindarajan, & Minshull, 2004; Novoa & Ribas de Pouplana, 2012). It is well-known that a protein secretion in the eukaryotic cell is translocated into the endoplasmic reticulum (ER) before transport into the Golgi complex achieving by a signal peptide (SP). However, SPs are identified as a limiting step in the classical secretory pathway. Therefore, the selection of appropriate SP is an important issue for improving the efficiency of protein secretion (Haryadi et al., 2015; Tole et al., 2009; You et al., 2018).

Some alterations to CHO cells have used to identify the highest-producing clones via metabolic selection systems. The glutamine synthetase (GS) selection system is more stringent selection than dihydrofolate reductase (DHFR) system, leading to a shorter timelines for identifying high-producing clones (Fan et al., 2012). However, the selection of those clones among a large population for low and non-productive clones in the bulk cultures is a critical step for cell line generation process development to produce recombinant Ab in CHO cells. The GS-CHO system is an alternative approach to efficiently identify high producing and stable clones. This system is used to generate the highly producing population by increasing the selection stringency in combination with methionine sulfoxinime (MSX), a GS inhibitor. However, the productivity of individual top producer was not improved (Fan et al., 2012). The optimization of culture media and

feeding strategies can produce maximal amounts of protein, increasing the expression levels about 100-fold over initial condition(Hacker, Nallet, & Wurm, 2008).

Several technologies are available to improve the performance of CHO cell lines. For instance, homologous recombination is induced by using the recombinant adeno associated virus (rAAV). However, this technology can direct to target at only one allele per a time, which makes the introduction of multiple events both a time-consuming and laborious process (Luo, Kofod-Olsen, Christensen, Sorensen, & Bolund, 2012; Schultz & Chamberlain, 2008). Zinc finger nucleases (ZFNs) can be engineered to target specific desired DNA sequences which work on principles similar the CRISPR/Cas9 system, but ZFNs have lower efficiency and specificity than CRISPR (Gaj, Gersbach, & Barbas, 2013; Pattanayak, Ramirez, Joung, & Liu, 2011).

The CRISPR/Cpf1 system has recently increased more popularity and more efficient version of a gene editing tool. Therefore, the CRISPR/Cpf1 system is interesting to revolutionize CHO cell line development. Now, scientists are known the sequencing of the CHO genome, which has potential to be driven for genome editing and allowed to designed efficient targeting vectors. CHO cells have engineered to improve the effectiveness and efficiency of their parental cell lines regarding metabolism, apoptosis resistance, growth, productivity or the ability to express recombinant Abs with modified glycosylation patterns (Fischer, Handrick, & Otte, 2015). Therefore, expression host cell engineering is a powerful technique to significantly increase efficiency of CHO based production development processes. However, this research is not done in Thailand. Therefore, we introduced these technologies which may contribute to improve CHO cell performance to establish highly productive processes in the future.

1.2 Research objectives

The overall objective of my thesis will be focusing on development of efficient bacterial and animal expression system for the production of human recombinant Abs. The thesis objective is divided into three sub-objectives as follows.

1. To evaluate a suitable *Escherichia coli* (*E. coli*) expression system for the production of human recombinant single-chain variable fragment (scFv)-Emerald Green Fluorescent Protein (EmGFP) Abs.

2. To compare the effects of different optimized codons and various signal peptides (SPs) on the productivity of therapeutic Abs, expressed from monocistronic expression vectors from transiently transfected CHO cells.

3. To establish the single and double glutamine synthetase (GS)-knockout CHO-S and CHO-K1 cells, eliminating the endogenous GS expression, and then the single and double GS-knockout CHO-S and CHO-K1 cells were characterized and evaluated to improve selection stringency in bulk cell line generation.

1.3 Scope of the study

My thesis is focusing on two key expression systems, i.e., *E. coli* and CHO cell lines. scFv-EmGFP, Adalimumab and Trastuzumab Abs were used as model Abs. Only the expression in a lab-scale was investigated.

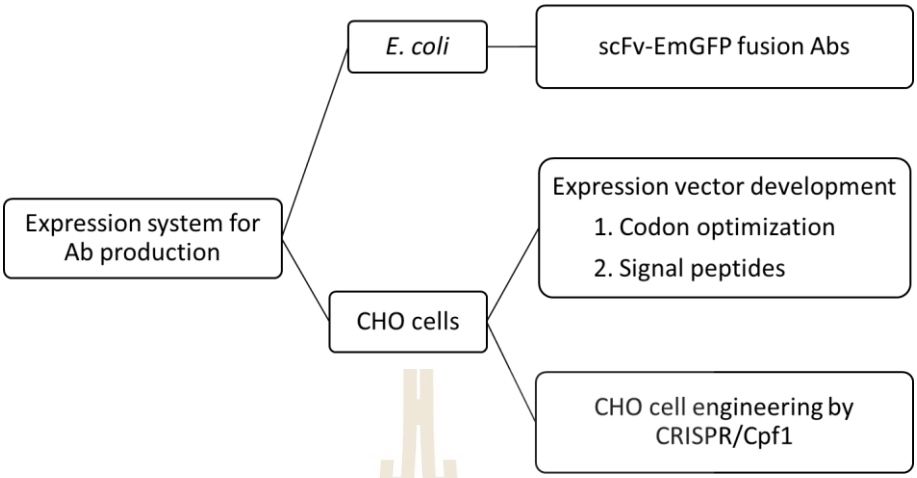

Figure 1.1 Schematic representation of the scope of this thesis.

1.4 References

Chusainow, J., Yang, Y. S., Yeo, J. H., Toh, P. C., Asvadi, P., Wong, N. S., & Yap, M. G. (2009). A study of monoclonal antibody-producing CHO cell lines: what makes a stable high producer? *Biotechnology and Bioengineering, 102*(4), 1182-1196.

Dolinar, R. O., & Reilly, M. S. (2013). The future of biological therapy: a pathway forward for biosimilars. *Generics and Biosimilars Initiative Journal, 2*(1), 36-40.

Ecker, D. M., Jones, S. D., & Levine, H. L. (2015). The therapeutic monoclonal antibody market. *Monoclonal Antibodies, 7*(1), 9-14.

Fan, L., Kadura, I., Krebs, L. E., Hatfield, C. C., Shaw, M. M., & Frye, C. C. (2012). Improving the efficiency of CHO cell line generation using glutamine synthetase gene knockout cells. *Biotechnology and Bioengineering, 109*(4), 1007-1015.

Feng, Y. Q., Seibler, J., Alami, R., Eisen, A., Westerman, K. A., Leboulch, P., Fiering, S., & Bouhassira, E. E. (1999). Site-specific chromosomal integration in mammalian cells: highly efficient CRE recombinase-mediated cassette exchange. *Journal of Molecular Biology, 292*(4), 779-785.

Fischer, S., Handrick, R., & Otte, K. (2015). The art of CHO cell engineering: a comprehensive retrospect and future perspectives. *Biotechnology Advances, 33*(8), 1878-1896.

Frenzel, A., Hust, M., & Schirrmann, T. (2013). Expression of recombinant antibodies. *Frontiers in Immunology, 4*, 217.

Gaj, T., Gersbach, C. A., & Barbas, C. F. (2013). ZFN, TALEN and CRISPR/Cas-based methods for genome engineering. *Trends in Biotechnology, 31*(7), 397-405.

Gustafsson, C., Govindarajan, S., & Minshull, J. (2004). Codon bias and heterologous protein expression. *Trends in Biotechnology, 22*(7), 346-353.

Hacker, D., Nallet, S., & Wurm, F. (2008). Recombinant protein production yields from mammalian cells: past, present, and future. *BioPharm International*(5), 1-6.

Haryadi, R., Ho, S., Kok, Y. J., Pu, H. X., Zheng, L., Pereira, N. A., Li, B., Bi, X., Goh, L.-T., Yang, Y., & Song, Z. (2015). Optimization of heavy chain and light chain signal peptides for high level expression of therapeutic antibodies in CHO cells. *PLOS One, 10*(2), e0116878-e0116878.

Hung, F., Deng, L., Ravnikar, P., Condon, R., Li, B., Do, L., Saha, D., Tsao, Y. S., Merchant, A., Liu, Z., & Shi, S. (2010). mRNA stability and antibody production in CHO cells: improvement through gene optimization. *Biotechnology Journal, 5*(4), 393-401.

Jenkins, N., Meleady, P., Tyther, R., & Murphy, L. (2009). Strategies for analysing and improving the expression and quality of recombinant proteins made in mammalian cells. *Biotechnology and Applied Biochemistry, 53*(Pt 2), 73-83.

Kanaya, S., Yamada, Y., Kinouchi, M., Kudo, Y., & Ikemura, T. (2001). Codon usage and tRNA genes in eukaryotes: correlation of codon usage diversity with translation efficiency and with CG-dinucleotide usage as assessed by multivariate analysis. *Journal of Molecular Evolution, 53*(4-5), 290-298.

Luo, Y., Kofod-Olsen, E., Christensen, R., Sorensen, C. B., & Bolund, L. (2012). Targeted genome editing by recombinant adeno-associated virus (rAAV) vectors for generating genetically modified pigs. *Journal of Genetics and Genomics, 39*(6), 269-274.

Nelson, K. M., & Gallagher, P. C. (2014). Biosimilars lining up to compete with Herceptin – opportunity knocks. *Expert Opinion on Therapeutic Patents, 24*(11), 1149-1153.

Novoa, E. M., & Ribas de Pouplana, L. (2012). Speeding with control: codon usage, tRNAs, and ribosomes. *Trends in Genetics, 28*(11), 574-581.

Ou, K.-C., Wang, C.-Y., Liu, K.-T., Chen, Y.-L., Chen, Y.-C., Lai, M.-D., & Yen, M.-C. (2014). Optimization protein productivity of human interleukin-2 through codon usage, gene copy number and intracellular tRNA concentration in CHO cells. *Biochemical and Biophysical Research Communications, 454*(2), 347-352.

Pattanayak, V., Ramirez, C. L., Joung, J. K., & Liu, D. R. (2011). Revealing off-target cleavage specificities of zinc-finger nucleases by in vitro selection. *Nature Methods, 8*(9), 765-770.

Schultz, B. R., & Chamberlain, J. S. (2008). Recombinant adeno-associated virus transduction and integration. *Molecular therapy : the Journal of the American Society of Gene Therapy, 16*(7), 1189-1199.

Tole, S., Mukovozov, I. M., Huang, Y. W., Magalhaes, M. A., Yan, M., Crow, M. R., Liu, G. Y., Sun, C. X., Durocher, Y., Glogauer, M., & Robinson, L. A. (2009). The axonal repellent, Slit2, inhibits directional migration of circulating neutrophils. *Journal of Leukocyte Biology, 86*(6), 1403-1415.

van Beers, M. M., & Bardor, M. (2012). Minimizing immunogenicity of biopharmaceuticals by controlling critical quality attributes of proteins. *Biotechnology Journal, 7*(12), 1473-1484.

You, M., Yang, Y., Zhong, C., Chen, F., Wang, X., Jia, T., Chen, Y., Zhou, B., Mi, Q., Zhao, Q., An, Z., Luo, W., & Xia, N. (2018). Efficient mAb production in CHO cells with optimized signal peptide, codon, and UTR. *Applied Microbiology and Biotechnology, 102*(14), 5953-5964.

Zhu, J. (2012). Mammalian cell protein expression for biopharmaceutical production. *Biotechnology Advances, 30*(5), 1158-1170.

CHAPTER II

RECOMBINANT ABTIBODY PRODUCTION

2.1 Abstract

Monoclonal antibodies (mAbs) dominate the market with the largest revenue share due to their use in diagnosis, prevention, or treatment of diseases. More mAbs will be on the market in the coming years. The growing significance of biologics has resulted in the development of technologies for different types of high quality and productivity expression systems. mAbs are mainly produced in mammalian and microbial host cells, with in addition to some other hosts including transgenic models, avian, insect, and transgenic animals. Bacterial expression systems are used for simple proteins that do not require complex glycosaccharides for their efficacy or stability. While mammalian expression systems are applied to produce the complex proteins that require the posttranslational modifications. Chinese hamster ovary (CHO) cells are the main expression system for the production of therapeutic Abs. They can secrete high levels of recombinant mAbs and provide a human-like glycosylation pattern with few concerns for immunogenic reactions.

Keywords: monoclonal antibody; recombinant antibody; expression system; *Escherichia coli*; mammalian cell; Chinese hamster ovary (CHO) cells

2.2 Recombinant human Abs

Most of therapeutic Abs are mAbs that bind specifically to target cell, particularly to cell surface antigens. Currently, many research and development are focused on creating various types of mAbs for numerous serious diseases, especially infections, and immunological disorders (Geng et al., 2015). In addition to full-length Abs, several types of Ab fragments are also being developed as potential therapeutics (Figure 2.1). A single-chain variable fragment (scFv) consists only of variable (V) regions of the heavy (V_H) and light chains (V_L) of mAb. V regions are connected with a soluble and flexible peptide linker for stabilization of the molecule (Bird et al., 1988; Rangnoi, Jaruseranee, O'Kennedy, Pansri, & Yamabhai, 2011). scFv fragment still retains the specificity of the original immunoglobulin for antigen. To obtain a Fab fragment, the V regions are connected to the constant (C) domains (Flanagan & Jones, 2004). Recently, both fragments are the most commonly utilized Ab fragments which are produced in prokaryotic expression systems. Other Ab formats have been produced in prokaryotic and eukaryotic expression systems, such as single chain Fab fragments (scFab) which linked combined Fab and scFv fragments (Hust et al., 2007), disulfide-bond stabilized scFv (ds-scFv) (Weatherill et al., 2012) and multimeric Ab formats like dia-, tria-, or tetra-bodies (Cuesta, Sainz-Pastor, Bonet, Oliva, & Alvarez-Vallina, 2010) or minibodies consisting of scFvs connected to CH3 domain of mAb (Hu et al., 1996), leucin zipper, helix turn helix motif streptavidin, or scFv-scFv tandems. Bispecific Ab compose of two different antigen binding domains in one fragment (de Kruif & Logtenberg, 1996). VHHs of cameloide heavy chain Abs are the smallest Ab fragments (Harmsen & De Haard, 2007). In the present, several techniques have been developed to generate recombinant human mAbs (Nogales-Gadea et al., 2015) for various applications.

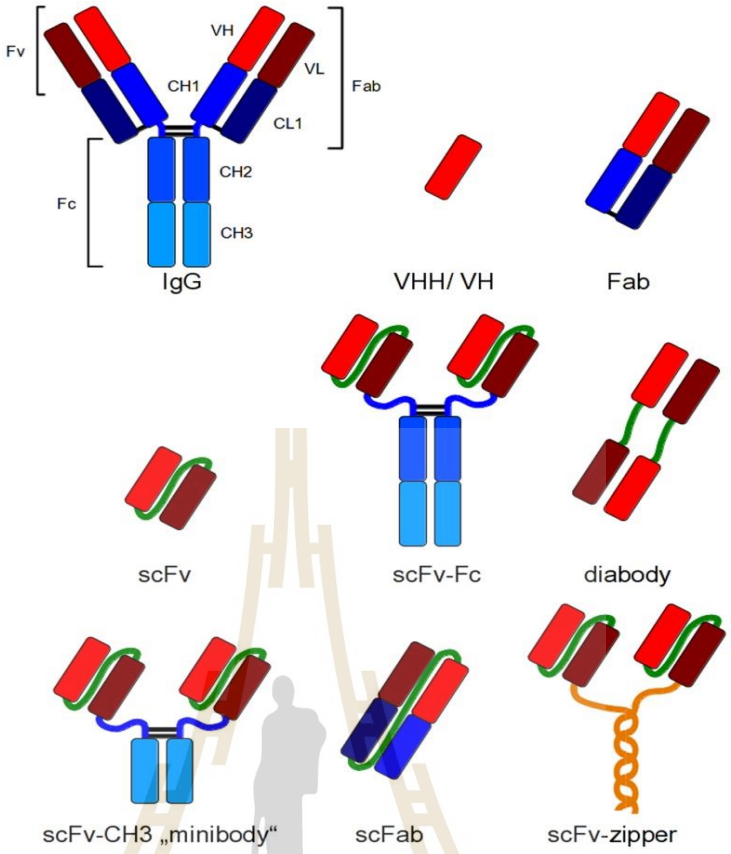

Figure 2.1 A full-length of IgG and recombinant Ab formats for various applications (Frenzel, Hust, & Schirrmann, 2013).

2.3 Expression of recombinant human Abs

The mAbs are mainly produced in mammalian and microbial host cells, with an addition of some other hosts including transgenic models, avian, insect, and transgenic animals. Therefore, only microbial and mammalian and expression host cells are discussed here.

2.3.1 Bacterial Expression

Now, Ab phage display is a wide spread method for the development of Ab fragments such as scFv or Fab. *E. coli* is used as an expression host and it has been extensive study of the biology resulting in large numbers of molecular tools and protein purification applications. Therefore, *E. coli* is the most essential expression system for

the production of recombinant Ab fragments. The production of recombinant Ab fragments in the reducing environment in cytosol of *E. coli* results mostly in non-functional aggregates. Recovery of inclusion bodies of Ab fragments from cytoplasmic compartment by complete denaturation and refolding is often not efficient (Martineau, Jones, & Winter, 1998). For production of recombinant Ab fragments, a major achievement is the secretion of recombinant Ab fragments into the periplasmic space and the culture supernatant of *E. coli* where the oxidizing environment permits the formation of disulfide bonds and correct folding. Therefore, the most recombinant Ab fragments are produced in the periplasm of *E. coli* using signal peptides (Rangnoi et al., 2011; Sletta et al., 2007; Vu et al., 2017).

In addition, expression of eukaryotic proteins can frequently fail in *E. coli* due to their lack of a glycosylation apparatus which limits in genetic repertoire of *E. coli* for proper folding. Fortunately, the novel expression strains of *E. coli* have developed such as Shuffle which a unique strain is able to catalyze the formation and maintenance of stable disulfide bonds within its cytoplasm (Lobstein et al., 2012). The SHuffle cells have been used to produce the VHH nanobody (Habib et al., 2013), Fab (Abe et al., 2014) and full length IgG Ab (Robinson et al., 2015).

2.3.2 Mammalian cells

The mammalian cell lines are most widely applied to produce the therapeutic Abs (Butler, 2005; Zhang & Shen, 2012; Zhu, 2012) due to their provide folding, secretion and post-translational apparatus is able to produce the Abs with least concerns for immunogenic modifications (Jenkins, Meleady, Tyther, & Murphy, 2009; Zhu, 2012). However, they still have some disadvantages such as relatively high production costs and difficult in handling.

Among mammalian cells, CHO cells are the most frequently used in the commercial production of biopharmaceuticals due to their high safety profile regarding human pathogenic virus, ability to growth in large-scale chemically defined and serum-free suspension culture, and ability to produce human-like glycosylated Abs (Kim, Kim, & Lee, 2012). However, although glycosylation patterns are very similar to that in humans, recombinant proteins derived from CHO cells have shown to be sometimes immunogenic (Butler & Spearman, 2014). Moreover, CHO cell system is the ease to establish the highly productive and stable recombinant CHO cells with adequate yields and acceptable quality for human use. This can be accomplished by using either site-specific integration of GOI into the host cell genome or random integration of GOI followed by gene amplification using the DHFR or GS systems (Durocher & Butler, 2009; Krämer, Klausing, & Noll, 2010).

CHO cells are derived from a clonal and spontaneously immortalized cells which the derived cell lines are deficient in proline synthesis (Puck, Cieciura, & Robinson, 1958). Currently, five different CHO cell lines are commonly used for biologic production: (i) the CHO-K1 and CHO-S cell lines having a functional DHFR gene, (ii) the CHO-DXB11 line containing a mono-allelic DHFR knockout (iii) the CHO-DG44 line which removed bi-allelic modification on the CHO DHFR gene (iv) GS-knockout CHOK1SV cell line with a bi-allelic deletion on the CHO GS gene eliminating the endogenous GS activity (Fan et al., 2012; Noh, Shin, & Lee, 2018; Urlaub & Chasin, 1980; Urlaub, Käs, Carothers, & Chasin, 1983; Wurm & Hacker, 2011).

Nowadays, genome information, transcriptome, miRnome, proteome as well as translatome data of the CHO cell became available, thus facilitating genetic manipulation (Baycin-Hizal et al., 2012; Becker et al., 2011; Brinkrolf et al., 2013;

Clarke et al., 2012; Courtes et al., 2013; Hackl et al., 2011; Lewis et al., 2013; Xu et al., 2011). More recently, transcription start sites were unraveled (Jakobi et al., 2014), which gives rise to more detailed bioinformatics analyses (www. chogenome.org). All these data significantly help to better characterize and engineer CHO cell for biotechnological application. CHO cells have been genetically engineered with several technologies corresponding glycosylation profile, improved the Ab production, improved metabolism, reduced apoptosis, and inducible cell cycle arrest which allows prolonged production times for high-cell viability and cell densities (Fischer, Handrick, & Otte, 2015).

The CRISPR/Cas9 system is an extremely powerful and easy tool for CHO cell engineering due to it is easy to establish, less time-consuming and much more cost effective. Therefore, this makes the CRISPR/Cas9 system particularly interesting for CHO cell engineering to more rapidly generate knockout cell lines harboring advantageous characteristics as a potential route for rational design of CHO cell factories. (Lee, Grav, Lewis, & Faustrup Kildegaard, 2015).

Recently, CRISPR/Cpf1-mediated genome editing has more potential than CRISPR/Cas9 (Bin Moon et al., 2018) due to Cpf1 endonuclease is much smaller than Cas9, making it easier for the enzyme to enter cells, requires shorter CRISPR RNA (crRNA) to work properly and does not require trans-activating crRNA (tracrRNA) (Liu et al., 2017; Schmieder et al., 2018; Zhang et al., 2017). Thus, this system has increased more popular than CRISPR/Cas9 since it is simpler and easier to use than the CRISPR-Cas9 system. CRISPR/Cpf1 (Clustered Regularly Interspaced Short Palindromic Repeats from *Prevotella* and *Francisella 1*) is a genome editing technology similar to the CRISPR/Cas9 system (Zetsche et al., 2015). The CRISPR/Cpf1 system composes of a Cpf1 enzyme and a guide RNA that binds

downstream of the protospacer adjacent motif (PAM) and cleaves target DNA. The Cpf1 endonuclease generates staggered ends at its PAM-distal region which cuts DNA strands at different places (Zetsche et al., 2015) whereas Cas9 endonuclease creates blunt ends at its PAM-proximal region which cuts both DNA strands at the same place (Garneau et al., 2010). For the PAM sequence, Cpf1 recognizes T-rich PAM sequences, i.e. 5'-TTTN-3' (Zetsche et al., 2015) whereas Cas9 prefers a G-rich PAM sequence (5'-NGG-3'). Now, the Cpf1-database is an online tool that help to find a potential target within the genome and design gRNA in which can recognize AsCpf1 and LbCpf1 nucleases via DNA recognition sequences (Park & Bae, 2017). Several reported have demonstrated the use of Cpf1 system for genome editing in eukaryotes (Hur et al., 2016; Kim et al., 2017; Kleinstiver et al., 2016; Tang et al., 2017; Zetsche et al., 2015).

2.7 References

Abe, R., Jeong, H.-J., Arakawa, D., Dong, J., Ohashi, H., Kaigome, R., Saiki, F., Yamane, K., Takagi, H., & Ueda, H. (2014). Ultra Q-bodies: quench-based antibody probes that utilize dye-dye interactions with enhanced antigen-dependent fluorescence. *Scientific Reports, 4*, 4640.

Baycin-Hizal, D., Tabb, D. L., Chaerkady, R., Chen, L., Lewis, N. E., Nagarajan, H., Sarkaria, V., Kumar, A., Wolozny, D., Colao, J., Jacobson, E., Tian, Y., O'Meally, R. N., Krag, S. S., Cole, R. N., Palsson, B. O., Zhang, H., & Betenbaugh, M. (2012). Proteomic Analysis of Chinese Hamster Ovary Cells. *Journal of Proteome Research, 11*(11), 5265-5276.

Becker, J., Hackl, M., Rupp, O., Jakobi, T., Schneider, J., Szczepanowski, R., Bekel, T., Borth, N., Goesmann, A., Grillari, J., Kaltschmidt, C., Noll, T., Pühler, A., Tauch, A., & Brinkrolf, K. (2011). Unraveling the Chinese hamster ovary cell

line transcriptome by next-generation sequencing. *Journal of Biotechnology*, *156*(3), 227-235.

Bin Moon, S., Lee, J. M., Kang, J. G., Lee, N.-E., Ha, D.-I., Kim, D. Y., Kim, S. H., Yoo, K., Kim, D., Ko, J.-H., & Kim, Y.-S. (2018). Highly efficient genome editing by CRISPR-Cpf1 using CRISPR RNA with a uridinylate-rich 3′-overhang. *Nature Communications*, *9*(1), 3651.

Bird, R. E., Hardman, K. D., Jacobson, J. W., Johnson, S., Kaufman, B. M., Lee, S. M., Lee, T., Pope, S. H., Riordan, G. S., & Whitlow, M. (1988). Single-chain antigen-binding proteins. *Science*, *242*(4877), 423-426.

Brinkrolf, K., Rupp, O., Laux, H., Kollin, F., Ernst, W., Linke, B., Kofler, R., Romand, S., Hesse, F., Budach, W. E., Galosy, S., Muller, D., Noll, T., Wienberg, J., Jostock, T., Leonard, M., Grillari, J., Tauch, A., Goesmann, A., Helk, B., Mott, J. E., Puhler, A., & Borth, N. (2013). Chinese hamster genome sequenced from sorted chromosomes. *Nature Biotechnology*, *31*(8), 694-695.

Butler, M. (2005). Animal cell cultures: recent achievements and perspectives in the production of biopharmaceuticals. *Applied Microbiology and Biotechnology*, *68*(3), 283-291.

Butler, M., & Spearman, M. (2014). The choice of mammalian cell host and possibilities for glycosylation engineering. *Current Opinion in Biotechnology*, *30*, 107-112.

Clarke, C., Henry, M., Doolan, P., Kelly, S., Aherne, S., Sanchez, N., Kelly, P., Kinsella, P., Breen, L., Madden, S. F., Zhang, L., Leonard, M., Clynes, M., Meleady, P., & Barron, N. (2012). Integrated miRNA, mRNA and protein expression analysis reveals the role of post-transcriptional regulation in

controlling CHO cell growth rate. *BMC Genomics, 13*(1), 656.

Courtes, F. C., Lin, J., Lim, H. L., Ng, S. W., Wong, N. S. C., Koh, G., Vardy, L., Yap, M. G. S., Loo, B., & Lee, D.-Y. (2013). Translatome analysis of CHO cells to identify key growth genes. *Journal of Biotechnology, 167*(3), 215-224.

Cuesta, A., Sainz-Pastor, N., Bonet, J., Oliva, B., & Alvarez-Vallina, L. (2010). *Multivalent antibodies: When design surpasses evolution* (Vol. 28).

de Kruif, J., & Logtenberg, T. (1996). Leucine zipper dimerized bivalent and bispecific scFv antibodies from a semi-synthetic antibody phage display library. *The Journal of biological chemistry, 271*(13), 7630-7634.

Durocher, Y., & Butler, M. (2009). Expression systems for therapeutic glycoprotein production. *Current Opinion in Biotechnology, 20*(6), 700-707.

Fan, L., Kadura, I., Krebs, L. E., Hatfield, C. C., Shaw, M. M., & Frye, C. C. (2012). Improving the efficiency of CHO cell line generation using glutamine synthetase gene knockout cells. *Biotechnology and Bioengineering, 109*(4), 1007-1015.

Fischer, S., Handrick, R., & Otte, K. (2015). The art of CHO cell engineering: A comprehensive retrospect and future perspectives. *Biotechnology Advances, 33*(8), 1878-1896.

Flanagan, R. J., & Jones, A. L. (2004). Fab antibody fragments: some applications in clinical toxicology. *Drug Safety, 27*(14), 1115-1133.

Frenzel, A., Hust, M., & Schirrmann, T. (2013). Expression of recombinant antibodies. *Frontiers in Immunology, 4*, 217.

Garneau, J. E., Dupuis, M., Villion, M., Romero, D. A., Barrangou, R., Boyaval, P.,

Fremaux, C., Horvath, P., Magadán, A. H., & Moineau, S. (2010). The CRISPR/Cas bacterial immune system cleaves bacteriophage and plasmid DNA. *Nature*, *468*(7320), 67-71.

Geng, X., Kong, X., Hu, H., Chen, J., Yang, F., Liang, H., Chen, X., & Hu, Y. (2015). Research and development of therapeutic mAbs: An analysis based on pipeline projects. *Human Vaccines & Immunotherapeutics*, *11*(12), 2769-2776.

Habib, I., Smolarek, D., Hattab, C., Grodecka, M., Hassanzadeh-Ghassabeh, G., Muyldermans, S., Sagan, S., Gutierrez, C., Laperche, S., Le-Van-Kim, C., Aronovicz, Y. C., Wasniowska, K., Gangnard, S., & Bertrand, O. (2013). V(H)H (nanobody) directed against human glycophorin A: a tool for autologous red cell agglutination assays. *Analytical Biochemistry, 438*(1), 82-89.

Hackl, M., Jakobi, T., Blom, J., Doppmeier, D., Brinkrolf, K., Szczepanowski, R., Bernhart, S. H., Siederdissen, C. H. z., Bort, J. A. H., Wieser, M., Kunert, R., Jeffs, S., Hofacker, I. L., Goesmann, A., Pühler, A., Borth, N., & Grillari, J. (2011). Next-generation sequencing of the Chinese hamster ovary microRNA transcriptome: Identification, annotation and profiling of microRNAs as targets for cellular engineering. *Journal of Biotechnology, 153*(1), 62-75.

Harmsen, M. M., & De Haard, H. J. (2007). Properties, production, and applications of camelid single-domain antibody fragments. *Applied Microbiology and Biotechnology, 77*(1), 13-22.

Hu, S., Shively, L., Raubitschek, A., Sherman, M., Williams, L. E., Wong, J. Y., Shively, J. E., & Wu, A. M. (1996). Minibody: A novel engineered anti-carcinoembryonic antigen antibody fragment (single-chain Fv-CH3) which exhibits rapid, high-level targeting of xenografts. *Cancer Research, 56*(13), 3055-3061.

Hur, J. K., Kim, K., Been, K. W., Baek, G., Ye, S., Hur, J. W., Ryu, S. M., Lee, Y. S., & Kim, J. S. (2016). Targeted mutagenesis in mice by electroporation of Cpf1 ribonucleoproteins. *Nature Biotechnology, 34*(8), 807-808.

Hust, M., Jostock, T., Menzel, C., Voedisch, B., Mohr, A., Brenneis, M., Kirsch, M. I., Meier, D., & Dubel, S. (2007). Single chain Fab (scFab) fragment. *BMC Biotechnology, 7*, 14.

Jakobi, T., Brinkrolf, K., Tauch, A., Noll, T., Stoye, J., Pühler, A., & Goesmann, A. (2014). Discovery of transcription start sites in the Chinese hamster genome by next-generation RNA sequencing. *Journal of Biotechnology, 190*, 64-75.

Jenkins, N., Meleady, P., Tyther, R., & Murphy, L. (2009). Strategies for analysing and improving the expression and quality of recombinant proteins made in mammalian cells. *Biotechnology and Applied Biochemistry, 53*(Pt 2), 73-83.

Kim, H. K., Song, M., Lee, J., Menon, A. V., Jung, S., Kang, Y. M., Choi, J. W., Woo, E., Koh, H. C., Nam, J. W., & Kim, H. (2017). In vivo high-throughput profiling of CRISPR-Cpf1 activity. *Nature Methods, 14*(2), 153-159.

Kim, J. Y., Kim, Y. G., & Lee, G. M. (2012). CHO cells in biotechnology for production of recombinant proteins: current state and further potential. *Applied Microbiology and Biotechnology, 93*(3), 917-930.

Kleinstiver, B. P., Tsai, S. Q., Prew, M. S., Nguyen, N. T., Welch, M. M., Lopez, J. M., McCaw, Z. R., Aryee, M. J., & Joung, J. K. (2016). Genome-wide specificities of CRISPR-Cas Cpf1 nucleases in human cells. *Nature Biotechnology, 34*(8), 869-874.

Krämer, O., Klausing, S., & Noll, T. (2010). Methods in mammalian cell line engineering: from random mutagenesis to sequence-specific approaches.

Applied Microbiology and Biotechnology, 88(2), 425-436.

Lee, J. S., Grav, L. M., Lewis, N. E., & Faustrup Kildegaard, H. (2015). CRISPR/Cas9-mediated genome engineering of CHO cell factories: Application and perspectives. *Biotechnology Journal, 10*(7), 979-994.

Lewis, N. E., Liu, X., Li, Y., Nagarajan, H., Yerganian, G., O'Brien, E., Bordbar, A., Roth, A. M., Rosenbloom, J., Bian, C., Xie, M., Chen, W., Li, N., Baycin-Hizal, D., Latif, H., Forster, J., Betenbaugh, M. J., Famili, I., Xu, X., Wang, J., & Palsson, B. O. (2013). Genomic landscapes of Chinese hamster ovary cell lines as revealed by the Cricetulus griseus draft genome. *Nat Biotech, 31*(8), 759-765.

Liu, Y., Han, J., Chen, Z., Wu, H., Dong, H., & Nie, G. (2017). Engineering cell signaling using tunable CRISPR–Cpf1-based transcription factors. *Nature Communications, 8*(1), 2095.

Lobstein, J., Emrich, C. A., Jeans, C., Faulkner, M., Riggs, P., & Berkmen, M. (2012). SHuffle, a novel Escherichia coli protein expression strain capable of correctly folding disulfide bonded proteins in its cytoplasm. *Microbial Cell Factories, 11*, 56.

Martineau, P., Jones, P., & Winter, G. (1998). Expression of an antibody fragment at high levels in the bacterial cytoplasm11Edited by J. Karn. *Journal of Molecular Biology, 280*(1), 117-127.

Nogales-Gadea, G., Saxena, A., Hoffmann, C., Hounjet, J., Coenen, D., Molenaar, P., Losen, M., & Martinez-Martinez, P. (2015). Generation of Recombinant Human IgG Monoclonal Antibodies from Immortalized Sorted B Cells. *Journal*

of Visualized Experiments(100), e52830.

Noh, S. M., Shin, S., & Lee, G. M. (2018). Comprehensive characterization of glutamine synthetase-mediated selection for the establishment of recombinant CHO cells producing monoclonal antibodies. *Scientific Reports, 8*(1), 5361.

Park, J., & Bae, S. (2017). Cpf1-Database: web-based genome-wide guide RNA library design for gene knockout screens using CRISPR-Cpf1. *Bioinformatics, 34*(6), 1077-1079.

Puck, T. T., Cieciura, S. J., & Robinson, A. (1958). Genetics of somatic mammalian cells. III. Long-term cultivation of euploid cells from human and animal subjects. *The Journal of experimental medicine, 108*(6), 945-956.

Rangnoi, K., Jaruseranee, N., O'Kennedy, R., Pansri, P., & Yamabhai, M. (2011). One-step detection of aflatoxin-B(1) using scFv-alkaline phosphatase-fusion selected from human phage display antibody library. *Molecular Biotechnology, 49*(3), 240-249.

Robinson, M.-P., Ke, N., Lobstein, J., Peterson, C., Szkodny, A., Mansell, T. J., Tuckey, C., Riggs, P. D., Colussi, P. A., Noren, C. J., Taron, C. H., DeLisa, M. P., & Berkmen, M. (2015). Efficient expression of full-length antibodies in the cytoplasm of engineered bacteria. *Nature Communications 6*, 8072.

Schmieder, V., Bydlinski, N., Strasser, R., Baumann, M., Kildegaard, H. F., Jadhav, V., & Borth, N. (2018). Enhanced Genome Editing Tools For Multi-Gene Deletion Knock-Out Approaches Using Paired CRISPR sgRNAs in CHO Cells. *Biotechnology Journal 13*(3), e1700211.

Sletta, H., Tøndervik, A., Hakvåg, S., Aune, T. E. V., Nedal, A., Aune, R., Evensen, G., Valla, S., Ellingsen, T. E., & Brautaset, T. (2007). The Presence of N-

Terminal Secretion Signal Sequences Leads to Strong Stimulation of the Total Expression Levels of Three Tested Medically Important Proteins during High-Cell-Density Cultivations of Escherichia coli. *Applied and Environmental Microbiology*, *73*(3), 906-912.

Tang, X., Lowder, L. G., Zhang, T., Malzahn, A. A., Zheng, X., Voytas, D. F., Zhong, Z., Chen, Y., Ren, Q., Li, Q., Kirkland, E. R., Zhang, Y., & Qi, Y. (2017). A CRISPR-Cpf1 system for efficient genome editing and transcriptional repression in plants. *Nature Plants*, *3*, 17018.

Urlaub, G., & Chasin, L. A. (1980). Isolation of Chinese hamster cell mutants deficient in dihydrofolate reductase activity. *Proceedings of the National Academy of Sciences*, *77*(7), 4216-4220.

Urlaub, G., Käs, E., Carothers, A. M., & Chasin, L. A. (1983). Deletion of the diploid dihydrofolate reductase locus from cultured mammalian cells. *Cell*, *33*(2), 405-412.

Vu, N. X., Pruksametanan, N., Srila, W., Yuttavanichakul, W., Teamtisong, K., Teaumroong, N., Boonkerd, N., Tittabutr, P., & Yamabhai, M. (2017). Generation of a rabbit single-chain fragment variable (scFv) antibody for specific detection of Bradyrhizobium sp. DOA9 in both free-living and bacteroid forms. *PLoS One*, *12*(6), e0179983.

Wurm, F. M., & Hacker, D. (2011). First CHO genome. *Nature Biotechnology*, *29*(8), 718-720.

Xu, X., Nagarajan, H., Lewis, N. E., Pan, S., Cai, Z., Liu, X., Chen, W., Xie, M., Wang, W., Hammond, S., Andersen, M. R., Neff, N., Passarelli, B., Koh, W., Fan, H. C., Wang, J., Gui, Y., Lee, K. H., Betenbaugh, M. J., Quake, S. R., Famili, I.,

Palsson, B. O., & Wang, J. (2011). The genomic sequence of the Chinese hamster ovary (CHO)-K1 cell line. *Nature Biotechnology, 29*(8), 735-741.

Zetsche, B., Gootenberg, J. S., Abudayyeh, O. O., Slaymaker, I. M., Makarova, K. S., Essletzbichler, P., Volz, S. E., Joung, J., van der Oost, J., Regev, A., Koonin, E. V., & Zhang, F. (2015). Cpf1 is a single RNA-guided endonuclease of a class 2 CRISPR-Cas system. *Cell, 163*(3), 759-771.

Zhang, R. Y., & Shen, W. D. (2012). Monoclonal antibody expression in mammalian cells. *Methods in Molecular Biology, 907*, 341-358.

Zhang, X., Wang, J., Cheng, Q., Zheng, X., Zhao, G., & Wang, J. (2017). Multiplex gene regulation by CRISPR-ddCpf1. *Cell Discovery, 3*(1), 17018.

Zhu, J. (2012). Mammalian cell protein expression for biopharmaceutical production. *Biotechnology advances, 30*(5), 1158-1170.

CHAPTER III

EXPRESSION AND CHARACTERIZATION OF SCFV-GFP FUSION ANTIBODIES

3.1 Abstract

Fluorescence-linked immunosorbent assay (FLISA) has become one of the most efficient analytical methods for immune analysis because it is a time-saving technique, with high sensitivity and reliability. This is because the secondary Ab and substrate for conjugated enzyme can be avoided. In this research, an expression vector for the expression of scFv-EmGFP antibody was constructed. Then, scFv Ab against rabies virus, aflatoxin B1 (AFB1) and Zearalenone (ZEN) were engineered to fuse with the EmGFP and expressed in different *E. coli* expression hosts. Our results indicated that *E. coli* C3029 (B cell) is the best host, when compared with *E. coli* C3026 (K12) and BL21 (DE3). Three cytoplasmic fluobodies were characterized by ELISA and FLISA, which revealed that they retained both affinity binding of native Abs and fluorescence activity of EmGFP. Furthermore, application of the purified yZA8B2-scFv-EmGFP for the detection of ZEN by competitive FLISA was demonstrated. This system has potential to be developed for both quantitative and qualitative analysis in various applications.

Keywords: Single-chain variable fragment (scFv); Green fluorescent protein (GFP); Immunofluorescence; Fluobody; Fusion protein, Fluorescence-linked immunosorbent assay (FLISA)

3.2 Introduction

Currently, many research and development are focused on creating various types of mAbs for therapeutics and diagnostics. In addition to full-length Abs, Recombinant Ab formats are also being developed as potential therapeutics and diagnostics (Frenzel, Hust, & Schirrmann, 2013). The smallest antigen binding fragment of immunoglobulins retaining its the antigen-binding affinity of the intact parental Ab is the scFv, which consists of the variable domains of the HC and LC are covalently linked together by a flexible peptide linker (Bird et al., 1988; Rangnoi, Jaruseranee, O'Kennedy, Pansri, & Yamabhai, 2011). Recently, scFv are the most widely used Ab fragments which can be expressed *E. coli*. Several techniques have been developed to generate recombinant human mAbs (Nogales-Gadea et al., 2015). Among these, the phage display technology is commonly used to create and select the recombinant Abs (Griffiths & Duncan, 1998). Moreover, scFvs are usually fused to other molecules to chimera protein which have bifunctional chimeric fusion protein (Rangnoi et al., 2011). The ability of chimera protein is interesting useful tool in biotechnology applications.

For analytical application, a high level of sensitivity can be increased by chemical conjugation between fluorescent labels and Abs (Hermanson, 2008; Holmes & Lantz, 2001). Fluorescein isothiocyanate (FITC) is one of the most widely used organic fluorophores in various applications. It can bind to the free amino group of the proteins leading to a stable thiourea bond formation. However, the FITC may conjugate with an antigen-binding site, which results in a partial or complete loss of reactivity of the Ab (Luria, Raichlin, & Benhar, 2012; Reimann et al., 1994; Sakamoto et al., 2012). To overcome the these drawbacks of this method, fusion protein of a *Aequorea victoria* green fluorescent protein (GFP) (Tsien, 1998) and a scFv Ab, which is call a fluobody,

has been developed by genetic engineering as an alternative to conjugate scFv-GFP. In this system, it is always produced in a 1:1 ratio between the scFv and GFP and retained the fluorescent properties of GFP and the antigen binding property of a native Ab, which should improve the accuracy of the quantitative analysis (Schwalbach, Sibler, Choulier, Deryckère, & Weiss, 2000). At present, fluobodies has been widely employed as probe in various fields, such as immunolabeling, fluorescence-activated cell sorter (FACS), fluorescent-linked immunosorbent assay (FLISA), yeast display and determine the scFv concentration in crude sample (Ferrara, Listwan, Waldo, & Bradbury, 2011; Gerdes & Kaether, 1996; Sakamoto, Shoyama, Tanaka, & Morimoto, 2014).

Fluobodies have been expressed in *Escherichia coli* (Casey, Coley, Tilley, & Foley, 2000; Ferrara et al., 2011; Olichon & Surrey, 2007; Sakamoto et al., 2012; Schwalbach et al., 2000), but the folding efficacy and the yield are frequently poor. Because scFvs have disulfide bonds, they require an oxidizing environment in the periplasm of *E. coli* or express in eukaryotic cells for correct folding, whereas GFP can be correctly folded in the cytosol of *E. coli* (Olichon & Surrey, 2007). To avoid of these obstacles, *E. coli* Shuffle strains, which is engineered to promote correctly folding disulfide bond formation in the cytoplasm, have been developed as an alternative to express e scFv-GFP (Lobstein et al., 2012). Here, we developed a suitable expression vector system for the production of various scFv-GFP Abs. The Abs which are constructed in our laboratory, namely IRA7c-scFv, 3E3-scFv and yZA8B2-scFv Abs against rabies virus, aflatoxin B1 (AFB1) and Zearalenone (ZEN), respectively, were used as model Abs in this study. In addition, scFv-GFP Abs were also characterized and applied for FLISA.

3.3 Materials and Methods

3.3.1 Construction of expression vector for the production of fluorescent Ab conjugates

To construct of pWS-Green vector containing EmGFP, the EmGFP gene from pSERT/EmGFP (Invitrogen, USA) was amplified by PCR technique using two primers (EmGFPNcoIEcoRINotIFW: 5'-CTGTGCCCATGGGAATTCAAGCTTGCGGCCGCAGGTGGCGGAGGGATGGTGAGCAAGGGCGAGGAG-3' and EGFPFlag6HisXhoIRv: 5'-GCACAGCTCGAGCTAGTGGTGGTGGTGGTGGTGCTTGTCGTCATCGTCTTTGTAGTCCCCCTTGTACAGCTCGTCCATGCC-3' in which containing the *Nco*I and *Xho*I restriction sites, respectively. And then the amplified product was digested with *Nco*I and *Xho*I, ligated into the expression vector pET15b which was cut using the same restriction enzymes. This resulted in the overexpression plasmid pWS-Green encodig C-terminal 6xHis and FLAG tagged recombinant EmGFP for further purification. The DNA sequence of the construct was confirmed by automated DNA sequencing (Macrogen, Korea).

3.3.2 Cloning and expression of scFv-EmGFP fusion proteins

To cloning of IRA7c-scFv, 3E3-scFv and yZA8B2-scFv Abs into pWS-Green, the scFv genes were digested with the *Nco*I and *Not*I restriction enzymes and ligated into digested pWS-Green. This resulted in the expression vector scFv-pWS-Green encodes scFv linked EmGFP protein via $(G)_4$ linker and followed by 6xHis tag that easy to purify the recombinant protein. The fused protein is under control of T7 promoter and could be induced for the overexpression using IPTG. The DNA sequence of the constructs was determined with automated DNA sequencer.

To produce the scFv-EmEGP fusions, the pWS-Green vectors containing scFv genes were transformed into *E. coli* strain SHuffle B (*E. coli* C3029 (B cell)), Shuffle K12 (*E. coli* C3026 (K12)) (New England Biolabs, USA) and BL21 (DE3) to evaluate a suitable expression host. The fusion proteins were expressed according to a previously published method (Lobstein et al., 2012) with some modifications. A single colony of each *E. coli* harboring recombinant plasmid was inoculated in 5 mL LB media containing 100 µg/mL of ampicillin and cultured at 30ºC with shaking 250 rpm for overnight. Four mL of overnight culture were used to inoculate 400 mL of LB medium containing 100 µg/mL of ampicillin next day. Cells were cultured at 30ºC to OD_{600} = 0.6, followed by induction by adding 0.4 mM isopropyl-β-D-thiogalactopyranoside (IPTG) at 25ºC for 16 h before harvesting the cells. The level of EmGFP-expressing *E. coli* was determined by a CytoFLEX S flow cytometer (Beckman Coulter, Germany) with 488 nm excitation and 523 emission wavelengths and and the data were analysed using the Kaluza 1.2 software program (Beckman Coulter). For a control, the pET27b harboring scFv gene was also expressed in the same time for comparison of binding activity.

3.3.3 Purification of scFv-EmGFP fusion proteins

The cell pellets were harvested by centrifugation at 8000 rpm for 10 min, which were re-suspended in binding buffer (20 mM Tris-HCl, 300 mM NaCl and 20 mM imidazole, pH 7.9) with 1 mg/ml lysozyme. Cells were disrupted by intermittent sonication at 25% amplitude for 7 min on ice using 30s pulse and 30s break for cooling after adding 1 mM phenylmethylsulfonyl fluoride (PMSF). The cell debris was removed by centrifugation at 15,000 x g for 20 min at 4°C, and the clear supernatant was applied directly into Ni-NTA column, pre-equilibrated with binding buffer. The

column was washed with biding buffer. Finally, the fusion protein was eluted with elution buffer (20 mM Tris-HCl, 300 mM NaCl and 250 mM imidazole, pH 7.9). Fractions containing scFv-EmGFP fusion protein were pooled and exchanged by dialysis into PBS buffer, respectively at 4ºC. The samples were collected and kept at 4ºC. The soluble fraction and purity of the samples were assessed by denaturing sodium dodecyl sulfate-polyacrylamide gel electrophoresis (SDS-PAGE). The purified protein were determined by Bradford method (1976) using bovine serum albumin as a standard.

3.3.4 Gel electrophoresis and western blot analysis

The purified fusion proteins were analyzed by 12% SDS-PAGE. Protein bands were visualized by staining with Coomassie brilliant blue R-250 (BioRad) (Laemmli, 1970). The Precision Plus Protein Standard (10-250 kDa) from Bio-Rad (Bio-Rad Laboratories, USA) was used as a molecular weight marker. Western blot was analyzed according to the manufacturer's protocol (Bio-Rad Laboratories, USA). The proteins were electroblotted to PVDF membrane at 100 volts for 1.5 h at 4ºC. Subsequently, the membrane was blocked for 1 h with 2% skim milk in 1xPBS (MPBS) at 4ºC for overnight. The membrane was then washed 3 times with 1xPBS by rocking at room temperature for 1 min each time. After HisProbe-HRP conjugate (1:5000; ThermoFisher Sceintific, USA) incubation for 1 h, the membrane was washed again. Finally, the protein target was visualized using Amersham ECL Prime Western Blotting Detection Reagent (GE Healcare Life Sciences, USA).

3.3.5 Conventional ELISA

The fused IRA7c-scFv-EmGFP Ab was confirmed the binding activity by ELISA (Pruksametanan, Yamabhai, & Khawplod, 2012). For the bind activity of 3E3-

scFv-EmGFP and yZA8B2-scFv-EmGFP were performed according to a previously published method (Rangnoi et al., 2011).

3.3.6 Fluorescence-linked immunosorbent assay (FLISA)

Binding activity of each fusion Abs was determined by FLISA. A black Nunc-Immuno 96 well plates were coated with 1 μg of AFB1-BSA in 1xPBS (for 3E3-scFv-EmGFP), 1 μg of ZEN-BSA in 1xPBS (for yZA8B2-scFv-EmGFP), 0.1 IU of rabies virus vaccine 100 mM $NaHCO_3$, pH 8.5 (for IRA7c-scFv-EmgFP). In this experiment, 1% BSA was used as a negative control. After incubation at 4°C overnight, the plates were blocked with 2% MPBS at room temperature for 1 h, followed by washing 3 times with PBS. Fifty microliters of 4% MPBS and 100 μL of each fusion Ab were added to each well and incubated at room temperature for 1 h. The wells were washed three times with PBS containing 0.05% Tween 20 (PBST) and twice times with PBS. Finally, 100 μL of PBS were added into the plates. The fluorescence intensity was measured by a fluorescent microplate reader (ThermoFisher Sceintific, USA). The excitation and emission wavelengths were 478-484 and 560-509 nm, respectively.

3.3.7 Competitive FLISA

To confirm the yZA8B2-scFv-EmGFP fusion Ab that can bind to free ZEN by competitive FLISA, inhibition FLISA was developed to determine the sensitivities and specificities of the yZA8B2-scFv-EmGFP fusion Ab. Two μg of ZEN-BSA, ZEN-OVA and ZEN-KLH were coated on a black Nunc-Immuno 96 well plate. The different yZA8B2-scFv-EmGFP dilutions were pre-incubated with varying concentrations of soluble ZEN. After incubation at 37ºC with shaking 300 rpm in dark for 30 min, the mixture was transferred to the coated plate and incubated for 1 h. The unbound Abs were washed away 3 times with 0.05% PBST and 2 times with PBS. The wells were

added 100 µL of PBS and measured the fluorescent signal with an excitation peak at 487-484 nm and an emission peak at 506-509 nm.

3.4 Results

3.4.1 Construction of expression vector for the production of fluorescent Ab conjugates

To construct plasmid that can produce the scFv-EmGFP fusion Abs, we firstly cloned EmGFP into pET15b by PCR technique, yielding pWS-Green without the SP for the secretion of protein. Then, the scFvs of each Ab were fused to the N-terminal residue of the EmGFP of the pWS-Green expression vector (Figure 3.1). This expression carrying the scFv-EmGFP gene under the control of T7 promoter could be induced for overexpression using IPTG. In addition to the fusion Abs were fused with DNA encoding 6xHis tag and followed by FLAG tag at the C-terminus for further purification and detection. For comparative, we also used the vectors containing scFv alone and EmGFP alone. The expression vector was designed such that the construct with scFv- EmGFP fusion will generate brighter fluorescent signal than those without the inserts, due to the position of ribosomal binding site and the start codon.

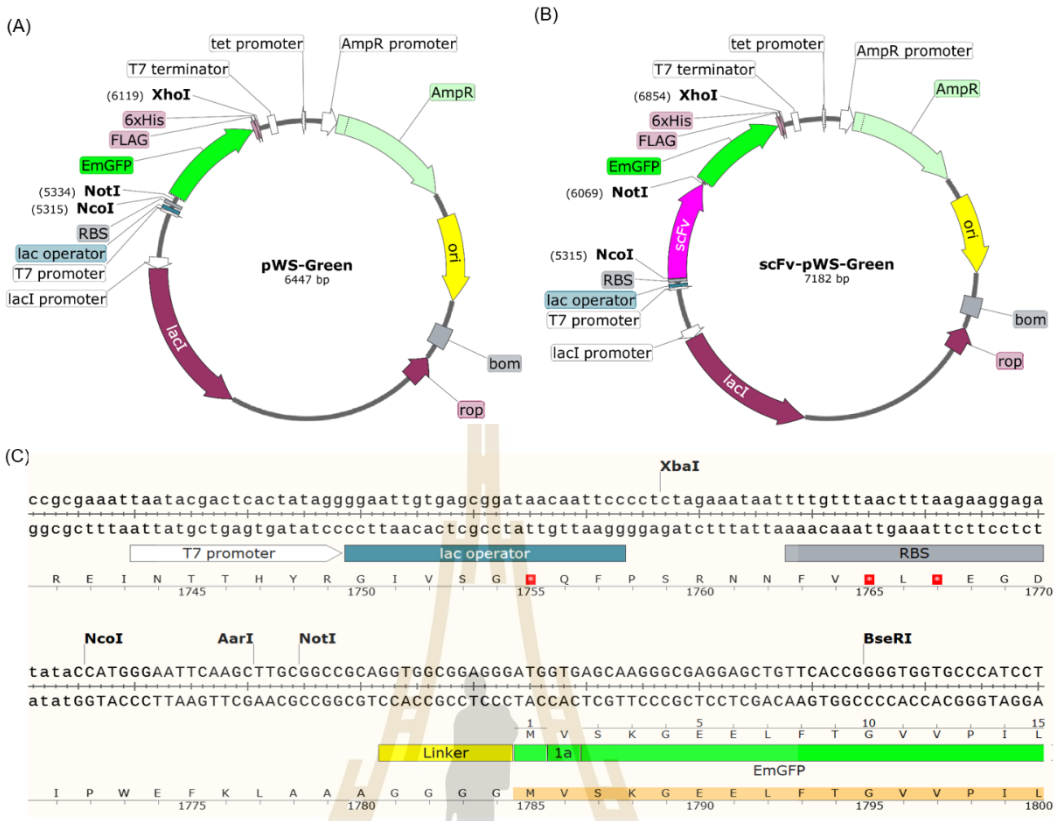

Figure 3.1 Map of pWs-Green (A) and scFv-pWS-Green (B) expression vectors. The EmGFP and scFv-EmGFP genes were under the control of the T7 promoter and fused with DNA encoding 6xHis tag, followed by FLAG tag at the C-terminus. The vector carries the gene for ampicillin resistance (Amp_r) for the selection and maintenance of the plasmid, and the lac repressor (*lac*I), which represses the T7 promoter. The scFv and EmGFP are liked with G_4 liker. (C) Multiple cloning site (MCS) of pWs-Green vector.

3.4.2 Expression of scFv-EmGFP fusion proteins

To evaluate a suitable expression host, the 3E3-scFv-EmGFP and IR7c-scFv-EmGFP were transformed to three strains of *E. coli* expression hosts for fusion protein expression. Then the fusion proteins from each *E. coli* expression host were tested by flow cytometer, ELISA, FLISA and western blot. The level of the scFv fusion

proteins was evaluated by measuring the fluorescence intensity of induced *E coli* cultures by flow cytometry (Figure 3.2A-B). The results demonstrate that EmGFP fluorescence peak separated from scFv-EmGFP fusion protein expressing three *E. coli* hosts. EmGFP fluorescence peak from *E. coli* B cell and K12 were found to be more overlapped with the fluorescence peak of pET15b transformed *E. coli* hosts when compared to EmGFP fluorescence peak from *E. coli* DE3. Among three expression hosts, the separation of the fluorescence peak between scFv-EmGFP fusion protein and EmGFP alone was clearly more observed in *E. coli* B cell than in *E. coli* K12 and DE3 under the same scFv-fusion expression. Surprisingly, the level of fluorescence intensity was observed only in cell lysates from three *E. coli* expression hosts harboring the scFv-EmGFP construct while the fluorescence intensity level was not observed in cell lysates from three *E. coli* expression hosts harboring only EmGFP construct (Figure 3.3). The specific binding of the fused 3E3-scFv-EmGFP protein has still remained comparing to the activity binding of 3E3-scFv expressed under the same condition, whereas the specific binding of the fused IR7c-scFv-EmGFP protein highly reduced comparing to the activity binding of IR7c-scFv expressed under the same condition (Figure 3.4A-D). In addition, our results indicated that *E. coli* B cell is the most suitable host, when compared with *E. coli* K12 and DE3. The activity binding of the fused protein from different expression hosts related to the band as indicated by western blot (Figure 3.5A-B). Therefore, the fused proteins were expressed in *E. coli* B cell for purification in the next step.

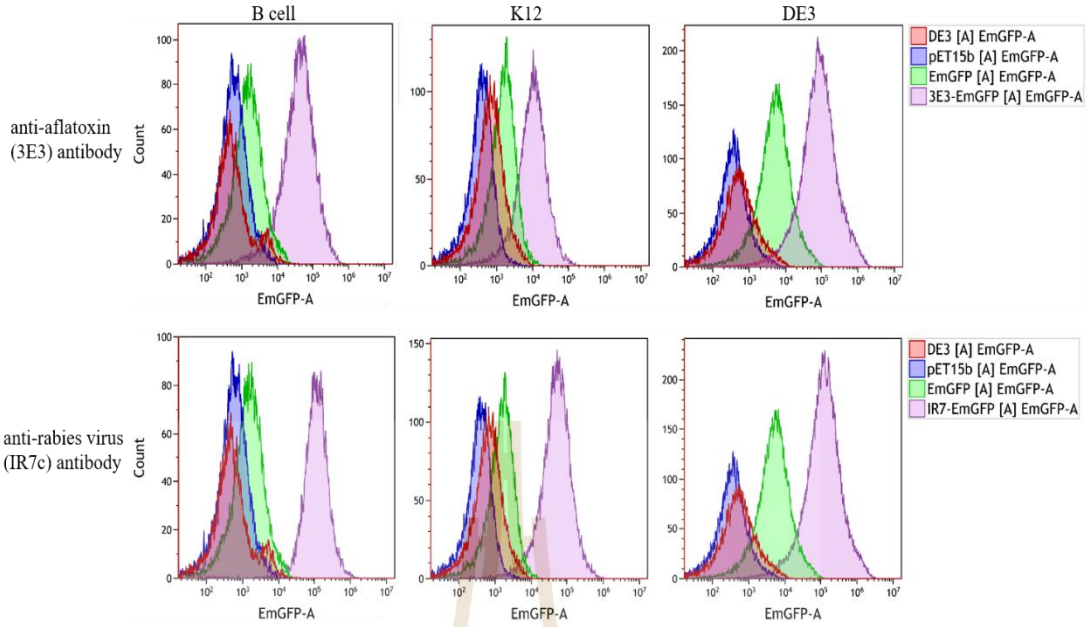

Figure 3.2 Flow cytometry analysis of three *E. coli* expression hosts (B cell, K12 and DE3) harboring scFv-EmGFP constructs of IR7c and 3E3 Abs and EmGFP construct. Empty three *E. coli* expression hosts and pET15b vector were used as negative controls.

(A)

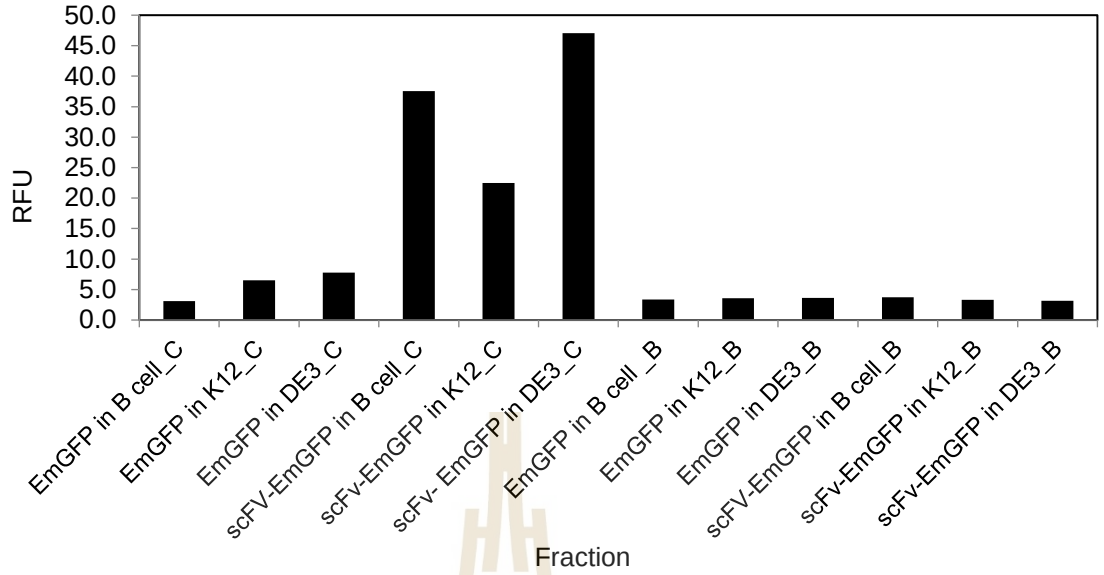

(B)

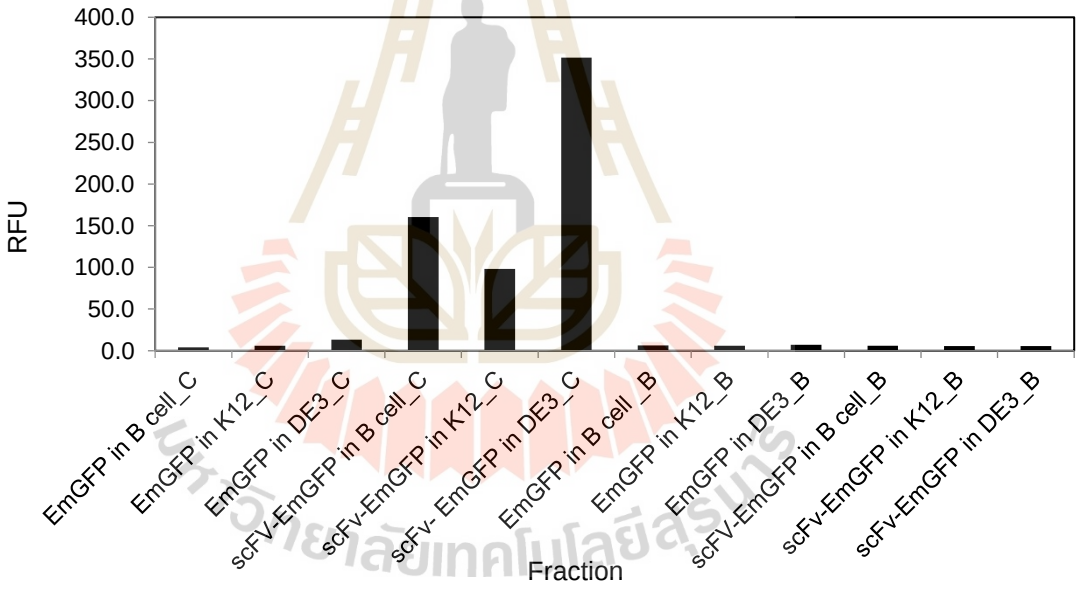

Figure 3.3 The fluorescence intensity of EmGFP and scFv-EmGFP of E3E (A) and IR7c Abs (B) from cell lysate (C at end of name) and broth (B at end of name) in different hosts. The fluorescence intensity was measured by a fluorescent microplate reader (excitation 484 nm and 509 nm).

(A)

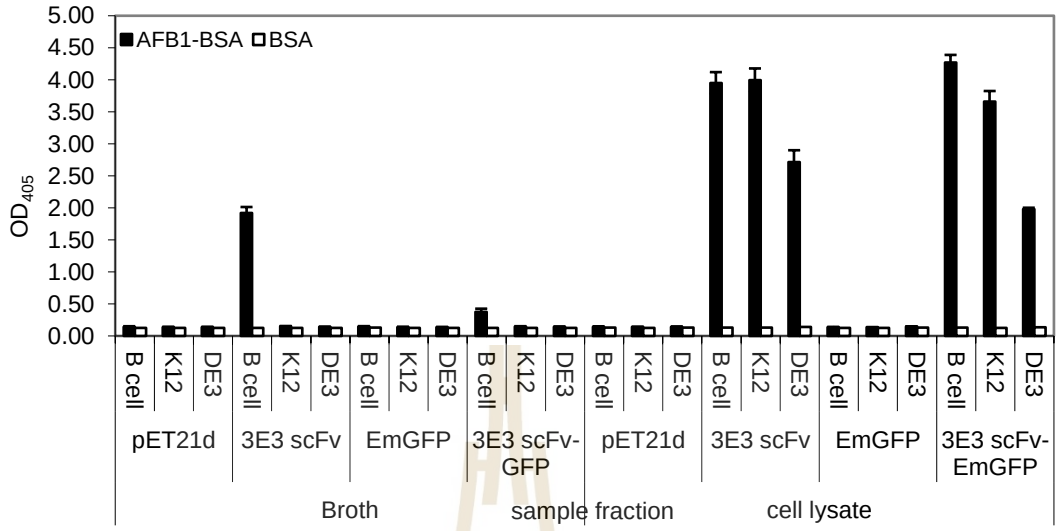

(B)

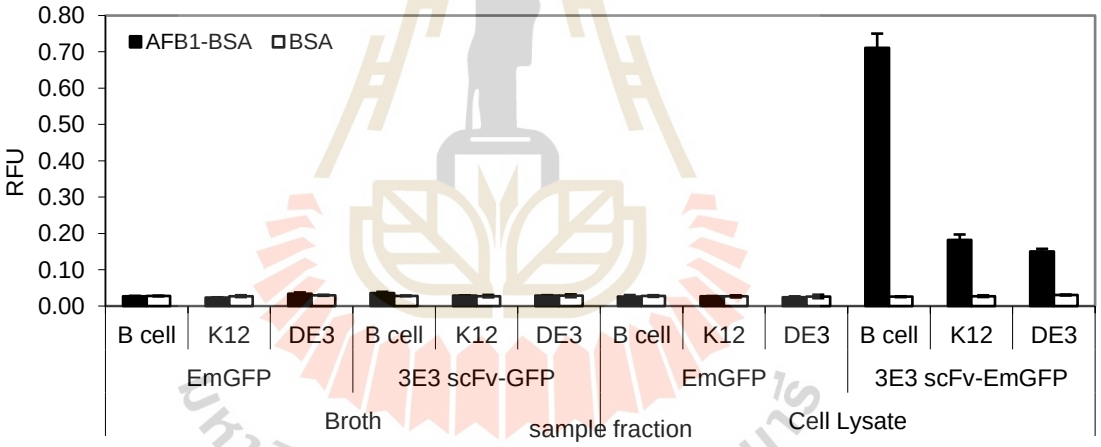

Figure 3.4 Specific binding of scFv and scFv-EmGFP of E3E (A and B) and IR7c (C and D) Abs. ELISA (A and C) and FLISA (B and D) results of the binding of scFv and scFv-EmGFP Abs in cytoplasmic space and broth are shown. BSA and skim milk were used as a negative control in this assay. The average optical density (OD) at 405 nm and relative fluorescence units (RFU) values and standard errors from triplicate wells are shown.

(C)

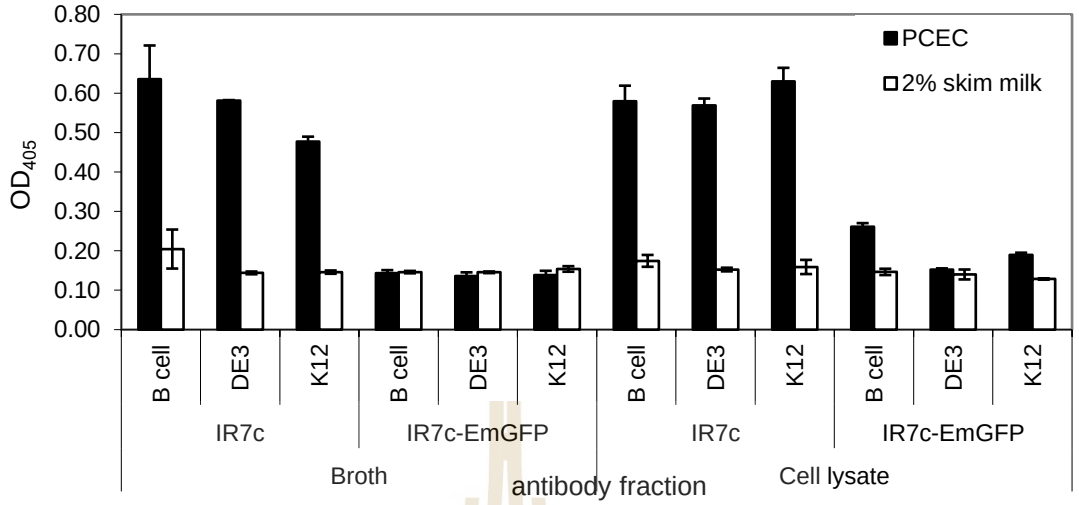

(D)

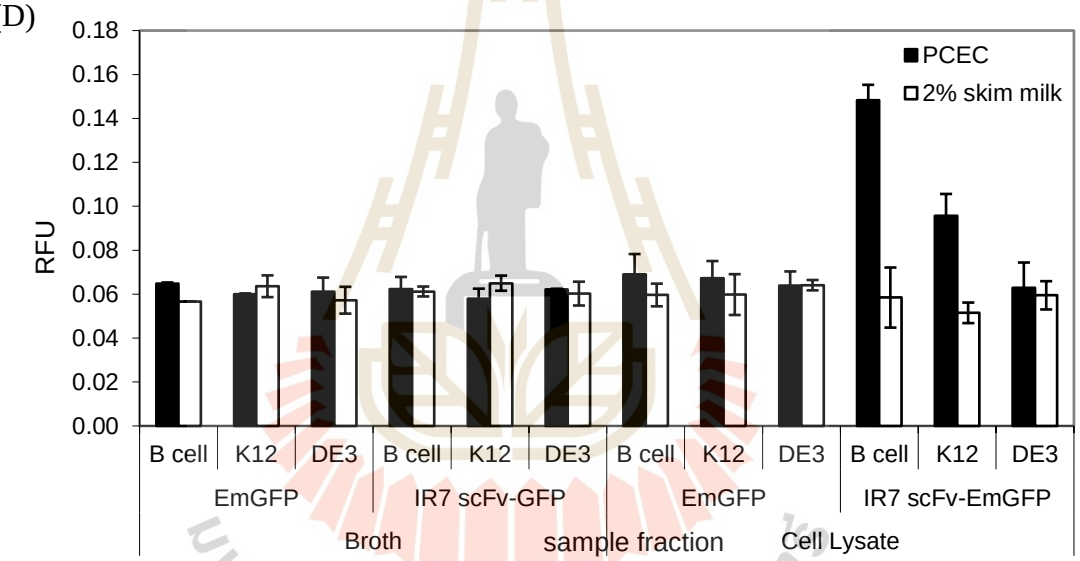

Figure 3.4 (continued).

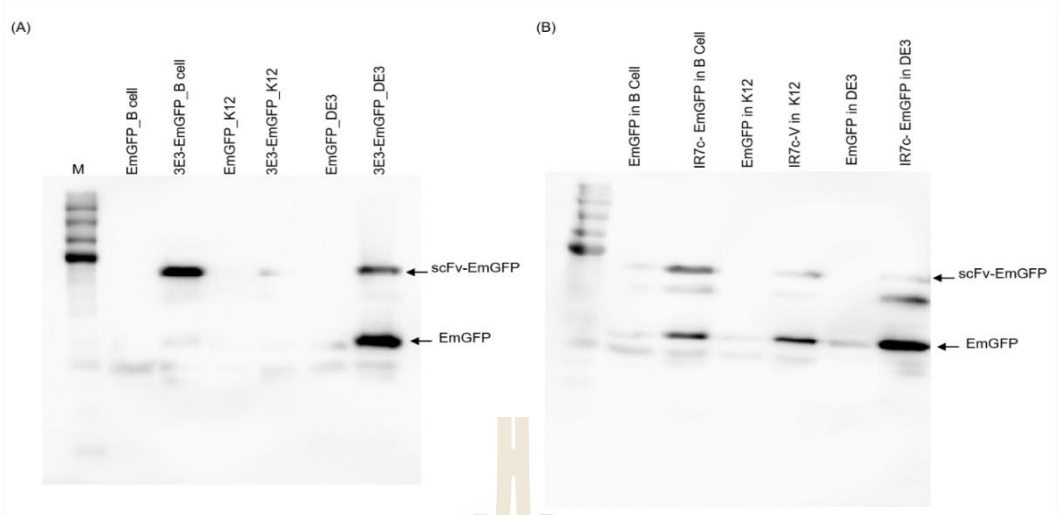

Figure 3.5 Western blot analysis of EmGFP and scFv-EmGFP of of E3E (A) and IR7c (B) Abs from cytoplasmic space. Abs from cell lysate were transferred from 12% SDS-PAGE to PVDF membrane. Then they were probed with HisProbe-HRP conjugate and visualized using Amersham ECL Prime Weatern Bloting Detection Reagent. The Precision plus Protein Standard was used as a protein marker.

3.4.3 Purification of scFv-EmGFP fusion protein

The SHuffle T7 Express strain (*E. coli* C3029 (B cell), which carries cytoplasmic expression of chaperone DsbC in addition to trxB/gor mutations, was chosen further for the expression of scFv-EmGFP fusion of yZA8B2 and IR7c Abs due to it show the highest fluorescent signal of activity biding of scFv-EmGFP fusion of 3E3 and IR7c Abs. After IPTG induction, the fusion Abs were mainly expressed as a soluble protein containing a hexa-histidine tag at the carboxyl terminus in the cytosol of *E. coli* cells. The Abs were purified in one purification step of Ni^{2+} affinity chromatography. The purified scFv-EmGFP fusion Abs of IR7c and yZA8B2 were obtained with a yield of 8.05 mg/L and 5.95 mg/L, respectively. The fusion Ab of IR7c and yZA8B2 Abs appeared to be non-homogeneous, as indicated by SDS-PAGE. The

molecular weight of scFv-EmGFP Abs was approximately 55.5 kDa by SDS-PAGE whereas the molecular mass of EmGFP and scFv was estimated at 26 kDa (Figure 3.6). The specific binding of the purified IR7C-scFv-EmGFP and yZA8B2-scFv-EmGFP Abs (each 20 µg of purified Abs) have still remained comparing to the activity binding of negative control under the same condition (Figure 3.7). In addition, this result indicated that yZA8B2-scFv-EmGFP still bound specific to ZEN conjugated with three proteins when compared to negative control (Figure 3.7).

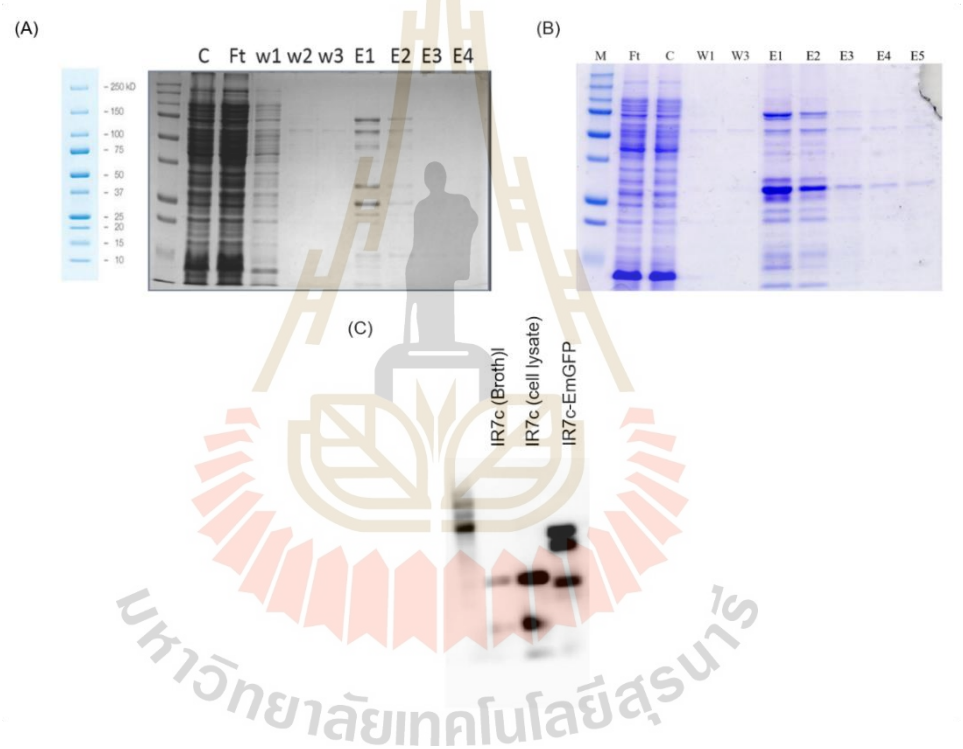

Figure 3.6 SDS-PAGE analysis of purified IR7c-scFv-EmGFP (A) and yZA8B2-scFv -EmGFP (B). Lane M: protein marker (Precision plus Protein Unstained Standards, Biorad), lane C: cell lysate, Ft: flow-through, lane W and E are number of wash and elute fraction of purification step. Western blot analysis of the purified scFv and scFv-EmGFP of IR7c Ab (C). This experiment was performed as previously described on materials ad methods.

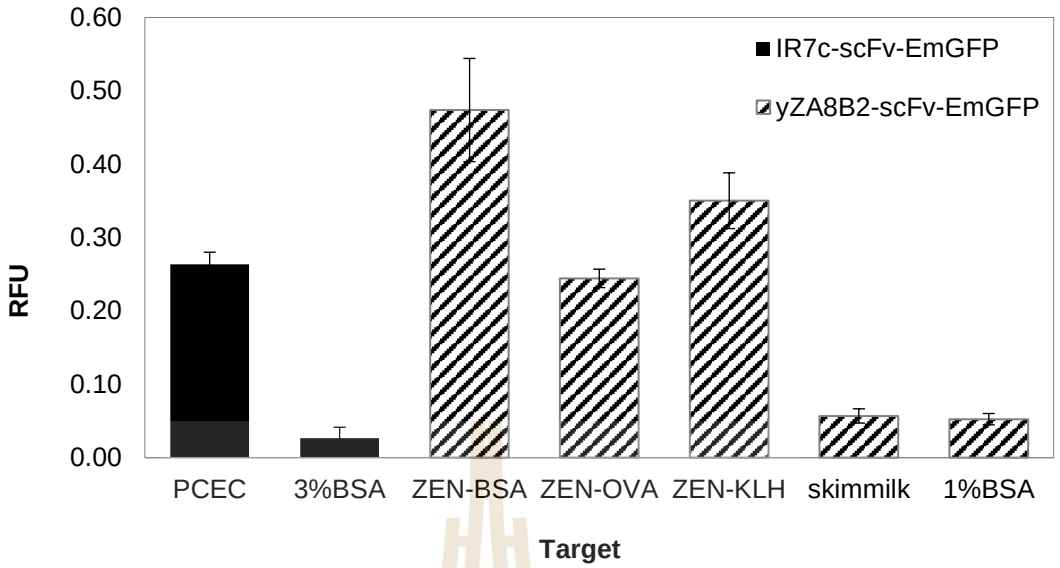

Figure 3.7 Specific binding of scFv-EmGFP of IR7c and yZA8B2 Abs. FLISA of the purified Abs was performed as previously described on materials ad methods. Binding of yZA8B2-scFv-GFP Ab was tested with ZEN-BSA, ZEN-OVA and ZEN-KLH as targets. Negative control is 2% skim milk, 1 and 3 % BSA. The data is expressed as absorbance at excitation peak at 484 nm and an emission peak at 509 nm.

3.4.4 Optimization of FLISA

The optimum ZEN-BSA, ZEN-OVA and ZEN-KLH concentration required for coating onto the microtiter plate, and the best working concentration of the recombinant yZA8B2-scFv-EmGFP was determined using checkerboard titration. In the titration procedure, appropriate concentrations of the coating antigen were prepared with varied concentration per well from 0.5 and 1 µg of ZEN-BSA, ZEN-OVA and ZEN-KLH in 1xPBS. The yZA8B2-scFv-EmGFP fusion protein was serially diluted with 2-fold dilutions from 1:10 to 1:1,280 in 0.05% PBST. A set of experimental parameters including concentration of ZEN-BSA, ZEN-OVA and ZEN-KLH and dilutions of fusion Ab were optimized sequentially to improve the sensitivity of the

immunoassay. The optimal condition was used to test affinities of fusion Abs with free ZEN by competitive FLISA. The result demonstrated that the concentration of 0.5 and 1 µg/well of ZEN-BSA, 1 ug/well of ZEN-OVA and the dilution 1:20 of the fusion Ab were further used for inhibition assay (Figure 3.8).

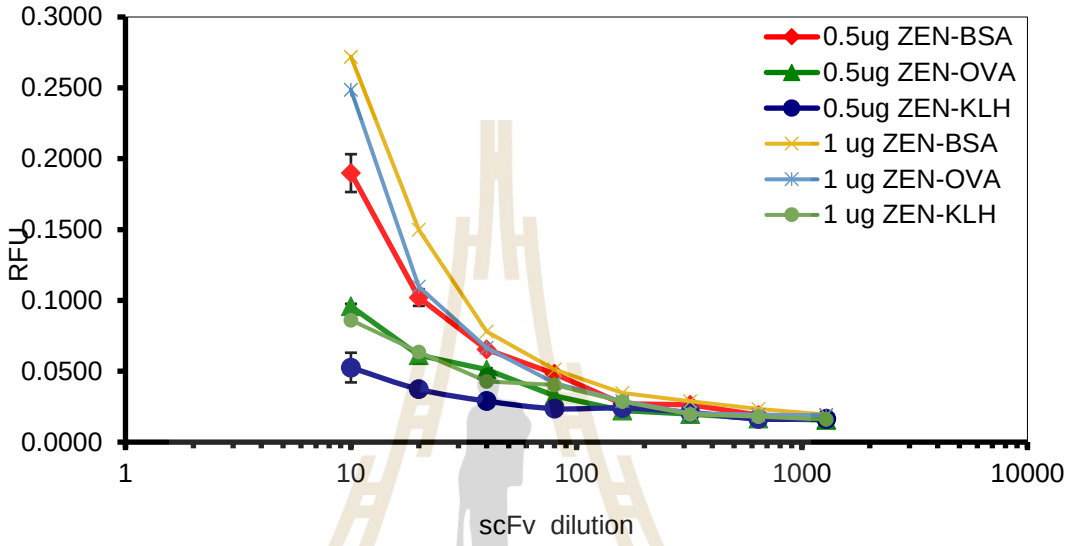

Figure 3.8 Checker broad of yZA8B2-scFv-EmGFP Ab by using ZEN-BSA (A) ZEN-OVA (B) and ZEN-KLH (C) as targets. The best working concentration of the yZA8B2-scFv-EmGFP Ab was determined using checkerboard titration by varying the concentration from 0.5 and 1 µg per well of ZEN-BSA, ZEN-OVA and ZEN-KLH in 100 µL of 1xPBS.

3.4.5 Completive FLISA

To examine the yZA8B2 scFv Ab that can be bound with free ZEN, competitive FLISA was developed and used to determine the sensitivities and specificities of the scFv-EmGFP fusion Ab. The yZA8B2-scFv-EmGFP Ab had binding specific to free ZEN. The IC_{50} of this scFv-GFP was 300 ng/ml and detection limit of this scFv Ab was 100 ng/ml, with a linear range 100 to 5000 ng/ml when used 0.5 µg/well of ZEN conjugated BSA as a target (Figure 3.9).

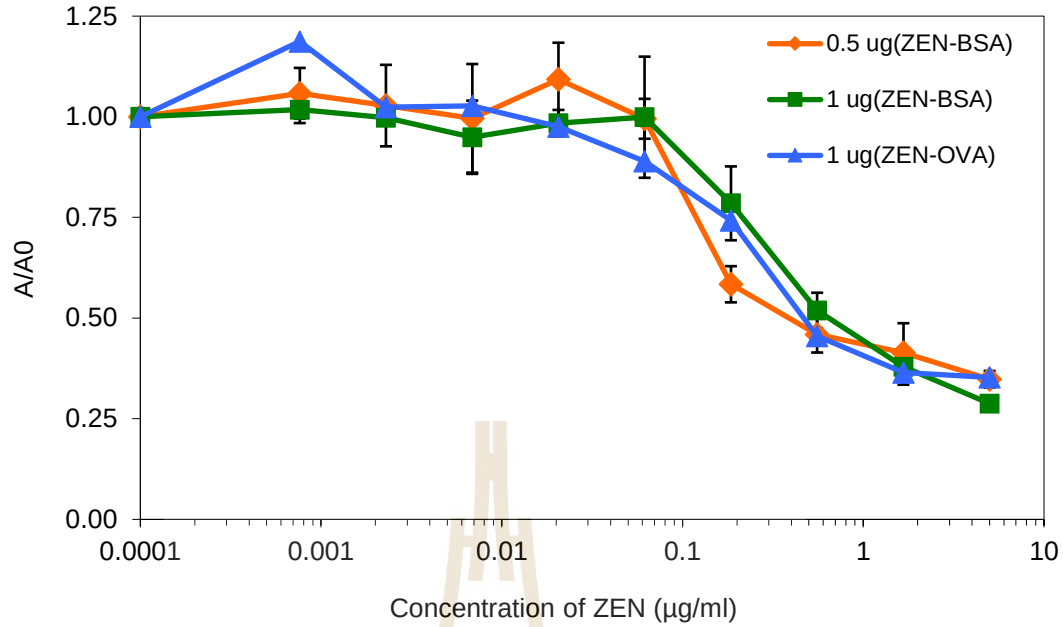

Figure 3.9 Competitive inhibition curves of yAZ8B2-scFv-GFP Ab and ZEN conjugated proteins. 0.5 µg/well of ZEN-BSA (orange line) was used to detect free ZEN by comparison with 1 µg/well of ZEN-BSA (green line) and 1 µg/well of ZEN-OVA (light blue line).

3.5 Discussion

FITC-labeled Ab has been widely utilized in various fields. However, FITC is sensitive to photobleaching (Schots & van der Wolf, 2002). The conjugation reaction of Ab to FITC require a large amount of purified protein, complicated manipulations and several purification steps (Casey et al., 2000). This reaction results in a heterologous mixture of labeled Abs that a different in number and location of bound FITC molecules per Ab (Luria et al., 2012). Also, if the fluorophores conjugate with an antigen-binding site, resulting in a partial or complete loss of reactivity of the Ab (Reimann et al., 1994). In addition, the presence of some fluorophores in close proximity may reduce fluorescence intensity via self-quenching of the fluorescence (Chen & Knutson, 1988). To circumvent these disadvantages, genetic fusion of scFv

and GFP (fluobody) has been constructed and used for diagnosis, immunoassay, immunolabeling of cancer cells, FACS and FLISA (Casey et al., 2000; Hudson & Souriau, 2001; Peipp et al., 2004; Sakamoto et al., 2012; Sakamoto et al., 2014; Schots & van der Wolf, 2002). GFP has been commonly used for monitoring proteins localization in living cells and gene expression (Misteli & Spector, 1997). GFP fusion does not require the fixation or cell permeabilization when GFP is fused to Ab (Cao, Zhang, Zhang, & Wang, 2006; Tsien, 1998) and the scFv-GFP fusion contains a stable GFP tag without interfering the native Ab function (Chalfie, Tu, Euskirchen, Ward, & Prasher, 1994). GFP has much less intrinsic environmental sensitivity than FITC and much less susceptible to self-quenching (Pawley, 2006). Moreover, GFP is more resistant to photobleaching than FITC (Patterson, Knobel, Sharif, Kain, & Piston, 1997). Using of scFv-GFP fusion Ab does not require the purification and any special filter attachment(Casey et al., 2000). Also, direct labelling with can remove background due to non-specific binding of the primary and secondary Abs to target other than the antigen (Wang & Hazelrigg, 1994).

In this study, we have described a rapid and a simple cloning method to construct the fluobodies comprising of scFv liked to EmGFP which can be express a scFv-EmGFP fusion proteins in a 1:1 ratio molecule in cytoplasmic *E. coli*. The fluorescence intensity level of fluobodies (scFv-EmGFP) and EmGFP alone were estimated by florescent microplate reader. Interestingly, no fluorescence intensity was observed for EmGFP alone (pWS-Green) (Figure 3.2 and 3.3). This could be because the start codon was positioned too far from ribosomal binding site of the expression vector, consequently, this has become an advantage of this expression system. Using this expression vector, only the clones that harbor plasmids containing scFv fusion to

EmGFP will show fluorescent signal in the cytoplasm of *E. coli.* Even if the fluorescence intensity was found in *E. coli* DE3 expressing scFv-EmGFP constructs compared to the fluorescence intensity of engineered *E. coli* B cell and K12, the binding signal in FLISA was very low. The reason for this could be explained by western blot analysis (Figure 3.5). As shown Figure 3.5, the biggest band migrated at position of approximately 26 kDa, which is related to the size of EmGFP and scFv alone. These results suggested that the proteolysis occurred in *E. coli* DE3 more than engineered *E. coli* B cell and K12. It has been previously shown that the reducing environment in cytoplasm of no engineered *E. coli* suited correctly folding S-S bonded of GFP (Feilmeier, Iseminger, Schroeder, Webber, & Phillips, 2000). However, the position of Ab fusion (C or N terminal) may affect the fluorescence intensity, the Ab conformational changes and the binding activity of Ab. It was previously reported that cytoplasmic scFv-GFP fusion proteins retained both binding affinity of scFvs to the target molecules and fluorescent properties of GFP (Oelschlaeger, Srikant-Iyer, Lange, Schmitt, & Schmid, 2002; Schwalbach et al., 2000) while periplasmic scFv-GFP showed only fluorescent property of scFv-GFP was not stable in cytoplasmic *E. coli* (Casey et al., 2000). Sakamoto et al. (2012) also reported that fluorescence intensity of scFv-GFP dramatically reduced 600-fold more than GFP-scFv and it is presumed that difference in level of fluorescence intensity is mostly depended on different flexibility of the linker between GFP and scFv. Surprisingly, they also found that scFv-GFP in indirect ELISA showed the binding activity higher than GFP-scFv whereas the binding activity of scFv-GFP in direct ELISA was not detectable. In addition, it has been reported that the expression of human kringle domain (KD) fused to at the N terminus of GFP showed higher level of fluorescence intensity and expression when compared to the fusion at C terminus of GFP (Jeong, Kim, & Jeong, 2014).

The three *E. coli* expression hosts were optimized to accomplish the highest fluorescence intensity. *E. coli* B cell was found to be the best expression host for producing all fluobodies (Figure 3.4). The 3E3-scFv-EmGFP protein from *E. coli* B cell and K12 have retained the binding activity similar to binding activity of scFvs while the binding activity of IR7c-scFv-EmGFP protein in *E. coli* B cell and K12 dramatically decreased 45.2% and 29.0% of the binding activity, respectively, when compared to scFvs protein expressing in the same expression host (Figure 3.4A and C). We also found that the binding activity of 3E3-scFv-EmGFP protein from *E. coli* DE3 reduced the binding activity of about 72.9 %, comparing to scFvs (Figure 3.4A), whereas the binding activity of IR7c-scFv-EmGFP protein in *E. coli* DE3 was completely lost when compared to scFv protein expressing in the same expression host (Fig. 3C and 3D). This suggested that difference of scFv sequence fused to EmGFP and expression host affect to the binding activity of fluobodies differently. It has been previously reported that DNA sequence could affect the level of protein expression and the fluorescent as well as the antigen biding affinity properties of scFv-GFP fusion proteins (Schwalbach et al., 2000). The expression of 3E3-scFv and 3E3-scFv-EmGFP proteins in three expression hosts indicated that 3E3-scFv and 3E3-scFv-EmGFP proteins from *E. coli* B cell and K12 had stronger affinity binding toward target than proteins from *E. coli* DE3 (Figure 3.4A). The same results were observed for IR7c-scFv and IR7c-scFv-EmGFP expressions. The obtained results indicated that the *E. coli* B cell and K12 could improve correctly folding of disulfide bonded proteins in cytoplasm of engineered *E. coli* (Lobstein et al., 2012). It has been reported that the expression of KD fused to at the N terminus or C terminus of GFP in *E. coli* Shuffle (B cell) express didn't affect the fluorescent properties of GFP and the antigen biding

properties of KD (Jeong et al., 2014). In addition, we have also found that the binding activity of IR7c-scFv proteins from three *E. coli* showed higher the binding activity than IR7c-scFv-EmGFP proteins (Figure 3.4A). This result indicated that the EmGFP led to the conformational changes and consequently, the binding activity of IR7c-scFv Abs (Zhang et al., 2014).

The Ni^{2+} affinity chromatography was not able to purify the fluobodies to be homogeneous and fragmentation of fusion proteins were observed by SDS-PAGE. Similar results have been reported previously for the fluobodies purification (Griep, van Twisk, van der Wolf, & Schots, 1999; Oelschlaeger et al., 2002). However, we also demonstrated that the crude and the partial purified fluobodies could be used for ELISA, FLISA and competitive FLISA immunoassays which are reliable and time-saving techniques without purification step. Cell lysates of the fluobodies were analyzed for proteolysis by western blotting. Free EmGFP in the cytoplasmic *E. coli* was observed, indicating that the fluobodies may be cleaved by some enzymes in the cytoplasm. Proteolysis of the fluobody has previously been reported (Casey et al., 2000).

The partial purified fluobodies showed the binding reactivity to immobilized targets after purification. This is the first report of yZA8B2-scFv-EmGFP expression in *E. coli* SHuffle T7 Express (B cell) for application in FLISA immunoassay. The yZA8B2-scFv-EmGFP fusion protein is able to inhibit the free ZEN by competitive FLISA. The IC_{50} value was approximately 3-fold higher than competitive ELISA using scFv (data not shown). This result indicates that yZA8B2-scFv-EmGFP affect the binding reactivity of yZA8B2-scFv. This differed from N-fluoKD which could not

detect the signal of fluorescent in FLISA and competitive FLISA (Sakamoto et al., 2012; Sakamoto, Tanizaki, Pongkitwitoon, Tanaka, & Morimoto, 2011).

Compared with conventional ELISA, the FLISA technique does not use the secondary Ab and toxic substrates for the enzyme horseradish peroxidase (HRP). Therefore, this method reduces assay time, cost and labor by the removal a secondary reaction and limitation of the enzyme reaction. Furthermore, the competitive FLISA is not amplified the signal by conjugated secondary Ab and the enzyme reaction, which may enhance accuracy in quantitative analysis (Casey et al., 2000; Jeong et al., 2014; Oelschlaeger et al., 2002; Sakamoto et al., 2012; Sakamoto et al., 2011).

3.6 Conclusion

We have successfully developed an efficient expression system suitable for production of fluobodies, using a cloning method that facilitates the identification of correct construct. The efficacy of this system is shown via an application for detection of rabies virus and mycotoxins. This scFv-EmGFP expression system has potential to be used for both quantitative and qualitative analysis of various analytes.

3.7 References

Bird, R., Hardman, K., Jacobson, J., Johnson, S., Kaufman, B., Lee, S., Lee, T., Pope, S., Riordan, G., & Whitlow, M. (1988). Single-chain antigen-binding proteins. *Science, 242*(4877), 423-426.

Bradford, M. M. (1976). A rapid and sensitive method for the quantitation of microgram quantities of protein utilizing the principle of protein-dye binding. *Analytical Biochemistry, 72*, 248-254.

Cao, P., Zhang, S., Zhang, J., & Wang, M. (2006). Construction and characterization of a bi-functional EGFP/sBAFF fusion protein. *Biochimie, 88*(6), 629-635.

Casey, J. L., Coley, A. M., Tilley, L. M., & Foley, M. (2000). Green fluorescent antibodies: novel in vitro tools. *Protein Engineering, 13*(6), 445-452.

Chalfie, M., Tu, Y., Euskirchen, G., Ward, W. W., & Prasher, D. C. (1994). Green fluorescent protein as a marker for gene expression. *Science, 263*(5148), 802-805.

Chen, R. F., & Knutson, J. R. (1988). Mechanism of fluorescence concentration quenching of carboxyfluorescein in liposomes: energy transfer to nonfluorescent dimers. *Analytical Biochemistry, 172*(1), 61-77.

Feilmeier, B. J., Iseminger, G., Schroeder, D., Webber, H., & Phillips, G. J. (2000). Green fluorescent protein functions as a reporter for protein localization in *Escherichia coli*. *Journal of Bacteriology, 182*(14), 4068-4076.

Ferrara, F., Listwan, P., Waldo, G. S., & Bradbury, A. R. M. (2011). Fluorescent labeling of antibody fragments using split GFP. *PLOS One, 6*(10), e25727.

Frenzel, A., Hust, M., & Schirrmann, T. (2013). Expression of recombinant antibodies. *Frontiers in Immunology, 4*, 217.

Gerdes, H.-H., & Kaether, C. (1996). Green fluorescent protein: applications in cell biology. *FEBS Letters, 389*(1), 44-47.

Griep, R. A., van Twisk, C., van der Wolf, J. M., & Schots, A. (1999). Fluobodies: green fluorescent single-chain Fv fusion proteins. *Journal of Immunological Methods, 230*(1), 121-130.

Griffiths, A. D., & Duncan, A. R. (1998). Strategies for selection of antibodies by phage display. *Current Opinion in Biotechnology, 9*(1), 102-108.

Hermanson, G. T. (2008). Chapter 9 - Fluorescent probes. In *Bioconjugate Techniques (Second Edition)* (pp. 396-497). New York: Academic Press.

Holmes, K. L., & Lantz, L. M. (2001). Chapter 9 Protein labeling with fluorescent probes. In *Methods in Cell Biology* (Vol. 63, pp. 185-204): Academic Press.

Hudson, P. J., & Souriau, C. (2001). Recombinant antibodies for cancer diagnosis and therapy. *Expert Opinion on Biological Therapy*, *1*(5), 845-855.

Jeong, G. M., Kim, Y. S., & Jeong, K. J. (2014). A human kringle domain-based fluorescence-linked immunosorbent assay system. *Analytical Biochemistry*, *451*, 63-68.

Laemmli, U. K. (1970). Cleavage of structural proteins during the assembly of the head of bacteriophage T4. *Nature, 227*, 680.

Lobstein, J., Emrich, C. A., Jeans, C., Faulkner, M., Riggs, P., & Berkmen, M. (2012). SHuffle, a novel *Escherichia coli* protein expression strain capable of correctly folding disulfide bonded proteins in its cytoplasm. *Microbial cell factories, 11*, 56.

Luria, Y., Raichlin, D., & Benhar, I. (2012). Fluorescent IgG fusion proteins made in *E. coli*. *Monoclonal Antibodies*, *4*(3), 373-384.

Misteli, T., & Spector, D. L. (1997). Applications of the green fluorescent protein in cell biology and biotechnology. *Nature Biotechnology, 15*(10), 961-964.

Nogales-Gadea, G., Saxena, A., Hoffmann, C., Hounjet, J., Coenen, D., Molenaar, P., Losen, M., & Martinez-Martinez, P. (2015). Generation of recombinant human IgG monoclonal antibodies from immortalized sorted B cells. *Journal of Visualized Experiments*(100), e52830.

Oelschlaeger, P., Srikant-Iyer, S., Lange, S., Schmitt, J., & Schmid, R. D. (2002). Fluorophor-linked immunosorbent assay: a time- and cost-saving method for the characterization of antibody fragments using a fusion protein of a single-

chain antibody fragment and enhanced green fluorescent protein. *Analytical Biochemistry, 309*(1), 27-34.

Olichon, A., & Surrey, T. (2007). Selection of genetically encoded fluorescent single domain antibodies engineered for efficient expression in *Escherichia coli*. *Journal of Biological Chemistry, 282*(50), 36314-36320.

Patterson, G. H., Knobel, S. M., Sharif, W. D., Kain, S. R., & Piston, D. W. (1997). Use of the green fluorescent protein and its mutants in quantitative fluorescence microscopy. *Biophysical Journal, 73*(5), 2782-2790.

Pawley, J. B. (2006). *Handbook of biological confocal microscopy* (3rd ed. ed.): New York (N.Y.) : Springer.

Peipp, M., Saul, D., Barbin, K., Bruenke, J., Zunino, S. J., Niederweis, M., & Fey, G. H. (2004). Efficient eukaryotic expression of fluorescent scFv fusion proteins directed against CD antigens for FACS applications. *Journal of Immunological Methods, 285*(2), 265-280.

Pruksametanan, N., Yamabhai, M., & Khawplod, P. (2012, 4-7 Nov. 2012). *Selection of single chain human monoclonal antibody (scFv) against rabies virus by phage display technology.* Paper presented at the 2012 IEEE 6th International Conference on Nano/Molecular Medicine and Engineering (NANOMED).

Rangnoi, K., Jaruseranee, N., O'Kennedy, R., Pansri, P., & Yamabhai, M. (2011). One-step detection of aflatoxin-B1 using scFv-alkaline phosphatase-fusion selected from human phage display antibody library. *Molecular Biotechnology, 49*(3), 240-249.

Reimann, K. A., Waite, B. C., Lee-Parritz, D. E., Lin, W., Uchanska-Ziegler, B., O'Connell, M. J., & Letvin, N. L. (1994). Use of human leukocyte-specific

monoclonal antibodies for clinically immunophenotyping lymphocytes of rhesus monkeys. *Cytometry, 17*(1), 102-108.

Sakamoto, S., Pongkitwitoon, B., Nakahara, H., Shibata, O., Shoyama, Y., Tanaka, H., & Morimoto, S. (2012). Fluobodies against bioactive natural products and their application in fluorescence-linked immunosorbent assay. *Antibodies, 1*(2), 239-258.

Sakamoto, S., Shoyama, Y., Tanaka, H., & Morimoto, S. (2014). Application of green fluorescent protein in immunoassays. *Advances in Bioscience and Biotechnology, 5*(6), 7.

Sakamoto, S., Tanizaki, Y., Pongkitwitoon, B., Tanaka, H., & Morimoto, S. (2011). A chimera of green fluorescent protein with single chain variable fragment antibody against ginsenosides for fluorescence-linked immunosorbent assay. *Protein Expression and Purification, 77*(1), 124-130.

Schots, A., & van der Wolf, J. M. (2002). Green fluorescent protein fluobody immunosensors. Immunofluorescence with GFP-antibody fusion proteins. *Methods in Molecular Biology, 183*, 265-273.

Schwalbach, G., Sibler, A.-P., Choulier, L., Deryckère, F., & Weiss, E. (2000). Production of fluorescent single-chain antibody fragments in *Escherichia coli*. *Protein Expression and Purification, 18*(2), 121-132.

Tsien, R. Y. (1998). The green fluorescent protein. *Annual Review of Biochemistry, 67*, 509-544.

Wang, S., & Hazelrigg, T. (1994). Implications for bcd mRNA localization from spatial distribution of exu protein in *Drosophila oogenesis*. *Nature, 369*(6479), 400-403.

Zhang, F., Moniz, H. A., Walcott, B., Moremen, K. W., Wang, L., & Linhardt, R. J. (2014). Probing the impact of GFP tagging on Robo1-heparin interaction. *Glycoconjugate Journal, 31*(4), 299-307.

CHAPTER IV

CODON AND SIGNAL PEPTIDE OPTIMIZATION FOR THERAPEUTIC ANTIBODY PRODUCTION IN CHINESE HAMSTER OVARY (CHO) CELL

4.1 Abstract

Therapeutic Abs are one of the most promising biopharmaceuticals or biologics for targeted-therapy of various diseases. Recent expiration of different patents as well as emerging of infectious diseases have made the demand for cost-effective production of therapeutic antibodies (Abs) critical for equal healthcare access of the world population. Chinese Hamster Ovary (CHO) cells are the most widely used cell line for the manufacturing of biologics. While the amino acid sequences of therapeutic Abs have become accessible after patent expiration, signal peptides (SPs) and algorithm of codon optimization for efficient production of therapeutic Abs from CHO cells are mostly unknown. Therefore, in this study, we sought to compare the effects of different optimized codons and various SPs on the productivity of therapeutic Abs, expressed from monocistronic expression vectors from transiently transfected CHO cells. To compare the algorithm of codon optimization, Adalimumab was used as a model of the study. The light chain (LC) and heavy chain (HC) of human IgG1 of Adalimumab genes were codon-optimized and synthesized from GeneArt (GA, Adali_GA) and GenSript (GS, Adali_GS). While the yield and q_p of genes from GA was higher, the

mRNA expression level of both HC and LC derived from both GA and GS showed no significant difference. Subsequently, various combinations of SPs fused to the codon-optimized HC and LC of Adalimumab and Trastuzumab were evaluated for secretory production efficiency. The results indicated that different Ab required different combinations of SP for optimal production, which are different from previous reports. In this study, we observed that the best SP combinations for HC and LC of Adalimumab are SpSH and SpB, while for Trastuzumab the SpB is the most suitable for both HC and LC. The binding property of the produced Abs was confirmed by ELISA against target antigens and the ratio of HC and LC was validated by flow cytometry.

Keywords : Codon optimization; Signal peptide; Chinese Hamster Ovary (CHO) cells; Biologic/biopharmaceutical; Antibody production

4.2 Introduction

Biologics or biopharmaceuticals are medicines generated using biotechnology from living cells for therapeutic and diagnostic purposes (U.S. Food and Drug Administration, 2012), which are very complex and expensive. It has been predicted that worldwide biologics market will reach nearly USD 400 billion by 2025 (Ecker, Jones, & Levine, 2015). Amongst these, the sale of mAbs is expected to lead the market. mAbs dominated the market with largest revenue share due to higher usage of this category of drugs in different therapeutics areas including uncurbable diseases such as cancer and immune disorders. Most importantly, mAb is the type of drugs most suitable for precision medicine, which is the future of medicine in the 21st century (Garattini & Padula, 2019). The expiration of the patents and/or data protection for the first major group of originator's biotherapeutic including therapeutic Abs is expected to contribute to increased access to these products at an affordable price (World Health

Organization, 2019). Biosimilars is highly similar to, and has no clinically meaningful differences in safety, purity, and potency (safety and effectiveness) from an existing FDA-approved reference product, but product development cost is much cheaper than the originator products (Ventola, 2013). It has been estimated that biosimilar sales will potentially triple in size to $15 billion by 2020, or closely thereafter (Ying, Jennifer, Jennifer, & Jorge, 2018). Since a large number of companies are interested to begin investing in these drug medicals (Calo-Fernandez & Martinez-Hurtado, 2012), the possibility for larger population of patients, especially those living in low to middle income countries to get access of these types of drug have been increasing. However, currently the price of biosimilars are still relatively high and the accessibility is still limited.

The growing significance of biologics has resulted in the development of technologies for high quality and productivity in different types of expression systems (Tripathi & Shrivastava, 2019). Among mammalian cell lines, Chinese hamster ovary (CHO) are the most commonly used system for the manufacturing of biopharmaceutical because they can secrete high levels of the recombinant protein and provide a human-like glycosylation pattern with least concerns for immunogenic modifications (Zhu, 2012).

Gene expression levels of mammalian cells involve multiple parameters including codon, gene copy number, the chromosomal integration site of gene, transcriptional regulation, mRNA processing and stability, tRNA abundance, translation efficiency and SPs (Feng et al., 1999; Hung et al., 2010; Kanaya, Yamada, Kinouchi, Kudo, & Ikemura, 2001; Ou et al., 2014; You et al., 2018). The design of heterologous gene for recombinant expression has been identified as a bottleneck at

translation of protein and thus recognizes a key issue that necessaries to be solved to achieve high levels of gene expression. The expression vectors are often a key to success in production efficiency. They contain strong promoters (e.g., CMV or hybrid promoter CMV-EF1α) to drive the gene expression (Shukurov et al., 2014), Kozak sequence to help the translation of mRNA (Kozak, 1987), intron sequence to support the processing and splicing pathway of mRNA (Rose & Beliakoff, 2000), poly(A) tail and 3'untranslated regions (UTR) to increase the stability of mRNA (Wu & Brewer, 2012; You et al., 2018) that have been evaluated and revealed enhancing the protein expression. Codon optimization has been commonly used to improve the heterologous gene expression by using codon preference (codon usage bias) that are optimized in a particular host (Gustafsson, Govindarajan, & Minshull, 2004; Novoa & Ribas de Pouplana, 2012). The codon adaptation index (CAI) is commonly used to measure of the synonymous codon usage bias for a gene sequence in a certain organism (Sharp & Li, 1987). The synonymous codon substitution of target protein with higher tRNA abundances results in highly translation efficiency and lower missense error rates (Shah & Gilchrist, 2010). In addition, codon optimization also involve in different aspects of gene expression to improve yield in various expression systems, such as GC content adjustment that affect the mRNA levels and the mRNA stability lead to enhancement of transcription and translation (Cho et al., 2019; Fath et al., 2011; Graf, Deml, & Wagner, 2004; Hung et al., 2010; Khan, 2013; You et al., 2018), mRNA structure changing result in increasing its translation (Gu, Zhou, & Wilke, 2010; Kim, Lee, & Kim, 2010), high level expression by removing rare codons (Barnes, Bentley, & Dickson, 2004; Makoff, Oxer, Romanos, Fairweather, & Ballantine, 1989) and eliminate the cryptic polyadenylation signals result in the full-length mRNA production

(Tokuoka et al., 2008). It also can affect protein folding in eukaryotic expression systems (Zhao, Yu, & Liu, 2017). Previous studies have shown that the production of recombinant Abs in CHO cells can be achieve success by codon optimization (Cho et al., 2019; Hung et al., 2010; Ou et al., 2014; Shukurov et al., 2014; You et al., 2018).

Another way to increase the protein yield is the secretion of protein by SPs. It is known that a protein secretion in the eukaryotic cell is translocated into the endoplasmic reticulum (ER) before transport into the Golgi complex achieving by a SP. The SP is cleaved off by signal peptidase on the luminal side of the ER membrane (Blobel, 1980). However, SPs are identified as a limiting step in the classical secretory pathway. Therefore, the selection of appropriate SP is an important issue for improving the efficiency of protein secretion. Previous reported have been indicated that SPs are extremely heterogeneous and SPs are functionally interchangeable even between different species (Kober, Zehe, & Bode, 2013; von Heijne, 1985). Recent studies have demonstrated that the recombinant Ab secretion in CHO cells can be increased by different SPs (Haryadi et al., 2015; Tole et al., 2009; You et al., 2018).

In this research, the effects of different optimized codons and various SPs on the productivity of two biosimilar therapeutic Ab, i.e., Adalimumab and Trastuzumab are reported. The knowledge obtained from this research will be useful to help expedite the development of biosimilar and biologics production platforms, resulting in a more affordable price for wider accessibility in the future.

4.3 Material and Methods

4.3.1 Codon optimization and vector construction for Ab production

The amino acid sequences of Adalimumab (Accession Number DB00051) and Trastuzumab (Accession Number DB00072) were obtained from the DrugBank

database. The codons of genes encoding variable and constant regions of the recombinant Ab Adalimumab were optimized using the GeneOptimizer™ (GeneArt, Thermo Fisher Scientific, USA) and OptimumGene™ (GenScript, USA) software. The codons for the SP were optimized using the OptimumGene™ algorithm. A detailed diagram for the constructions of all recombinant plasmids in this study is explained in Figure 4.1.

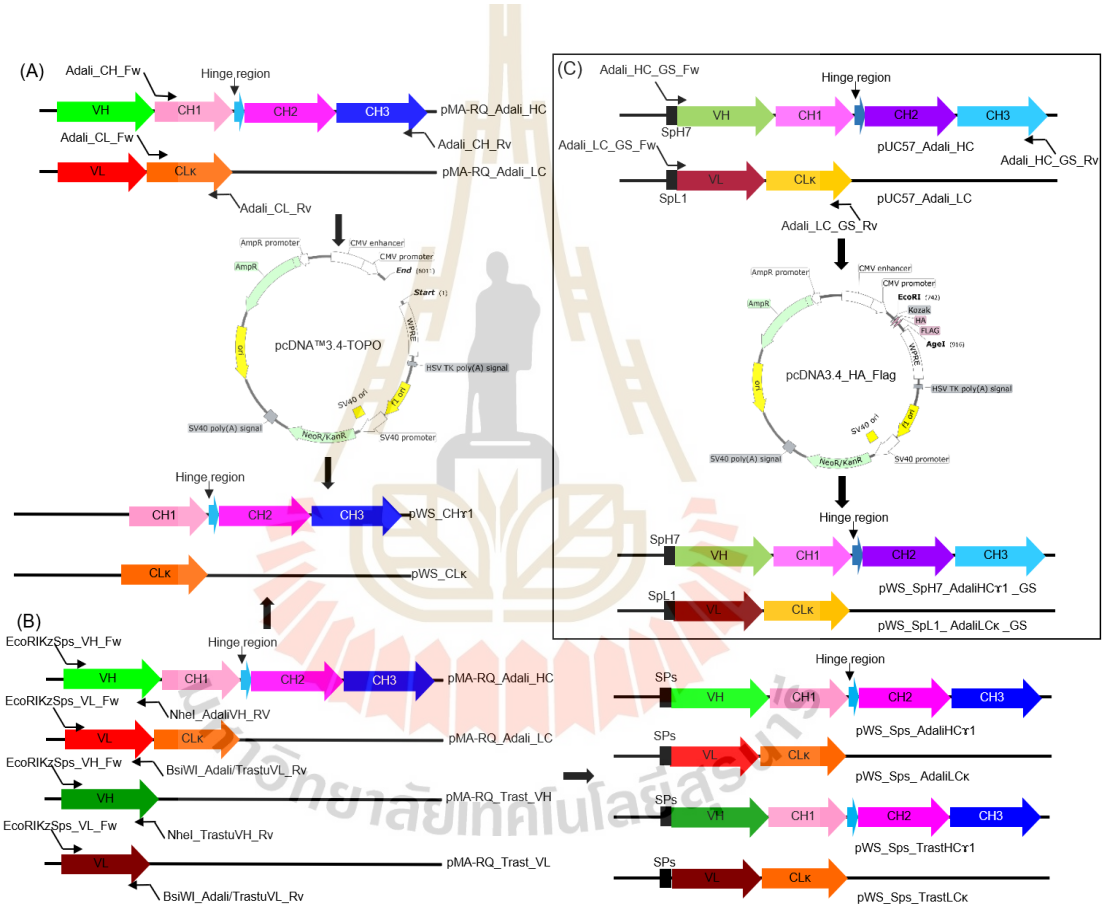

Figure 4.1 Overview of the methods for the constructions of all recombinant plasmids used in this study. (A) The vector expressing heavy (pWS_HC) and light (pWS_LC) chain of Ab was constructed based on pcDNA3.4 TOPO vector (Thermo Fisher Scientific, USA). The heavy chain (VH-CH_{IgG1}) and light chain (VL-CLκ) genes were codon optimized and synthesized by GA algorithm in the pMA-RQ plasmid. The genes were amplified by PCR

using Platinum *Pfx* DNA Polymerase (Thermo Fisher Scientific, USA) and appropriate primer pairs as indicated in Table 4.1. Then, the amplified products were inserted into the pcDNA3.4 TOPO vector. The integrity of the constructs was confirmed by automated DNA sequencing (Macrogen, Korea). (B) In the next step, the variable domain (V_H for the heavy chain and V_L for the light chain) of two Abs were cloned into pWS_CH and pWS_CL vectors, respectively by PCR cloning. The PCR primers contained kozak sequence (GCCACCATGG/A) (Kozak, 1987) (Kozak, 1987) followed by three different SPs for each V_H and V_L as indicated in Table 4.1. Three amplified fragments of V_H and V_L for each Ab were digested with restriction enzymes and ligated into pWS_CH and pWS_CL, cut with corresponding enzymes, respectively. These resulted in the expression vector with different SPs i.e., pWS_Sps_AdaliHC, pWS_Sps_TrastHC, pWS_Sps_AdaliLCκ and pWS_Sps_TrastLCκ, encoding different SPs linked with the optimized HC and LC of Adalimumab and Trastuzumab, respectively. The genes were fused with 3' WPRE (woodchuck posttranscriptional regulatory element) to enhance transcript expression. The constructs are under the control of human cytomegalovirus (CMV) immediate-early promoter/enhancer for high level gene expression in CHO cells. The DNA sequence of the constructs was confirmed by automated DNA sequencing. (C) To generate the constructs for the comparison of codon optimization by different vendors (GA and GS), the pcDNA3.4 TOPO vector was modified to contain certain restriction enzymes, HA, and Flag epitopes (designed pcDNA3.4_ HA_Flag) for further amplification and use. Then, the codon optimized HC

and LC genes of Adalimumab containing H7 and L1 SPs, respectively, synthesized by GS, were amplified by PCR using primers as indicated in Table 4.1. The primers contained *EcoR*I and kozak sequence at 5' and *Age*I restriction site at 3'end. The amplified fragments were digested with corresponding restriction enzymes and ligated into digested pcDNA3.4_HA_Flag vector. These resulted in the pWS_SpH7_AdaliHC_ GS and pWS_SpL1_AdaliLCκ _GS recombinant vectors. The integrity of the constructs was confirmed by automated DNA sequencing.

4.3.2 DNA sequence and RNA structure analysis

Plasmids containing HC or LC were prepared using a plasmid purification kit as suggested by the manufacturer (MiniPrep; Qiagen, USA). Automated DNA sequencing was performed by Macrogen (Korea) or Eurofins (Austria) using the specific primers as indicated in Table S1. The DNA sequences were analyzed with SnapGene version 4.2.6 (GSL Biotech). The RNA structures were analyzed by the Quikfold program (RNA 3.0; http://unafold.rna.albany.edu/?q=DINAMelt/Quickfold). The codon usage bias of codon-optimized Adalimumab from GA and GS was determined based on the tRNA genes of the CHO-K1 in genomic tRNA database (http://gtrnadb.ucsc.edu/genomes/eukaryota/Cgris1/).

Table 4.1 The primers for cloning and RT-qPCR used in this study.

Primer	Sequence (5'--->3')
Adali_CH_Fw	5' gaattcgtatacgctagcACCAAGGGACCCTCTGTGTTTC 3'
Adali_CH_Rv	5' TCATTTGCCGGGGCTCAGAGAC 3'
Adali_CL_Fw	5' gaattcgctagccgtacgGTGGCCGCTCCTTCCGTGTTC 3'
Adali_CL_Rv	5' TCAGCACTCGCCCCGGTTGAAAG 3'
EcoRIKzSpB_Adali/TrastuVH_Fw	5'ctgtgcgaattcgccaccatgaagtgggtgaccttcatctctctgctgttcctgttttccagcgcctactccGAAGTGCAGCTGGTTGAATCTGGC 3'
EcoRIKzSpH7_AdaliVH_Fw	5'ctgtgcgaattcgccaccatggagttcggcctgtcctgggtgttcctggtggccctgtttaggggcgtgcagtgcGAAGTGCAGCTGGTTGAATCTGGC 3'
EcoRIKzSpSH_Adali/TrastuVH_Fw	5'ctgtgcgaattcgccaccatgggagagctgttattactgctgctgctgggcctgaggctccagctgtccctgggcatcGAAGTGCAGCTGGTTGAATCTGGC 3'
EcoRISKzSpH5_TrastuVH_Fw	5'ctgtgcgaattcgccaccatggactggacctggaggttcctgtttgtggtggccgctgccacaggcgtgcagtccGAAGTGCAGCTGGTTGAATCTGGC 3'
NheI_AdaliVH_RV	5' gcacaggctagcAGATGACACTGTGACCAGGGTGCC 3'
NheI_TrastuVH_Rv	5' gcacaggctagcAGATGACACTGTGACCAGGGTGCCCTGG 3'
EcoRIKzSpB_Adali/TrastuVL_Fw	5'ctgtgcgaattcgccaccatgaagtgggtgaccttcatctctctgctgttcctgttttccagcgcctactccGACATCCAGATGACCCAGTCTCC 3'
EcoRIKzSpL1_Adali/TrastuVL_Fw	5'ctgtgcgaattcgccaccatggacatgagggtgcccgctcagctgctgggcctgctgctgctgtggctgtccggcgctcggtgcGACATCCAGATGACCCAGTCTCC 3'
EcoRIKzSpSH_Adali/TrastuVL_Fw	5'ctgtgcgaattcgccaccatgggagagctgttattactgctgctgctgggcctgaggctccagctgtccctgggcatcGACATCCAGATGACCCAGTCTCC 3'
BsiWI_Adali/TrastuVL_Rv	5' gcacagcgtacgCTTGATTTCCACCTTGGTGCCCTG 3'
Adali_LC_GS_Fw	5' ctgtgcgaattcgccaccATGGACATGCGGGTG 3'
Adali_LC_GS_Rv	5' gcacagaccggtTCAACACTCGCCCCGGTTGAAAG 3'
Adali_HC_GS_Fw	5' ctgtgcgaattcgccaccATGGAGTTCGGCCTG 3'
Adali_HC_GS_Rv	5' gcacagaccggtTCACTTGCCAGGGCTCAGGGAC 3'
qPCR_Adali_VH_Fw	5' GCTCCTATCGAAAAGACCATC 3'

Capital letters are binding to specific genes.

Table 4.1 (continued).

Primer	Sequence (5'--->3')
qPCR_Adali_VH_Rv	5' CTGGTTCTTGGTCAGCTC 3'
qPCR_Adali_VL_GA_Fw	5' TCTTCCCACCTTCCGACGAG 3'
qPCR_Adali_VL_GA_Rv	5' GACTGCAGAGCGTTGTCCAC 3'
qPCR_Adali_VL_GS_Fw	5' TCTTTCCCCCTAGCGACGAG 3'
qPCR_Adali_VL_GS_Rv	5' CTCTGGAGGGCGTTATCCAC 3'
qPCR_GAPDH_Fw	5' AACTTTGGCATTGTGGAAGG 3'
qPCR_GAPDH_Rv	5' ACACGTTGGGGGTAGGAACA 3'

Capital letters are binding to specific genes.

4.3.3 Cell lines and cell culture

CHO-S (cGMP Banked, Cat. No. A13696-01), was purchased from Thermo Fisher Scientific (USA). CHO-S and CHO-K1 were maintained in CD-CHO medium (Thermo Fisher Scientific) supplemented with 8 mM L-Glutamine (L-Gln; Thermo Fisher Scientific, USA) and 0.2% Anti-Clumping Agent (Thermo Fisher Scientific, USA). Cells were grown in TubeSpin Bioreactors 50 mL (TPP Techno Plastic Products, Switzerland) with a working volume of 15 mL medium. The cells were incubated at 37°C, 7% CO_2, and humidified air at a shaking speed of 250 rpm (standard condition). The cells were passaged twice a week with a seeding density of $2x10^5$ viable cells per mL. The cell cultures were mixed with trypan blue and counted by a ViCELL XR Cell Counter (Beckman Coulter, Germany) for viable cell density (VCD) and viability.

4.3.4 Cell transfection

For transient expression of recombinant Ab, appropriate expression vectors were transiently transfected into CHO-S or CHO-K1 cells by nucleofection according to a previously published protocol (Schmieder et al., 2018). In brief, $5x\ 10^6$ viable cells were electroporated with 10 µg of circular plasmid DNA using a Neon Nucleofector device and the 100 µL Neon Transfection Kit (Thermo Fisher Scientific, USA) with 1,700 V, 20 ms and 1 pulse. The transfected cells were transferred into 50 mL TubeSpin Bioreactors containing pre-warmed 15 mL medium and held in a static incubator at 37°C, 7% CO_2 and humidified air for 2 h. After that the transfected cells were cultured under standard condition. To check the transfection efficiency, the pcDNA3.4 plasmid bearing an emerald green gluorescent protein gene (EmGFP), designated pWS-EmGFP, was transfected in parallel. After 24h, the transfection efficiencies were

determined on a CytoFLEX S flow cytometer with a 488 nm excitation laser and 525/40 BP filter for emission signals (Beckman Coulter, Germany) to evaluate the percentage of EmGFP-expressing cells.

4.3.5 Intracellular staining

The Ab-expressing CHO cells were stained following a previously published protocol (Pichler, Galosy, Mott, & Borth, 2011). The cells expressing the HC and LC genes of the Ab were stained with anti-human IgG (γ-chain specific) Ab labelled with R-Phycoerythrin (Cat. No. P9170, Sigma–Aldrich, USA) and anti-human kappa light chain Ab labelled with FITC (Cat. No. F3761, Sigma–Aldrich, USA), respectively. The fluorescent signal intensity was measured using the CytoFLEX S flow cytometer (Beckman Coulter, Germany) using a 488nm laser with a 525/40 BP filter for FITC and a 561 nm laser with a 585/42 BP filter for PE detection, and the data were analysed using the CytExpert 2.4.0.28 software program (Beckman Coulter). The experiments were performed in duplicates.

4.3.6 Determination of mRNA expression by RT-qPCR

The total RNA was isolated from $1x10^6$ viable cells using the Direct-zol RNA Kit (Zymo Research, USA) with DNase treatment, following the manufacturer's instructions. RNA (800 ng) was converted to cDNA using a high-capacity cDNA reverse transcription kit with RNase inhibitor (Applied Biosystems, USA), according to the manufacturer's instructions. For quantitative PCRs (qPCRs), one microliter of the 4x diluted cDNA was used as a template in a 10 μL reaction using the SensiFAST SYBR Hi-ROX Kit (Bioline, UK). Samples were measured in quadruplicates on a Rotor-Gene qPCR cycler (Qiagen, Germany) with conditions as previously described (Nguyen et al., 2019). The primer pairs specific for CHO, i.e., GAPDH (glyceraldeyde-

3-phoshate dehydrogenase), constant domains of heavy (CH) and light (CL) chain genes of the two mAbs Adalimumab and Trastuzumab are listed in Table S1. Relative quantification of mRNA expression levels was normalized to GAPDH for calculation of fold change (FC) using the $2^{-\Delta\Delta C}{}_T$ method (Livak & Schmittgen, 2001).

4.3.7 Titer and cell-specific productivity (q_p)

The Ab titre of the transfectants was determined from cell supernatant 3 days post transfection by the Octet RED96e (ForteBio, USA) with protein A probes, using human IgG1 Trastuzumab as a standard. To assess the q_p (pg/cell/day) of cells, the viable cell density and Ab titer were evaluated and q_p was calculated as previously described (Meleady et al., 2011).

4.3.8 Purification of secreted Abs

After 3 days of cultivation, the supernatants of transfected cells containing the expressed mAb were harvested by centrifugation at 200 xg for 10 min at 4°C. The mAbs were purified as previously described (Bydlinski et al., 2018) with some modifications. For each sample, the clear supernatant was applied directly into Pierce Protein A agarose beads (Thermo Fisher Scientific, USA) in a 15 mL tube, pre-equilibrated with nuclease free water and phosphate-buffer saline (PBS). The mixture was incubated overnight by head-to-head rotation at 4°C. The beads were centrifuged at 500 xg for 2 min and washed five times with PBS. Finally, the mAb was eluted with 0.1 M glycine-HCl pH 2.7 and neutralized with 1 M Tris-HCl pH 9.0. The elution fractions were electrophoresed with 4-15% Mini-Protein TGX PreCast Gels (Biorad, USA). Protein bands were visualized by staining with Problue safe stain (Giotto Biotech, Italy). The protein standard PageRuler Plus (Thermo Fisher Scientific, USA) was used as a molecular weight marker. Fractions containing mAb were pooled and

exchanged into PBS buffer by ultrafiltration using a membrane with a 30 kDa cutoff (Millipore, USA). The sample was collected and kept at 4ºC. The concentration of the purified protein was determined by Octet RED96e using protein A probe.

4.3.9 Assessment of the binding activity by Enzyme-Linked Immunosorbent Assay (ELISA)

The binding activities of mAbs were confirmed by ELISA. A 96-well flat bottom ELISA maxisorp plate (Nunc, Thermo Fisher Scientific, USA) was coated with 1 µg of human HER2/ErbB2 protein (Sino Biological, USA) or 1 µg of human TNF-α (GenScript, USA) in a coating buffer (0.1 M Sodium-bicarbonate ($NaHCO_3$), pH 9.6) to test the binding of Trastuzumab or Adalimumab, respectively. In this experiment, 1% BSA was used as a negative control. After incubation at 4°C overnight, the plate was washed three times with PBS and blocked with blocking buffer (PBS containing 2% BSA) at room temperature for 1 h. The plate was then washed three times with PBS before 1 µg of corresponding Ab was added to each well. After incubation at 37ºC for 1 h, the wells were washed three times with 1xPBS containing 0.05% Tween 20 (PBST) and twice with PBS. To detect the bound mAb, 100 µL of goat anti-IgG human HRP (1:200 in blocking buffer, Thermo Fisher Scientific, USA) were added into each well and incubated at 37ºC for 1 h. After further washing, the color reactions were developed using OPD (*o*-Phenylenediamine dihydrochloride) peroxidase substrate (Sigma, USA) containing 0.018% H_2O_2. The plate was kept at room temperature in the dark for 10 min to allow color development. Then, the reactions were stopped by adding 100 µL of 3 M H_2SO_4 per well. The OD was measured by a TECAN Infinite M200 microplate reader (TECAN, Austria) at 492 nm. The assay was performed in triplicates.

4.3.10 Statistical analysis

Data were obtained from at least two independent experiments. All quantitative data are represented as mean ± standard deviations and were analyzed with the GraphPad Prism 8 software using Student's *t*-test or one-way ANOVA followed by Dunnett's test ($P < 0.05$) as mentioned in each experiment.

4.4 Results and discussion

4.4.1 Comparison of optimized codon for Adalimumab

To examine the effect of different codon optimization algorithms on recombinant Ab expression in CHO cells, the HC and LC genes encoding Adalimumab were optimized and synthesized by the Optimizer™ (GeneArt, GA) and Optimum GeneTM (GenScript, GS) algorithms, according to codon usage in Chinese hamster (*Cricetulus griseus*) as described in Materials and Methods. These algorithms take into account a variety of critical parameters involved in different aspects of Ab expression, such as GC content, mRNA structure, cryptic splicing sites and various cis-elements in transcription and translation. The amino acid sequences of the resulting optimized genes are identical. The Adalimumab synthetic genes were labeled as "Adali_GA" or "Adali_GS", according to the respective gene synthesis company. DNA sequence analysis revealed that the optimized HC and LC genes from GA and GS had a sequence identity relative to each other at 84.96% and 86.36%, respectively (Figure 4.2). CpG dinucleotides were avoided because recent research has shown that apart from codon optimization, intragenic CpG depletion increases transcriptional activity and protein expression in mammalian cells (Bauer et al., 2010).

Figure 4.2 DNA sequence alignment of GA and GS optimized genes. (A) Alignment of HC; AdaliHC_GA and AdaliHC_GS. (B) Alignment of LC; AdaliLC_GA and AdaliLC_GS. The dot indicates the identical nucleotides. Different domains are indicated as lines of different colors.

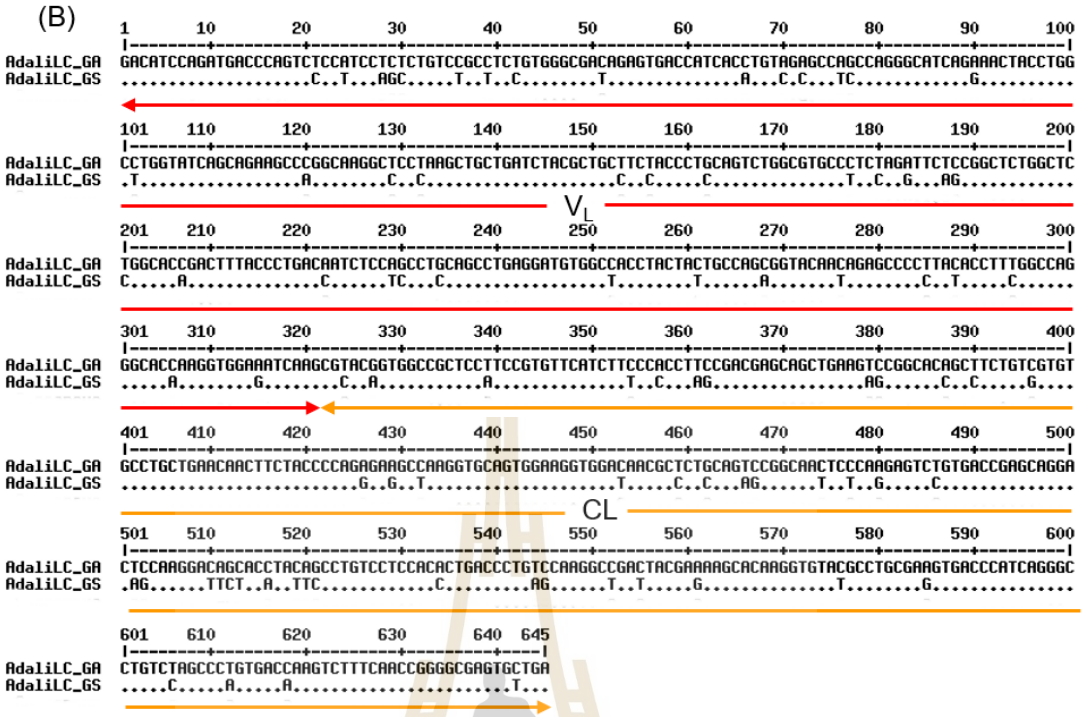

Figure 4.2 (continued).

The codon adaptation index (CAI), which is commonly used to analyze the codon usage bias for a gene sequence and can be used to predict the level of expression of a gene based on its codon sequence, was calculated. Optimized genes showing a higher CAI value have been suggested to increase the gene expression rate in CHO cells (Sharp & Li, 1987). From our analysis, the CAI of HC and LC from GA were 0.94 and 0.96, respectively, while those of HC and LC from GS were similar at 0.96. The GC content was also adjusted to enhance the transcriptional and translational efficiency and promote RNA stability. The average GC content of HCs/LCs for Adali_GA and Adali_GS was approximately 57.58% / 58.36%, and 58.56% / 59.48%, respectively (Figure 4.3A and B). In addition, the quality value, of which 100 is set for the codon with the highest usage frequency for a given amino acid in the desired expression organism, was also calculated. While the quality value in the 91-100 range for the HC sequences from both GA and GS showed 83%, those for the LC genes from

were 89% and 85%, respectively (Figure 4.3). In summary, as judged by CAI and GC content, the sequences optimized by GS had a slightly higher score.

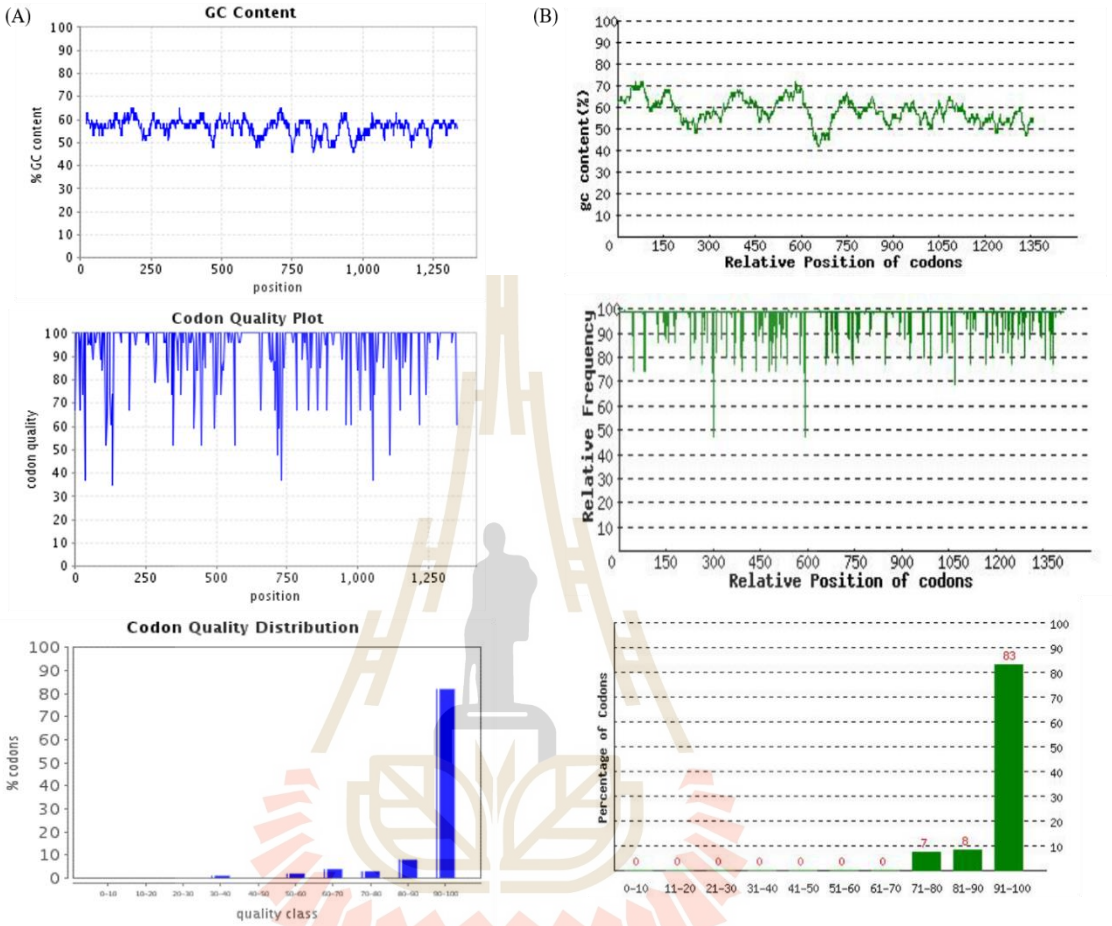

Figure 4.3 Analysis of codon usage bias. (A) The HC optimized by GeneOptimizer™ software from GeneArt (GA). (B) The HC optimized by OptimumGene™ algorithm from Genscript (GS). (C) The LC optimized by GeneOptimizer™ software from GeneArt (GA). (D) The HC optimized by OptimumGene™ algorithm from Genscript (GS).

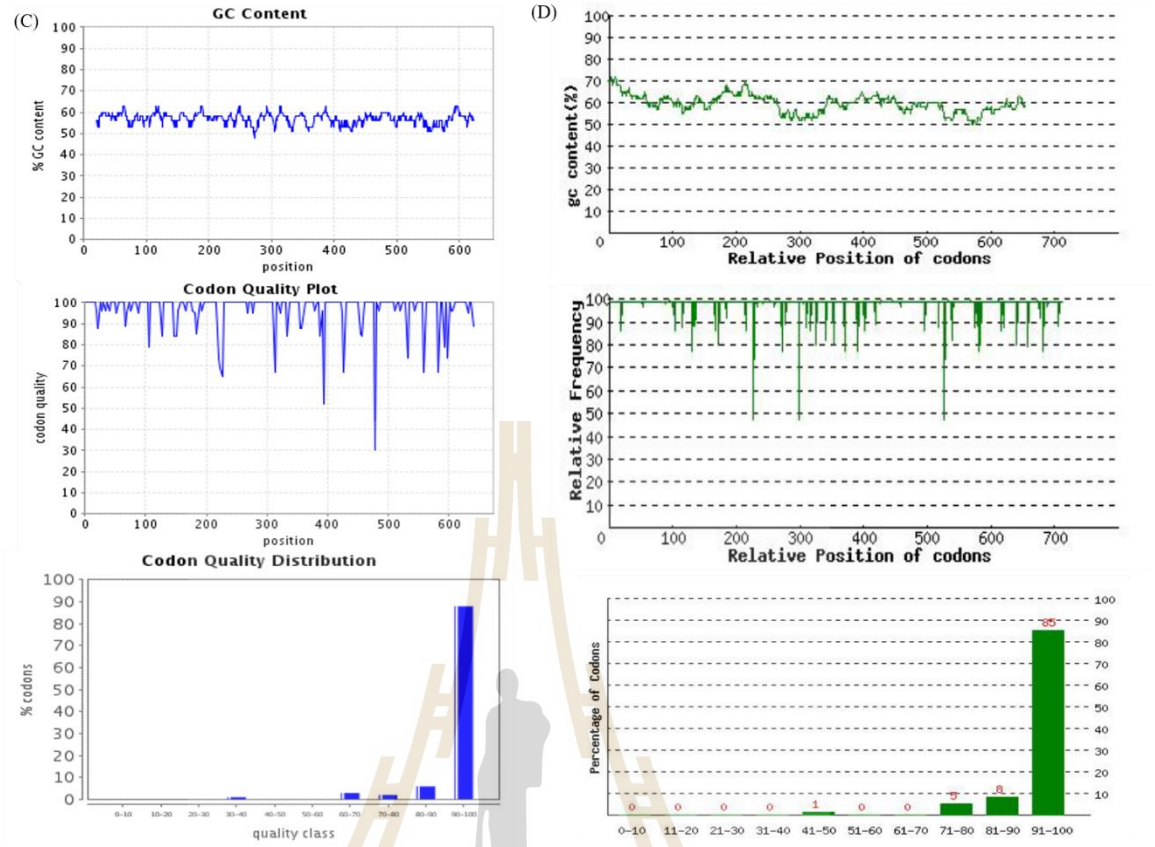

Figure 4.3 (continued).

4.4.2 The effect of codon optimization algorithm on the expression of Adalimumab from CHO-K1

The map of the expression vectors used for the comparison of the effect of codon optimization on the level of expression of Adalimumab from CHO-K1 cell is shown in Figure 4.4 The optimized genes were under the control of a CMV promoter/enhancer with 5’ Kozak and 3’ Woodchuck Hepatitis Virus (WHP) Posttranscriptional Regulatory Element (WPRE). The latter is a DNA sequence which, when transcribed, creates a tertiary structure that can enhance gene expression. The sequence is commonly used in molecular biology to increase expression of genes delivered by viral vectors (Lee, Glover, Cosgrave, Bienemann, & Uney, 2005). Previous studies have shown that the Kozak sequence is the most common 5’ UTR that

can enhance translation (Kozak, 1987) (Kozak, 1987; Lopez-Lastra, Rivas, & Barria, 2005), while WPRE can significantly increase mRNA stability, enhancing post-transcriptional processing and protein yield when used as the 3' UTR of a mammalian expression cassette (Donello, Loeb, & Hope, 1998; Klein et al., 2006). The full-length human CMV promoter has been shown to enhance the levels of protein expression in transient transfections in CHO cells (Xia et al., 2006). The selected SPs for HC and LC of Adalimumab genes in this study were H7 and LI, respectively, based on previous publication (Haryadi et al., 2015).

CHO-K1 cells were transiently co-transfected with the expression vectors containing the optimized GA or GS genes at a 1:1 molar ratio. The transient gene expression (TGE) systems have been used to quickly assess many parameters for producing Abs at an early stage of product development. (Cachianes et al., 1993; Codamo, Munro, Hughes, Song, & Gray, 2011). After 24 h, flow cytometry analysis indicated that the transfection efficiency was approximately 65.91%-68.59%. After 3 days, CHO-K1 cells co-transfected with vectors bearing the Adali_GA genes showed significantly higher level of secreted Adalimumab (Figure 4.5A) as well as cell-specific productivity (qp) (Figure 4.5B) compared to those transfected with constructs bearing the Adali_GS genes. Moreover, evaluation of viable cell density, viability, and size (Figure 4.5C-E) also showed that cells transfected with expression vectors bearing genes synthesized with the GA algorithm could grow faster, as apparent by the approx. 2-fold higher cell density, and the slightly higher % viability and size. These results indicated that codon optimization using the GA algorithm generates transcripts that can be efficiently translated in CHO-K1 cells. Further, the level of transcription of the codon optimized genes by GA and GS was evaluated 3 days after transient transfection

by RT-qPCR using GAPDH as a reference. Interestingly, despite the fact that the GA genes lead to higher Ab production, the mRNA level of both GA and GS optimized genes were the same. Significant differences were only observed between mRNA expression from heavy and light chain, where the mRNA from LC was significantly higher than that of HC for both GA and GS (Figure 4.5F).

Taken together, these results indicate that the higher productivity achieved by the codon optimized sequence from GA was not due to higher gene expression from the promoter or the increase in the half-life of the mRNA. Rather, the translation process of genes optimized by GA seemed to be more efficient resulting in a higher cell specific productivity. Recent results have shown that rare codons play an important role in reducing translational speed and thus assisting with proper folding of the nascent protein (Brule & Grayhack, 2017). Too rapid translation by use of the most frequent codons may thus well result in misfolded proteins causing unfolded protein response and stress. The fact that cells transfected with the GA gene variant grew to higher cell density seems to indicate such stress with the cells transfected with the GS sequence. A welcome side effect of the higher growth was a concomitant increase in total titer reached.

Contradictory results of codon optimization on the expression level of recombinant proteins have been reported. In some cases, the codon optimization could not improve the yield (Fath et al., 2011; Kim et al., 2010; Kudla, Murray, Tollervey, & Plotkin, 2009), but frequently gene optimization and GC content were shown to affect both the mRNA level and stability, so that Ab expression could be enhanced (Cho et al., 2019; Fath et al., 2011; Graf et al., 2004; Hung et al., 2010; Khan, 2013; You et al., 2018). In this study, the mRNA level was not affected, but the yields were improved.

Analysis of mRNA folding energy (ΔG) related to the secondary structure of the entire mRNA showed that the ΔG of HC from Adali_GA and Adali_GS were approximately -487.4 and -524.7 kcal/mol; while those of LC from Adali_GA and Adali_GS were -225.0 and -232.5 kcal/mol, respectively. These values could also explain the higher productivity of mRNA transcribed from Adali_GA, because weaker RNA folding have been shown to correlate with higher levels of protein expression (Jia & Li, 2005; Kim et al., 2010).

Analysis of codon usage indicated that Adali-GA codons targeted more abundant cognate tRNAs than those of Adali_GS (Table 4.2), leading to maximized translation rates (Cannarozzi et al., 2010; Ou et al., 2014; Parmley & Huynen, 2009). Compared to Adali_GS, Adali_GA also used different codons that encode the same amino acid, i.e., for Glu, Gly, Lys, Gln, Ser and Val. Generation of high codon concentration to a subset of the tRNA population could lead to an imbalance in the available tRNA pool, which may result in decreased growth rate due to tRNA depletion and increasing translational error. These considerations could explain why the growth rate of CHO cells expressing Adali_GS, was much lower than that of cells expressing Adali-GA (Gong, Gong, & Yanofsky, 2006; Plotkin & Kudla, 2011).

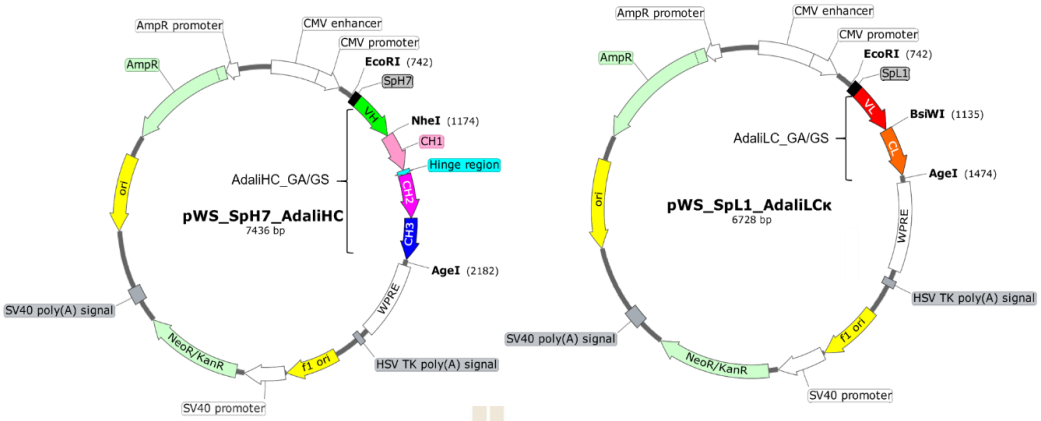

Figure 4.4 Map of constructs for the comparison of codon optimization algorithms. The map of vectors expressing HC (pWS_SpH7_AdaliHC), containing H7 SP, and LC (pWS_SpL1_AdaliLCκ), containing L1 SP of Adalimumab are illustrated. The genes were optimized by GA or GS algorithms. All genes were under the control of the CMV enhancer and promoter, WPRE indicated Woodchuck Hepatitis Virus (WHP) Posttranscriptional Regulatory Element. HSV TK poly (A) signal at the C-terminus is the terminator sequence for the stability of mRNA. The vector carries the gene for ampicillin resistance (Amp^R) for the selection and maintenance of the plasmid. Neomycin resistance gene is used for selection of stable cell lines with Geneticin. The pUC origin is for high copy number and maintenance of the plasmid in *E. coli*.

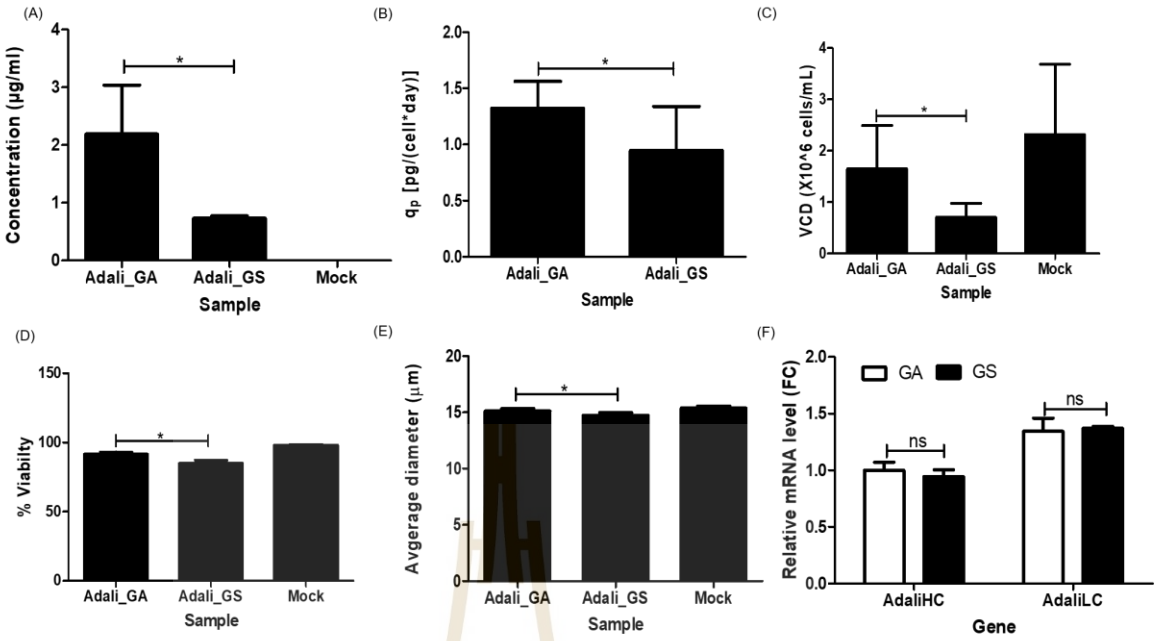

Figure 4.5 The effects of codon optimization algorithm on Adalimumab expression. CHO K1 cells were transfected with vectors containing Adalimumab genes optimized by GA (Adali_GA) and GS (Adali_GS), or empty vectors (Mock), as described in the materials and methods. (A): concentration of Ab secreted into culture supernatant; (B): q_p; (C): VCD; (D): cell viability; (E) cell size; (F): relative mRNA expression normalized with GAPDH. All values represent mean ± S.D. of two independent experiments. The date analysis was performed with Paired t-test. "*" indicates a statistically significant difference ($p<0.05$).

Table 4.2 Comparison of tRNA gene copy number and codon usage bias in *C. griseus* of the genes of Adalimumab codon-optimized with GA and GS.

no	amino acid	number of amino acid		codon	codon number				codon usage bias	anti-codon	tRNA Count
		HC	LC		HC		LC				
					GA	GS	GA	GS			
1	Ala (A)	24	15	GCT	8	12	6	7	22.40	AGC	18
				GCC	16	12	9	8	25.90	GGC	0
2	Cys (C)	11	5	TGT	4	6	1	2	9.10	ACA	0
				TGC	7	5	4	3	10.30	GCA	34
3	Asp(D)	20	9	GAC	12	12	8	4	28.10	GTC	12
				GAT	8	8	1	5	24.60	ATC	0
4	Glu, E	22	9	GAA	13	1	4	0	28.40	TTC	7
				GAG	9	21	5	9	41.10	CTC	10
5	Phe (F)	13	7	TTC	9	6	5	5	22.00	GAA	7
				TTT	4	7	2	2	19.60	AAA	0
6	Gly (G)	29	13	GGA	6	6	0	0	15.80	TCC	4
				GGC	22	23	13	13	21.30	GCC	12
				GGT	1	0	0	0	12.80	ACC	0
7	His (H)	11	2	CAC	10	6	1	1	12.90	GTG	11
				CAT	1	5	1	1	10.20	ATG	0
8	Ile(I)	8	7	ATC	8	8	7	7	24.80	GAT	0
9	Lys (K)	31	13	AAG	27	31	13	13	38.40	CTT	56
				AAA	4	0	0	0	24.60	TTT	10
10	Leu (L)	37	15	CTG	33	35	15	12	38.80	CAG	9
				CTC	2	2	0	3	18.40	GAG	0
				TTG	2	0	0	0	14.10	CAA	4
11	iMet/Met (M	4	1	ATG	4	4	1	1	23.00	CAT	14
12	Asn (N)	19	7	AAC	14	11	7	5	21.20	GTT	15
				AAT	5	8	0	2	17.40	ATT	0
13	Pro (P)	33	11	CCA	6	9	2	3	15.60	TGG	6
				CCC	6	14	3	4	17.00	GGG	0
				CCT	21	10	6	4	16.70	AGG	6
14	Gln (Q)	16	15	CAA	1	0	1	0	10.30	TTG	5
				CAG	15	16	14	15	33.40	CTG	11
15	Arg (R)	12	9	AGA	7	3	6	2	10.10	TCT	4
				AGG	1	4	0	4	10.20	CCT	4
				CGA	1	0	0	0	7.20	TCG	5
				CGG	3	2	2	1	10.10	CCG	3
				CGC	0	3	0	2	9.30	GCG	0
				CGT	0	0	1	0	5.60	ACG	7
16	Ser (S)	55	30	AGC	7	15	5	8	16.40	GCT	9
				TCA	2	0	0	0	10.30	TGA	3
				TCC	28	26	13	15	16.50	GGA	0
				TCT	18	14	12	7	16.00	AGA	7
17	Thr (T)	33	18	ACA	5	14	3	6	15.70	TGT	4
				ACC	28	19	14	12	20.30	GGT	0
				ACG	0	0	1	0	4.50	CGT	4
18	Val (V)	45	15	GTC	4	0	1	0	15.70	GAC	0
				GTG	39	45	14	15	30.10	CAC	9
				GTT	2	0	0	0	11.60	AAC	13
19	Trp (W)	9	2	TGG	9	9	2	2	13.10	CCA	6
20	Try (Y)	19	11	TAC	18	11	10	6	16.40	GTA	11
				TAT	1	8	1	5	13.10	ATA	0
21	STOP	1	1	TGA	1	1	1	1	1.20	TCA	0

4.4.3 Identification of optimal SP combinations for the expression of Adalimumab and Trastuzumab

SPs are amino acid residues at the N-terminus of a protein targeting the nascent polypeptide chains to the lumen of the ER, from where it is transported further to the Golgi apparatus and subsequently to the culture supernatant. These are the rate-limiting steps in the classical secretory pathway (Blobel, 1980). It has been shown that SP functionality is replaceable between different species (Stern, Olsen, Trösse, Ravneberg, & Pryme, 2007). Previous reports have shown that optimization of SP could help to produce maximal quantities of recombinant proteins in a mammalian cell and that different Abs require different combinations of SPs for HC and LC. (Cho et al., 2019; Haryadi et al., 2015; Kober et al., 2013). To identify optimal combinations of SPs for the secretion of two bestselling therapeutic Abs; i.e., Adalimumab and Trastuzumab, we have searched several published studies (as listed in Table 4.3) that suggested the best candidate SPs for HC and LC of these two Ab. Five promising SPs were selected and fused with the two Ab genes, codon optimized by GA, and cloned into the monocistronic expression vector for transient expression in CHO-S, an efficient expression host for rapid and high-yield production of recombinant Ab (Takeshi, Masayoshi, & Wook-Dong, 2010).

A diagram of all SPs tested in this study are shown in Figure 4.6A. For HC, three different SPs (SH, B and H7) and (SH, B and H5) were tested for Adalimumab and Trastuzumab, respectively. The SP H7 and H5 were chosen based on previous report on the optimization of HC and LC SPs for high level expression of therapeutic Abs in CHO-K1 cells (Haryadi et al., 2015). For LC, three different SPs (SH, B and

L1) were tested for both. Thus, a total of 9 combinations for each Ab were investigated by duplicate transfections for each pair of HC and LC combination. On day 3 after transfection, the Ab concentrations in the culture supernatant and number of cells were determined. As demonstrated in Figure 4.6B and C, the choice of SP combinations clearly affected the resulting Ab titer. While SpH7_HC+SpSH_LC pair was the worst combination for Adalimumab, SpL1 was the least efficient SP for a light chain for Trastuzumab (Figure 4.6D and 6E). These results are similar to a previous study (Cho et al., 2019). To confirm the best SP pair for each Ab, the top 6 SP pairs for each were selected. As shown in Figure 4.7A-D, analysis of both relative yield and cell-specific productivity (q_p) indicated that the best SP combination for production are SpSH_HC+SpB_LC for Adalimumab and SpB_HC+SpB_LC for Trastuzumab, respectively. Most importantly, flow cytometry analysis by intracellular staining of HC and LC demonstrated equal distribution of heavy and light chain in more than 99% of cells expressing either Ab, when the best SP combination pair were tested (Figure 4.7E).

These optimal combinations are different from previous reports using the same Abs (Haryadi et al., 2015; Kober et al., 2013; Tole et al., 2009; You et al., 2018). However, there is some consistency, for example, in these previous reports the human serum albumin preproprotein (SpB) SP was also the best SP for specific productivity across different Abs (Kober et al., 2013). This observation holds true for Trastuzumab in this study. However, for Adalimumab, the best combination was SpSH_HC+SpB_ LC, where the SP SH, an optimized SP for recombinant Ab secretion (Tole et al., 2009), was more efficient for HC production. These results confirmed previous observation that the variable domains of mAb can affect the secretion of Ab, and that different mAb

require different combinations of SP for optimal expression in CHO cells (Haryadi et al., 2015). They also stress the importance of individually testing available SP-product gene combinations for each new product, for instance using a pipeline as demonstrated in this study.

Table 4.3 Amino acid and DNA sequence* of SP used in this study.

SP	Optimized DNA sequence	Amino acid sequence	Protein	Reference
B	MKWVTFISLLF LFSSAYS	ATGAAGTGGGTGACCTTCATCTCTCTGC TGTTCCTGTTTTCCAGCGCCTACTCC	Human Serum albumin preproprotein	(Kober et al., 2013)
SH	MGELLLLLLLG LRLQLSLGI	ATGGGAGAGCTGTTATTACTGCTGCTGC TGGGCCTGAGGCTCCAGCTGTCCCTGGG CATC	Human Ig	NRC,USA)and(Tole et al., 2009)
H7	MEFGLSWVFL VALFRGVQC	ATGGAGTTCGGCCTGTCCTGGGTGTTCC TGGTGGCCCTGTTTAGGGGCGTGCAGTG C	Human Ig HC	(Haryadi et al., 2015)
H5	MDWTWRFLFV VAAATGVQS	ATGGACTGGACCTGGAGGTTCCTGTTTG TGGTGGCCGCTGCCACAGGCGTGCAGTC C	Human Ig HC	(Haryadi et al., 2015)
L1	MDMRVPAQLL GLLLLWLSGA RC	ATGGACATGAGGGTGCCCGCTCAGCTG CTGGGCCTGCTGCTGCTGTGGCTGTCCG GCGCTCGGTGC	Human Ig LC	(Haryadi et al., 2015)

*The DNA sequences were optimized by OptimumGene^{TM} algorithm from GS.

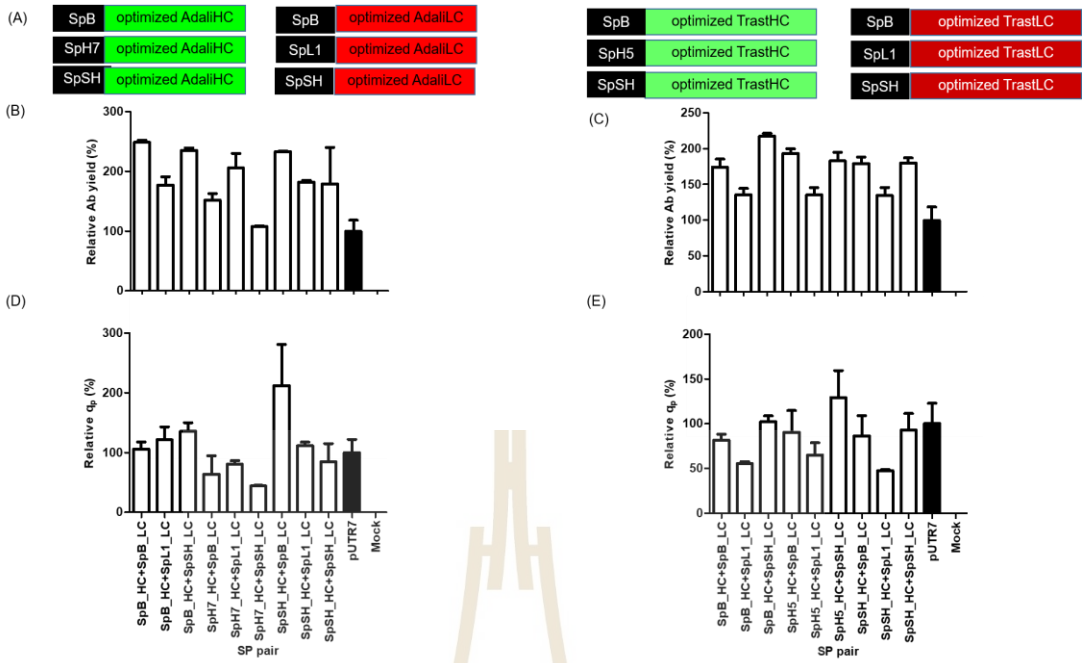

Figure 4.6 The effects of SP pairs on the secretory production of Adalimumab and Trastuzumab. Nine constructs of selected SPs fused with HC and LC of Adalimumab (AdaliHC/LC) and Trastuzumab (TrastHC/LC), optimized by GA, were generated and depicted in (A). CHO-S cells were transiently co-transfected with a total of 9 combinations for each Ab. Duplicate transfections for each pair of HC and LC combination were done. The Ab concentrations of Adalimumab and Trastuzumab (C) in the culture supernatant were determined on 3 days after post-transfection. q_p for Adalimumab (D) and Trastuzumab (E) are shown in the bottom panel. All values are normalized to a control vector pUT7, which was set as 100%.

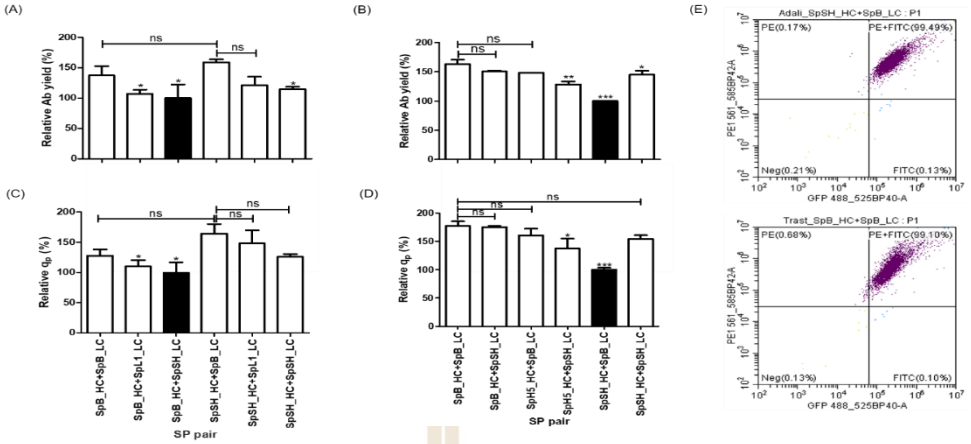

Figure 4.7 Identification of an optimal SP pair for the production of Adalimumab and Trastuzumab. The Ab concentrations of Adalimumab (A) and Trastuzumab (B) in the culture supernatant were determined on 3 days after post-transfection. The q_p of Adalimumab (C) and Trastuzumab (D) was also determined. The pUT7 vector was used in the experiments as a control to ensure the reproducibility of the experiments (data not shown). The Data are expressed as the percent relative to SpSH_HC+SpB_LC pair (for Adalimumab) and SpB_HC+SpB_LC pair (for Trastuzumab) which were set as 100%. The date analysis was performed with one-way ANOVA and followed by Dunnett's test. Symbol "*, **, ***" indicate a statistically significant difference $p<0.05$, 0.01 and 0.001, respectively and ns indicates no significant difference. All values represent mean ± S.D. of duplicate. (E) CHO-S cells were co-transfected with SpSH_HC+SpB_LC and SpSH_HC+SpL1_LC pairs for expression of Adalimumab and Trastuzumab. The LC and HC of Ab were stained with anti-human Kappa light chain Ab labelled with FITC and anti-human IgG (γ-chain specific) Ab, labelled with R-Phycoerythrin, respectively. The fluorescent signal intensity was measured using a CytoFLEX S flow cytometer.

4.4.4 Binding properties of two purified Abs transiently expressed withoptimized SPs and codons

Finally, the binding of two optimized therapeutic Abs to their cognate therapeutic targets were confirmed by ELISA. CHO-S cells were co-transfected with the optimal SP pairs for Adalimumab (SpSH_HC+SpB_LC) and Trastuzumab (SpB_HC+SpB_LC), identified in this study. The Abs were purified by one-step protein A affinity chromatography. The yields of crude and purified Ab were 134.5±13.0 and 5.6 μg for Adalimumab, and 139.7±8.6 and 7.7 μg for Trastuzumab, respectively. The purified Abs appeared to be homogeneous, as indicated by SDS-PAGE (Figure 4.8A). The molecular weight of HC and LC of Adalimumab and Trastuzumab were approximately 50 kDa and 24 kDa, respectively. Specific bindings of the two Abs were demonstrated by using 1μg of purified and crude Abs against their specific targets, human HER2/ErbB2 for Trastuzumab and human TNF-α for Adalimumab. The ELISA results clearly demonstrated that both purified and crude Ab could bind well to their corresponding targets (Figure 4.8B). Further investigation on physicochemical properties and functional analysis, which must be done to investigate the biosimilarity of the products, are beyond the scope of this research.

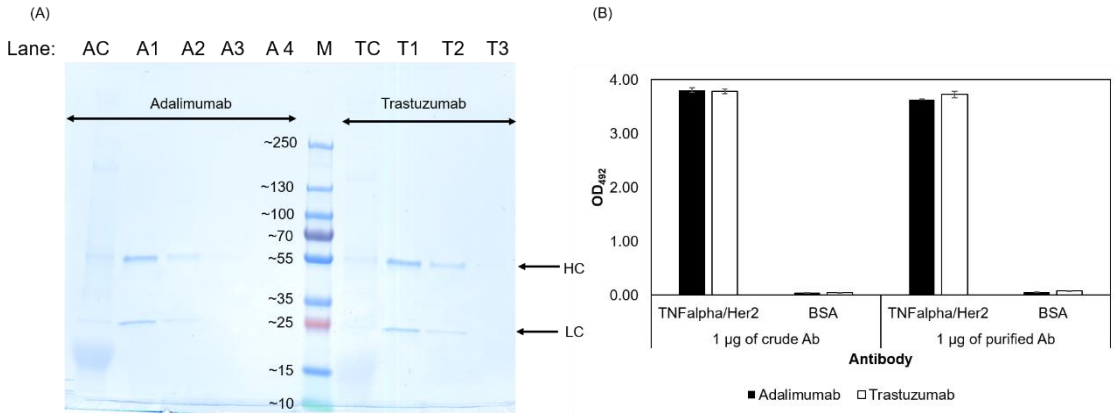

Figure 4.8 Purification and binding activity of Adalimumab and Trastuzumab. (A) SDS-PAGE of Adalimumab and Trastuzumab purified from CHO-S expressing optimal constructs; i.e., Adalimumab (SpSH_HC+SpB_LC) and Trastuzumab (SpSH_HC+SpL1_LC). M: protein standard PageRuler Plus, AC and TC: crude Ab, A1 and T1: elute 1, A2 and T2: elute 2, A3 and T3: elute 3 and A4: elute 4). The fractions from elute 1 and 2 were pooled together and concentrated by ultrafiltration with a 30 kDa MWCO for further analysis. (B) ELISA of purified Adalimumab and Trastuzumab against human TNF-α and human HER2/ErbB2. All values are the average ± SD of triplicate wells.

4.5 Conclusions

While the production of recombinant monoclonal Abs for human therapy have developed into a platform technology over the last 25 years, with this wider experience also comes the realization that for highly rapid and efficient production, individual differences of each new Ab need to be taken into account. Many studies have shown that different limitations may apply in each case and that these may depend on the cell line, the product gene as well as the bioprocess conditions (Tripathi & Shrivastava, 2019). The limitations that apply can be in gene transcription, mRNA processing and

stability, translational efficiency, protein folding and post translational processing as well as the availability of sufficient energy and precursors. Thus, for vector design, several critical parameters need to be individually optimized for a new product. In this report, we have demonstrated the benefits of applying a rapid pipeline of reproducible transient expression experiments to quickly identify the best settings before the development of a stable cell line. The parameters included in this pipeline were codon optimized gene sequences and combinations of different SPs. Obviously, this can be expanded for other parameters, such as different promoters, 3´UTR and 5´UTR sequences or other vector borne elements. An important aspect of such a pipeline would have to include careful characterization of cell behavior, such as growth rate and specific productivity, single cell secretion or intracellular product content, to rapidly determine the degree of stress that the individual constructs cause. The rapid selection of individual elements on a case by case basis would hugely benefit the efficient and timely generation of production clones for biosimilar therapeutic Ab manufacturing.

4.6 References

Barnes, L. M., Bentley, C. M., & Dickson, A. J. (2004). Molecular definition of predictive indicators of stable protein expression in recombinant NS0 myeloma cells. *Biotechnology and Bioengineering, 85*(2), 115-121.

Bauer, A. P., Leikam, D., Krinner, S., Notka, F., Ludwig, C., Längst, G., & Wagner, R. (2010). The impact of intragenic CpG content on gene expression. *Nucleic Acids Res, 38*(12), 3891-3908.

Blobel, G. (1980). Intracellular protein topogenesis. *Proceedings of the National Academy of Sciences of the United States of America, 77*(3), 1496-1500.

Brule, C. E., & Grayhack, E. J. (2017). Synonymous Codons: Choose Wisely for

Expression. *Trends Genet, 33*(4), 283-297.

Bydlinski, N., Maresch, D., Schmieder, V., Klanert, G., Strasser, R., & Borth, N. (2018). The contributions of individual galactosyltransferases to protein specific N-glycan processing in Chinese Hamster Ovary cells. *J Biotechnol, 282*, 101-110.

Cachianes, G., Ho, C., Weber, R. F., Williams, S. R., Goeddel, D. V., & Leung, D. W. (1993). Epstein-Barr virus-derived vectors for transient and stable expression of recombinant proteins. *Biotechniques, 15*(2), 255-259.

Calo-Fernandez, B., & Martinez-Hurtado, J. L. (2012). Biosimilars: company strategies to capture value from the biologics market. *Pharmaceuticals (Basel), 5*(12), 1393-1408.

Cannarozzi, G., Schraudolph, N. N., Faty, M., von Rohr, P., Friberg, M. T., Roth, A. C., Gonnet, P., Gonnet, G., & Barral, Y. (2010). A role for codon order in translation dynamics. *Cell, 141*(2), 355-367.

Cho, H. J., Oh, B. M., Kim, J. T., Lim, J., Park, S. Y., Hwang, Y. S., Baek, K. E., Kim, B. Y., Choi, I., & Lee, H. G. (2019). Efficient interleukin-21 production by optimization of codon and signal peptide in Chinese Hamster Ovarian Cells. *Journal of Microbiology and Biotechnology, 29*(2), 304-310.

Codamo, J., Munro, T. P., Hughes, B. S., Song, M., & Gray, P. P. (2011). Enhanced CHO cell-based transient gene expression with the epi-CHO expression system. *Molecular Biotechnology, 48*(2), 109-115.

Donello, J. E., Loeb, J. E., & Hope, T. J. (1998). Woodchuck hepatitis virus contains a tripartite posttranscriptional regulatory element. *J Virol, 72*(6), 5085-5092.

Ecker, D. M., Jones, S. D., & Levine, H. L. (2015). The therapeutic monoclonal antibody market. *MAbs*, *7*(1), 9-14.

Fath, S., Bauer, A. P., Liss, M., Spriestersbach, A., Maertens, B., Hahn, P., Ludwig, C., Schafer, F., Graf, M., & Wagner, R. (2011). Multiparameter RNA and codon optimization: a standardized tool to assess and enhance autologous mammalian gene expression. *PLoS One*, *6*(3), e17596.

Feng, Y. Q., Seibler, J., Alami, R., Eisen, A., Westerman, K. A., Leboulch, P., Fiering, S., & Bouhassira, E. E. (1999). Site-specific chromosomal integration in mammalian cells: highly efficient CRE recombinase-mediated cassette exchange. *J Mol Biol*, *292*(4), 779-785.

Garattini, L., & Padula, A. (2019). Precision medicine and monoclonal antibodies: breach of promise? *Croat Med J*, *60*(3), 284-289.

Gong, M., Gong, F., & Yanofsky, C. (2006). Overexpression of tnaC of *Escherichia coli* inhibits growth by depleting tRNA2Pro availability. *Journal of Bacteriology*, *188*(5), 1892-1898.

Graf, M., Deml, L., & Wagner, R. (2004). Codon-optimized genes that enable increased heterologous expression in mammalian cells and elicit efficient immune responses in mice after vaccination of naked DNA. *Methods in Molecular Medicine*, *94*, 197-210.

Gu, W., Zhou, T., & Wilke, C. O. (2010). A universal trend of reduced mRNA stability near the translation-initiation site in prokaryotes and eukaryotes. *PLoS Computational Biology*, *6*(2), e1000664-e1000664.

Gustafsson, C., Govindarajan, S., & Minshull, J. (2004). Codon bias and heterologous protein expression. *Trends Biotechnol*, *22*(7), 346-353.

Haryadi, R., Ho, S., Kok, Y. J., Pu, H. X., Zheng, L., Pereira, N. A., Li, B., Bi, X., Goh, L.-T., Yang, Y., & Song, Z. (2015). Optimization of heavy chain and light chain signal peptides for high level expression of therapeutic antibodies in CHO cells. *PloS One, 10*(2), e0116878-e0116878.

Hung, F., Deng, L., Ravnikar, P., Condon, R., Li, B., Do, L., Saha, D., Tsao, Y. S., Merchant, A., Liu, Z., & Shi, S. (2010). mRNA stability and antibody production in CHO cells: improvement through gene optimization. *Biotechnology Journal, 5*(4), 393-401.

Jia, M., & Li, Y. (2005). The relationship among gene expression, folding free energy and codon usage bias in Escherichia coli. *FEBS Lett, 579*(24), 5333-5337.

Kanaya, S., Yamada, Y., Kinouchi, M., Kudo, Y., & Ikemura, T. (2001). Codon usage and tRNA genes in eukaryotes: correlation of codon usage diversity with translation efficiency and with CG-dinucleotide usage as assessed by multivariate analysis. *Journal of Molecular Evolution, 53*(4-5), 290-298.

Khan, K. H. (2013). Gene expression in mammalian cells and its applications. *Advanced Pharmaceutical Bulletin, 3*(2), 257-263.

Kim, H. J., Lee, S. J., & Kim, H.-J. (2010). Optimizing the secondary structure of human papillomavirus type 16 L1 mRNA enhances L1 protein expression in *Saccharomyces cerevisiae*. *Journal of Biotechnology*, *150*(1), 31-36.

Klein, R., Ruttkowski, B., Knapp, E., Salmons, B., Günzburg, W. H., & Hohenadl, C. (2006). WPRE-mediated enhancement of gene expression is promoter and cell line specific. *Gene, 372*, 153-161.

Kober, L., Zehe, C., & Bode, J. (2013). Optimized signal peptides for the development of high expressing CHO cell lines. *Biotechnology and Bioengineering, 110*(4),

1164-1173.

Kozak, M. (1987). An analysis of 5'-noncoding sequences from 699 vertebrate messenger RNAs. *Nucleic Acids Research, 15*(20), 8125-8148.

Kudla, G., Murray, A. W., Tollervey, D., & Plotkin, J. B. (2009). Coding-sequence determinants of gene expression in *Escherichia coli*. *Science 324*(5924), 255-258.

Lee, Y. B., Glover, C. P., Cosgrave, A. S., Bienemann, A., & Uney, J. B. (2005). Optimizing regulatable gene expression using adenoviral vectors. *Exp Physiol, 90*(1), 33-37.

Livak, K. J., & Schmittgen, T. D. (2001). Analysis of relative gene expression data using real-time quantitative PCR and the $2^{-\Delta\Delta CT}$ method. *Methods, 25*(4), 402-408.

Lopez-Lastra, M., Rivas, A., & Barria, M. I. (2005). Protein synthesis in eukaryotes: the growing biological relevance of cap-independent translation initiation. *Biological Research, 38*(2-3), 121-146.

Makoff, A. J., Oxer, M. D., Romanos, M. A., Fairweather, N. F., & Ballantine, S. (1989). Expression of tetanus toxin fragment C in E.coli : high level expression by removing rare codons. *Nucleic Acids Research, 17*(24), 10191-10202.

Meleady, P., Doolan, P., Henry, M., Barron, N., Keenan, J., O'Sullivan, F., Clarke, C., Gammell, P., Melville, M. W., Leonard, M., & Clynes, M. (2011). Sustained productivity in recombinant Chinese Hamster Ovary (CHO) cell lines: proteome analysis of the molecular basis for a process-related phenotype. *BMC Biotech, 11*(1), 78.

Nguyen, L. N., Baumann, M., Dhiman, H., Marx, N., Schmieder, V., Hussein, M.,

Eisenhut, P., Hernandez, I., Koehn, J., & Borth, N. (2019). Novel Promoters Derived from Chinese Hamster Ovary Cells via In Silico and In Vitro Analysis. *Biotech J, 14*(11), 1900125.

Novoa, E. M., & Ribas de Pouplana, L. (2012). Speeding with control: codon usage, tRNAs, and ribosomes. *Trends Genet, 28*(11), 574-581.

Ou, K.-C., Wang, C.-Y., Liu, K.-T., Chen, Y.-L., Chen, Y.-C., Lai, M.-D., & Yen, M.-C. (2014). Optimization protein productivity of human interleukin-2 through codon usage, gene copy number and intracellular tRNA concentration in CHO cells. *Biochemical and Biophysical Research Communications, 454*(2), 347-352.

Parmley, J. L., & Huynen, M. A. (2009). Clustering of Codons with Rare Cognate tRNAs in Human Genes Suggests an Extra Level of Expression Regulation. *PLoS Genet, 5*(7), e1000548.

Pichler, J., Galosy, S., Mott, J., & Borth, N. (2011). Selection of CHO host cell subclones with increased specific antibody production rates by repeated cycles of transient transfection and cell sorting. *Biotech Bioeng, 108*(2), 386-394.

Plotkin, J. B., & Kudla, G. (2011). Synonymous but not the same: the causes and consequences of codon bias. *Nat Rev Genet 12*(1), 32-42.

Rose, A. B., & Beliakoff, J. A. (2000). Intron-mediated enhancement of gene expression independent of unique intron sequences and splicing. *Plant physiology, 122*(2), 535-542.

Schmieder, V., Bydlinski, N., Strasser, R., Baumann, M., Kildegaard, H. F., Jadhav, V., & Borth, N. (2018). Enhanced genome editing tools for multi-gene deletion knock-out approaches using aaired CRISPR sgRNAs in CHO Cells.

Biotechnology Journal, 13(3), e1700211.

Shah, P., & Gilchrist, M. A. (2010). Effect of Correlated tRNA Abundances on Translation Errors and Evolution of Codon Usage Bias. *PLOS Genetics, 6*(9), e1001128.

Sharp, P. M., & Li, W. H. (1987). The codon Adaptation Index--a measure of directional synonymous codon usage bias, and its potential applications. *Nucleic Acids Res, 15*(3), 1281-1295.

Shukurov, R. R., Kazachenko, K. Y., Kozlov, D. G., Nurbakov, A. A., Sautkina, E. N., Khamitov, R. A., & Seryogin, Y. A. (2014). Optimization of genetic constructs for high-level expression of the darbepoetin gene in mammalian cells. *Applied Biochemistry and Microbiology, 50*(9), 802-811.

Stern, B., Olsen, L., Trösse, C., Ravneberg, H., & Pryme, I. (2007). Improving mammalian cell factories: The selection of signal peptide has a major impact on recombinant protein synthesis and secretion in mammalian cells. *Trends Cell Mol Biol, 2*, 1-17.

Takeshi, O., Masayoshi, O., & Wook-Dong, K. (2010). Cell Engineering and Cultivation of Chinese Hamster Ovary (CHO) Cells. *Appl Biochem Microbiol, 11*(3), 233-240.

Tokuoka, M., Tanaka, M., Ono, K., Takagi, S., Shintani, T., & Gomi, K. (2008). Codon Optimization Increases Steady-State mRNA Levels in Aspergillus oryzae Heterologous Gene Expression. *Applied and Environmental Microbiology, 74*(21), 6538-6546.

Tole, S., Mukovozov, I. M., Huang, Y. W., Magalhaes, M. A., Yan, M., Crow, M. R.,

Liu, G. Y., Sun, C. X., Durocher, Y., Glogauer, M., & Robinson, L. A. (2009). The axonal repellent, Slit2, inhibits directional migration of circulating neutrophils. *Journal of Leukocyte Biology*, *86*(6), 1403-1415.

Tripathi, N. K., & Shrivastava, A. (2019). Recent Developments in Bioprocessing of Recombinant Proteins: Expression Hosts and Process Development. *Front Bioeng Biotechnol, 7*(420).

Ventola, C. L. (2013). Biosimilars: part 1: proposed regulatory criteria for FDA approval. *P t, 38*(5), 270-287.

von Heijne, G. (1985). Signal sequences: The limits of variation. *Journal of Molecular Biology, 184*(1), 99-105.

Wu, X., & Brewer, G. (2012). The regulation of mRNA stability in mammalian cells: 2.0. *Gene, 500*(1), 10-21.

Xia, W., Bringmann, P., McClary, J., Jones, P. P., Manzana, W., Zhu, Y., Wang, S., Liu, Y., Harvey, S., Madlansacay, M. R., McLean, K., Rosser, M. P., MacRobbie, J., Olsen, C. L., & Cobb, R. R. (2006). High levels of protein expression using different mammalian CMV promoters in several cell lines. *Protein Expression Purif*, *45*(1), 115-124.

Ying, C., Jennifer, D., Jennifer, H., & Jorge, S. d. S. (2018, 17 Jul 2018). Five things to know about biosimilars right now. Retrieved from https://www.mckinsey.com/industries/pharmaceuticals-and-medical-products/ourinsights/five-things-to-know-about-biosimilars-right-now

You, M., Yang, Y., Zhong, C., Chen, F., Wang, X., Jia, T., Chen, Y., Zhou, B., Mi, Q., Zhao, Q., An, Z., Luo, W., & Xia, N. (2018). Efficient mAb production in CHO cells with optimized signal peptide, codon, and UTR. *Applied Microbiology*

and Biotechnology, 102(14), 5953-5964.

Zhao, F., Yu, C.-H., & Liu, Y. (2017). Codon usage regulates protein structure and function by affecting translation elongation speed in Drosophila cells. *Nucleic acids research, 45*(14), 8484-8492.

Zhu, J. (2012). Mammalian cell protein expression for biopharmaceutical production. *Biotechnol Adv, 30*(5), 1158-1170.

CHAPTER V

IMPROVEMENT OF THE SELECTION EFFICIENCY OF RECOMBINANT CHINESE HAMSTER OVARY (CHO) CELL BY GLUTAMINE SYNTHETASE GENE KNOCKOUT USING CRISPR/CPF1 TECHNOLOGY

5.1 Abstract

Chinese Hamster Ovary (CHO) cells are the most commonly used cell line for the manufacturing of biologics. The selection of high producing stable clones from a large population of low and non-productive clones from the transiently transfected bulk cultures, which is crucial step for recombinant Ab production from CHO cells, was explored. The Glutamine synthetase (GS)-CHO system is an alternative approach to efficiently identify high producing and stable clones in the cell line generation process. This system is used to generate the highly producing population by using a combination of increasing selection stringency with methionine sulfoximine (MSX), a GS inhibitor, and a GS-knockout CHO cell line, where the endogenous CHO GS gene expression was removed. The hypothesis of this study was that since there are three GS genes in CHO cells, deleting only 1 GS gene may result in the activation of one of the other 2 GS genes, consequently reducing the selection stringency. Therefore, in this study, to

further increase the selection stringency, two GS genes on chromosome 5 (GS5) and 1 (GS1) of CHO-S and CHO-K1, which express GS at high and low activity level, were deleted using CRISPR/Cpf1. The GS-knockout CHO cells were confirmed by RT-qPCR and DNA sequencing. The single and double GS-knockout CHO cells of CHO-S and CHO-K1 showed robust glutamine-dependent growth after eliminating GS activity. The bulk culture productivity of engineered CHO-S and CHO-K1 was significantly improved after a single round of 25 μM MSX selection, as non-transfected cells and cell populations of low and non-producing cells were removed, even in medium not supplemented with MSX. Our results suggest that CHO-K1 P1F3 is the most suitable host to establish highly producing clones when compared with other GS-knockout CHO cell lines.

Keywords: Chinese Hamster Ovary (CHO) cells; Glutamine synthetase (GS); recombinant antibody production, monoclonal antibody; knockout; CRISPR/Cpf1) system

5.2 Introduction

Since approval of the first mAb in 1986 (Ecker, Jones, & Levine, 2015), therapeutic Abs have become the predominant treatment of various diseases in recent years due to their high specificity. During this time, many technological advances have used to discover and develop the various therapeutic Abs such as humanization, phage display, and human Ab-producing mice. They are rapidly growing products in the pharmaceutical market due to their high specificity. Currently, 98 therapeutic mAbs have been approved by The United States Food and Drug Administration (US FDA) in 2020 (https://www.antibodysociety.org). Growing significance of biologics can lead to higher market revenues over the forecast period. The approved therapeutic mAbs are

on the market for treating various human diseases which achieved sales of $122 billion and the top ten selling mAb products had annual sales of more than $3 billion in 2018 (https://biopharmadealmakers. nature.com). The global biologics market is expected to reach nearly $400 billion (https://www.grandviewresearch.com), with the mAbs segment garnering sales of $300 billion by 2025 (Lu et al., 2020).

The growing significance of biologics has resulted in the development of technologies for high quality and productivity in different types of expression systems (Tripathi & Shrivastava, 2019). Among mammalian cell lines, CHO cells are the predominant system for biopharmaceutical production because they can secrete recombinant Abs at relatively high levels and provide a human-like glycosylation pattern with least concerns for immunogenic modifications (Zhu, 2012). Moreover, the knowledge about their genomes have been extensive studied, thus facilitating genetic manipulation. Manufacturing processes for biologics have improved significant increases in final yield over the past years which reached titer improvement up to or more than 10 g/L (Handlogten et al., 2018; Huang et al., 2010). However, establishing stable cell line is a critical process of biochemical production. To obtain a stable and high productivity clones, several rounds of selection amplification for stable pools are required and followed by isolation, screening and characterization a large number of clones, taking 6-12 months for cell line development (Jayapal, Wlaschin, Hu, & Yap, 2007; Kingston, Kaufman, Bebbington, & Rolfe, 2002). Due to the integration efficiency of the gene of interest (GOI) into the host cell genome is low and GOI will be integrated into a highly transcribed or hot spot region of only few cells which will produce adequate recombinant mAb expression levels (Ho, Tong, & Yang, 2013; Lacy, Roberts, Evans, Burtenshaw, & Costantini, 1983; Wurm, 2004). Often, the selection

efficiency is low, thus this process is both time-consuming and laborious (Fan et al., 2013; Lin et al., 2019; Nakamura & Omasa, 2015). Therefore, the efficiency of cell line development process requires improvement to drive biologic development, increase yield and reduce manufacturing costs in the pharmaceutical industry.

Generation of cell lines in CHO cell expression systems is the most commonly selected by either DHFR-based methotrexate (MTX) selection in DHFR-deficient cells or GS based-MSX selection in CHO cell or GS-knockout CHO lines (Matasci, Hacker, Baldi, & Wurm, 2008; Rita Costa, Elisa Rodrigues, Henriques, Azeredo, & Oliveira, 2010). In DHFR-based system, the -/-DHFR DG44 cell has been widely used by selection in the medium without hypoxanthine and thymidine (Chusainow et al., 2009; Wurm, 2004). The *DHFR* and GOI were amplified via rounds of increasing of MTX to improve productivity which this step increases the timeline for cell line generation (Kingston et al., 2002) and introduces increased mutation (suitability and genetic stability) rates to be caused by loss of gene copies after removing MTX selection pressure (Guo et al., 2010).

The GS-based system uses the GS enzyme catalyzes the ATP-dependent condensation of glutamate and ammonia to produce L-glutamine (L-Gln) as an essential nutrient and as a nitrogen donor in the amino acid and nucleotide synthesis (Meister, 1980; Neermann & Wagner, 1996; Wurm, 2004). This system also decreases ammonia accumulation in the cell culture medium without MSX (Noh, Shin, & Lee, 2018). Addition of an appropriate GS inhibitor (MSX) in the medium without L-Gln, MSX binds to the GS enzyme and prevents the L-Gln production, resulting in non-transfected cells death (Sanders & Wilson, 1984). The GS system was designed to use in cell lines lacking GS activity (such as NS0 myeloma cell line), in which case removal

the L-Gln from medium can be isolated the stable and high producing clones (Brown, Renner, Field, & Hassell, 1992) or expressing sufficient GS (such as CHO cells), in which case MSX selection pressure is applied to selected the productive stable cells (Cockett, Bebbington, & Yarranton, 1990; Wurm, 2004). Typically, this system used two rounds of MSX selection, the first round of 25–50 μM MSX for improved selection stringency and a second round of 100–1000 μM for gene amplification (Cockett et al., 1990; Jun, Kim, Hong, & Lee, 2006; Kingston et al., 2002; Liu et al., 2004). However, the selection of high producer clones in CHO cell lines was not efficiency improved due to some CHO cells can survive up to 5 mM MSX (Sanders & Wilson, 1984). In this case, large numbers of non and medium-to-low producing cells still exist and limit the efficiency of identifying the higher-producing clones. To improve stringency selection, GS-knockout CHO cells have been applied to improve cell line generation efficiency. The previous studies have been shown that the engineered SV40E promoter driving the GS gene expression (Fan et al., 2013) and attenuated GS as a selection maker to reduce GS activity level can improve highly-efficiency CHO cell line generation in absence of MSX (Lin et al., 2019). The GS-based system has some advantages over the DHFR-based system. For example, GS-based system requires a single round of MSX selection, resulting in fewer copies of transgene per cell for the survival of the stable cells, accomplishing faster selection and highly-efficiency CHO cell line generation (Bebbington et al., 1992; Brown et al., 1992). And also, this system does not require mutant hosts (Bebbington et al., 1992). The stable specific productivity of the clones is a vital attribute for the pharmaceutical industry. Therefore, after achievement for higher producer clones, the stability of long-term production has to be monitored. Previous reports have suggested that unstable specific productivity of some

GS-generated CHO cell lines lost more than 20% when compared with their original productivity in both absence and present of MSX (Dorai et al., 2012; Noh et al., 2018). To overcome this issue and future improve more selection stringency, I try to improve stability and high productivity without the use of MSX by completely knockout two GS genes on chromosome 5 (GS5) and 1 (GS1) of CHO-S and CHO-K1, which express the high and low GS activity level, using CRISPR/Cpf1. This technology has been successfully applied to generate the engineered CHO-K1 cells (Schmieder et al., 2018). In this study, two engineered (single (GS5) and double (GS5 and GS1) GS-knockout cells) in both CHO-S and CHO-K1 cells were established to completely eliminate the endogenous GS activity. After confirming the GS-engineered CHO cell lines by deletion PCR, non-deletion PCR and RT-qPCR, they were characterized and used to evaluate for selection stringency improvement in bulk cell line generation, as indicated by non-transfected cells and cell populations of low and non-producing cells removed, even in medium no supplemented with MSX.

5.3 Material and Method

5.3.1 Cloning of paired gRNAs into CRISPR/Cpf1 vector

The gRNA sequences of 23 nucleotide (nt) targeting GS genes were extracted and designed with a Bowtie program developed by Langmead et al. (Langmead, Trapnell, Pop, & Salzberg, 2009). The gRNA were chosen only if the 27 nt frame followed criteria: (1) started with TTT[ACG]; (2) does not contain TTTT, TTTTT, GGGGG, AAAAA, CCCCC; (3) does not contain recognition sites for restriction enzymes BsmbI and BbsI (CGTCTC, GAAGAC); (4) individual GC content is between 0.3-0.7; (5) without off-targets across entire genome with 0 mismatch in seed. Each possible gRNA in the upstream region (on left over the scaffold, irrespective

of direction) was paired with gRNAs in the downstream region (on right over the scaffold, irrespective of direction) along-with the scaffold sequences. Only the gRNAs in the frames that have GC content between 0.38-0.44 were selected (Table 5.1). The selected paired gRNAs were obtained as single-stranded (ss) oligonucleotides (Sigma-Aldrich, USA), annealed and cloned into the pY010 (AsCpf1) vector (Schmieder et al., 2018) according to Bauer et al. (Bauer, Canver, & Orkin, 2015). The sequences of recombinant plasmids were confirmed by Sanger sequencing (Eurofins, Austria) using the U6 promoter primer.

Table 5.1 The paired sgRNA sequences including additional information for AsCpf1.

Name	Sequence (5'-3')	PAM gRNA1 (5'-3')	PAM gRNA2 (5'-3')	Target
GS5_gRNA1_Fw	caccGTAATTTCTACTCTTGTAGATTAAGCGCTGCTCTGGCAGTTACAAATTTCTACTCTTGTAGATAAGGTGAGACAAGGGGACTAAGGTTTTTGCG	TTTA	TTTA	GS5
GS5_gRNA2_Fw	caccGTAATTTCTACTCTTGTAGATCAGTAGGGCTACCCATCTGTCAGAATTTCTACTCTTGTAGATACCTTAACCCGTGATTTGTCTCCTTTTTGCG	TTTA	TTTA	
GS5_gRNA3_Fw	caccGTAATTTCTACTCTTGTAGATACTCCAGGTCTGCCTGTCCTCCGAATTTCTACTCTTGTAGATAAAGGCTAACATATTCCTGGGAATTTTTGCG	TTTA	TTTA	
GS5_gRNA1_Rv	aaacCGCAAAAACCTTAGTCCCCTTGTCTCACCTTATCTACAAGAGTAGAAATTTGTAACTGCCAGAGCAGCGCTTAATCTACAAGAGTAGAAATTAC	TTTA	TTTA	
GS5_gRNA2_Rv	aaacCGCAAAAAGGAGACAAATCACGGGTTAAGGTATCTACAAGAGTAGAAATTCTGACAGATGGGTAGCCCTACTGATCTACAAGAGTAGAAATTAC	TTTA	TTTA	
GS5_gRNA3_Rv	aaacCGCAAAAATTCCCAGGAATATGTTAGCCTTTATCTACAAGAGTAGAAATTCGGAGGACAGGCAGACCTGGAGTATCTACAAGAGTAGAAATTAC	TTTA	TTTA	
GS1_gRNA1_Fw	caccGTAATTTCTACTCTTGTAGATTCTACATTTTCTCTGGGCTAAGCAATTTCTACTCTTGTAGATGTACCAAGACCATGCGGGAGGAGTTTTTGCG	TTTA	TTTA	GS1
GS1_gRNA2_Fw	caccGTAATTTCTACTCTTGTAGATGAATTCCGTTCATCATACCCATAAATTTCTACTCTTGTAGATAAGCCCGCTGCCCCTCTGCCAATTTTTTGCG	TTTA	TTTG	
GS1_gRNA3_Fw	caccGTAATTTCTACTCTTGTAGATTTCTACTGTGAGTTGGCCCTTATAATTTCTACTCTTGTAGATGTTGGCCTTCCGATGGCTTCCCTTTTTTGCG	TTTA	TTTG	
GS1_gRNA4_Fw	caccGTAATTTCTACTCTTGTAGATAGACACACGGTGTAAACGGATAATAATTTCTACTCTTGTAGATGGATCCTGCCTGTATCCTGTGAGTTTTTGCG	TTTA	TTTA	
GS1_gRNA5_Fw	caccGTAATTTCTACTCTTGTAGATGTTGGCCTTCCGATGGCTTCCCTAATTTCTACTCTTGTAGATGTCAAGCTCTGTTTGTGAAACTGTTTTTGCG	TTTG	TTTA	
GS1_gRNA1_Rv	aaacCGCAAAAACTCCTCCCGCATGGTCTTGGTACATCTACAAGAGTAGAAATTGCTTAGCCCAGAGAAAATGTAGAATCTACAAGAGTAGAAATTAC	TTTA	TTTA	
GS1_gRNA2_Rv	aaacCGCAAAAAATTGGCAGAGGGGCAGCGGGCTTATCTACAAGAGTAGAAATTTATGGGTATGATGAACGGAATTCATCTACAAGAGTAGAAATTAC	TTTA	TTTG	
GS1_gRNA3_Rv	aaacCGCAAAAAAGGGAAGCCATCGGAAGGCCAACATCTACAAGAGTAGAAATTATAAGGGCCAACTCACAGTAGAAATCTACAAGAGTAGAAATTAC	TTTA	TTTG	
GS1_gRNA4_Rv	aaacCGCAAAAACTCACAGGATACAGGCAGGATCCATCTACAAGAGTAGAAATTATTATCCGTTTACACGTGTGTCTATCTACAAGAGTAGAAATTAC	TTTA	TTTA	
GS1_gRNA5_Rv	aaacCGCAAAAACAGTTTCACAAACAGAGCTTGACATCTACAAGAGTAGAAATTAGGGAAGCCATCGGAAGGCCAACATCTACAAGAGTAGAAATTAC	TTTG	TTTA	
GS6_gRNA1_Fw	caccGTAATTTCTACTCTTGTAGATCATATGTCATTGCAGGGTGGAATAATTTCTACTCTTGTAGATGCACCAAGGCCATGTGGGAGGAATTTTTGCG	TTTA	TTTA	GS6
GS6_gRNA2_Fw	caccGTAATTTCTACTCTTGTAGATTAGTCCCAGTGCATCTCATGGGAAATTTCTACTCTTGTAGATACTGGAGGACTGCCTCTCACACTTTTTTGCG	TTTA	TTTA	
GS6_gRNA3_Fw	caccGTAATTTCTACTCTTGTAGATGGAACTGGTTCAGAACAGACCCAAATTTCTACTCTTGTAGATTACCTTATCTGCTTCCAGCTGACTTTTTGCG	TTTA	TTTA	
GS6_gRNA1_Rv	aaacCGCAAAAATTCCTCCCACATGGCCTTGGTGCATCTACAAGAGTAGAAATTATTCCACCCTGCAATGACATATGATCTACAAGAGTAGAAATTAC	TTTA	TTTA	
GS6_gRNA2_Rv	aaacCGCAAAAAAGTGTGAGAGGCAGTCCTCCAGTATCTACAAGAGTAGAAATTTCCCATGAGATGCACTGGGACTAATCTACAAGAGTAGAAATTAC	TTTA	TTTA	
GS6_gRNA3_Rv	aaacCGCAAAAAGTCAGCTGGAAGCAGATAAGGTAATCTACAAGAGTAGAAATTTGGGTCTGTTCTGAACCAGTTCCATCTACAAGAGTAGAAATTAC	TTTA	TTTA	

Color code: cloning overhangs, scaffold 1, sgRNA1, scaffold 2, sgRNA2, Poly(T)

5.3.2 Cell lines and cell culture

CHO-S (cGMP Banked, Cat. No. A13696-01), was purchased from Thermo Fisher Scientific (USA). CHO-S and CHO-K1 were maintained in CD-CHO medium (Thermo Fisher Scientific) supplemented with 8 mM L-Gln (Thermo Fisher Scientific, USA) and 0.2% Anti-Clumping Agent (Thermo Fisher Scientific, USA). Cells were grown in either TubeSpin Bioreactor 50 (TPP) tubes (TPP Techno Plastic Products, Switzerland) with a working volume of 15 mL medium or 125 mL shaking flasks (Corning, USA) with a working volume of 25-30 mL medium. The cell cultures in the tubes and shaking flasks were incubated at 37°C, 7% CO_2, and humidified air at a shaking speed of 250 and 140 rpm, respectively. The cells were passaged twice a week with a seeding density of $2x10^5$ viable cells per mL. The cell cultures were mixed with trypan blue and counted by ViCELL XR Cell Counter (Beckman Coulter, Germany) for viable cell density (VCD) and viability.

5.3.3 Cell transfection

For transient expression of recombinant Ab, appropriate expression vectors were transiently transfected into CHO-S or CHO-K1 cells by nucleofection method according to previously published method (Schmieder et al., 2018). In brief, $5x\ 10^6$ viable cells were electroporated with 10^{-12} µg of circular plasmid DNA using a Neon Nucleofector device and the 100 µL Neon Transfection Kit (Thermo Fisher Scientific, USA) with 1,700 V, 20 ms and 1 pulse. The transfected cells were transferred into TPP tube containing pre-warmed 15 mL medium and held in a static incubator at 37°C, 7% CO_2 and humidified air for 2 h. After that the transfected cells were cultured under standard condition. To check the transfection efficiency, the pY010 (AsCpf1) plasmid bearing a gene encoding green fluorescent protein (GFP) was

transfected in parallel. After 24 h post transfection, the transfection efficiencies were determined by CytoFLEX S flow cytometer with 488 nm excitation and 523 emission wavelengths (Beckman Coulter, Germany) to evaluate the percentage of the GFP-expressing cells.

5.3.4 Assessment of paired gRNA efficiency

To assess the efficiency of paired gRNA, the pY010 (AsCpf1) vector (3 μg each) containing different paired gRNAs were transfected into 2 x 10^6 CHO-S and CHO-K1 cells. After 5 days post transfection, the genomic DNA (gDNA) was isolated with the DNeasy1 Blood & Tissue Kit (Qiagen, USA) according to the manufacturer's protocol. The isolated gDNA was performed the deletion PCR for all targets with specific primers (Table 5.2) using GoTaq$^{@}$ G2 DNA polymerase (Promega, USA). The amplified products were visualized of DNA fragmentation by agarose gel electrophoresis using Midori Green Advance (Biozym, Germany) for DNA staining and documentation with the Gel Doc^{TM} XR system (Bio-Rad, USA). The paired gRNAs that showed the deletion PCR band were selected for further GS gene deletions.

Table 5.2 Primers for deletion PCR including further specifications.

Name	Sequence (5'-3')	Annealing temperature (°C)	Expected amplicon size (bp)	Detection	Target
D_GS5_Fw	GCAAGCTGGAAATGCTTCC	58	1745	GS5_gRNA2	GS5
D_GS5_Rv	CAAAAGGCCTGCTTTAGTGAC				
D_GS5_2_Fw	GTGGCTTGTTAGTCTTGCCC	58	837 and 1096	GS5_gRNA1 and 3	
D_GS5_2_Rv	GTGGAACTAGGAATTGCCAAGAC				
D_GS6_4_Fw	GCTTCTTGCTCTGAGGTGAG	58	1433	GS6_gRNA1	GS6
D_GS6_Cpf1_p1.2_Rv	CCCCCATCAGTAGCAATGTTC				
D_GS6_4_Fw	GCTTCTTGCTCTGAGGTGAG	58	1417 and 1260	GS6_gRNA2 and 3	
D_GS6_Cpf2.2/3.2_Rv	GGGACATGTGCATTTATTTGATGC				
D-GS1_Fw_3	TAGGGTTGGGTCATGTGC	62	1729, 1272 and 1638	GS6_gRNA1, 2 and 3	GS1
D_GS1_Rv_3	AGAAGAACGGGATTGTGGG				
D-GS1_F	CCTGAGTGGAATTTTGATGGC	52	690 and 550	GS1_gRNA4 and 5	
D-GS1_R	GAAAATGTAAGCTGTTCATGCTG				

Table 5.3 Primers for deletion PCR including further specifications.

Name	Sequence (5'-3')	Annealing temperature (°C)	Expected amplicon size (bp)	Detection	Target
ND_GS5_Fw	CTTGGGTGGTTCTTGTGATG	60	902	GS5_gRNA3	GS5
DN_GS5_Rv	CGCTTAAGTACGAATTACAGC				
ND_GS1_Fw	TACCTTTCAGTCTGAGGGCTC	60	185	GS1_gRNA2	GS1
ND_GS1_Rv	GCTGGTTGCTCACCATGTC				
ND_GS1_F	GCCTATCGCAGGGATATCATG	54.4	591	GS1_gRNA5	
ND-GS1_R	GTCGCCAGTCTCATTGAGAAG				
ND_GS6_Fw_2	CCACTGGTCCAGGAAACTTG	60	647	GS6_gRNA1	GS6
ND_GS6_Rv_2	GCATTGCAGCTGGTTAGTCAG				

5.3.5 Generation of cell lines with GS-knockout cells

For the generation of triple CHO-S and CHO-K1 knockout cell lines, they were transfected with appropriate three paired gRNA vector combinations using 4 μg each. Single cells were obtained by subcloning via fluorescence activated cell sorting (FACS) on day 3 after transfection (MoFlo Astrios Cell Sorter, Beckmann Coulter). The cells were sorted in 200 μL cultivation medium supplemented with 1x Penicillin–Streptomycin (10,000 units/ml Penicillin, 10 mg/mL Streptomycin, Sigma–Aldrich, USA) in 96 well plates. Single colonies were expanded into 48 well plates containing 900 μl cultivation medium and incubated at 37 °C, 7% CO_2 and humidified air at a shaking speed of 300 rpm.

For initial screening, Samples for colony PCR were prepared following by a previously published method (Bydlinski et al., 2018; Schmieder et al., 2018). The individual colonies were lysed in 20 μL 0.2 M NaOH, incubated for 10 min at 75 °C and neutralization with 180 μL 0.04 M Tris-HCl, pH 7.8. The crude cell lysates were subjected to GS5 non-deletion PCR with specific primers (Table 5.3) and then assessed with GS1 and GS6, respectively. Lysates of negative clones (no have non-deletion PCR band) were further evaluated by deletion PCR for all three genes. The candidate clones were confirmed with non-deletion PCR and deletion PCR again using pure gDNA as a template. All PCRs with either crude cell lysate or isolated gDNA were routinely done with GoTaq@ G2 DNA polymerase (Promega, USA) by following to the manufacturer's instructions. After screening and selection, cells showed no have triple GS knockouts were further transfected with pY010 (AsCpf1) vectors, containing paired sgRNAs, targeting the next gene to be deleted.

5.3.6 Confirmation of GS genes deletion by RT-qPCR

The total RNA was isolated from $1x10^6$ viable cells using Direct-zol RNA Kit (Zymo Research, USA) with DNase treatment, following the manufacturer's instructions. RNA (800 ng) was converted to cDNA using a High-Capacity cDNA Reverse Transcription Kit with RNase Inhibitor (Applied Biosystems, USA), according to the manufacturer's instructions. For Quantitative PCRs (qPCRs), one microliter of the 4x diluted cDNA was used as template in a 10 µL reaction using the SensiFAST SYBR Hi-ROX Kit (Bioline, UK). Samples were measured in quadruplicates on a Rotor-Gene qPCR cycler (Qiagen, Germany) with condition as previously described (Nguyen et al., 2019). The primer pairs specific for CHO, i.e., GAPDH (glyceraldeyde-3-phoshate dehydrogenase), Alpha-(1,6)-fucosyltransferase (FUT8) and three GS genes are listed in Table 5.4. Relative quantification of mRNA expression level was normalized to GAPDH (for mRNA) or FUT8 (for gDNA) for calculation of fold change (FC) by $2^{-\Delta\Delta C}{}_T$ method (Livak & Schmittgen, 2001).

5.3.7 Assessment of impact on growth

The growth curve experiments were performed in TPP tubes with a working volume of 15 mL medium supplemented with or without 8 mM L-Gln. Each tube was inoculated in triplicates with a viable cell concentration of 2 x 10^6 cells/ml and cultivated under standard condition. The samples were taken daily to measure VCD and viability.

Table 5.4 Primer used for qPCR including further specifications.

Name	Sequence (5'-3')	Annealing temperature (°C)	Target
qPCR_GS5_cpf1_Fw_2	ATCCGCATGGGAGATCAT		
qPCR_GS5_cpf1_RV2	CTGGGCAGGCATGACCTCAG	60	GS5
qPCR_GS6_cpf1_Fw	GGAGAAGGTGTTCACCGC		
qPCR_GS6_cpf1_Rv	CTACACGGGTCGTCCATCTTG	60	GS6
qPCR_GS1_cpf1_Fw	GAGTAGAGCCGACTGCCTGA		
qPCR_GS1_cpf1_Rv	CACAAGCCACGAGAACGAG	60	GS1
qGS1_F (2nd deletion)	GCCTATCGCAGGGATATCATG		
qGS1_R (2nd deletion)	TTGGAATTCCCACTGGGCATG	60	GS1
qPCR-FUT8_E7_fw	GCTGTGGCTATGGATGTCAA		
qPCR-FUT8_E7_rev	GTGCATGTCTCACTTACAGGTC	60	FUT8
RT-qPCR_GAPDH_fw	AACTTTGGCATTGTGGAAGG		
RT-qPCR_GAPDH_rev	ACACGTTGGGGGTAGGAACA	60	GAPDH

5.3.8 Evaluation of GS knockout cells in stable cell pool development

To evaluate the GS selection efficiency of each engineered cell, single and double GS knockout of both CHO-S and CHO-K1 cells were 5 transfected with a vector containing Trastuzumab and *gs* genes (Figure 5.1) using nucleofection method as previously described in section. At 24 hours post transfection, each bulk pool was centrifuged and resuspended in 15 mL CD-CHO medium with no L-Gln (GS selection media). The tubes were incubated with shaking under standard condition. After the pools recover from GS selection (viability >90 %), the bulk pools were further selected with Gln-free medium supplemented with 25 µM MSX. The bulk pools were further characterized.

In order to compare the efficiency of expression host and to monitor the improvement in Ab productivity during batch culture, the cell pools (selected with and with no MSX) were seed 2 x 10^5 cells/mL into TPP tubes containing 15 mL GS selection medium supplemented with or without 25 µM MSX which depended on selection condition. Samples were taken for cell viability, density, intracellular staining, and titer analysis on day 3 and 7 post inoculation. Cell specific productivity was calculated.

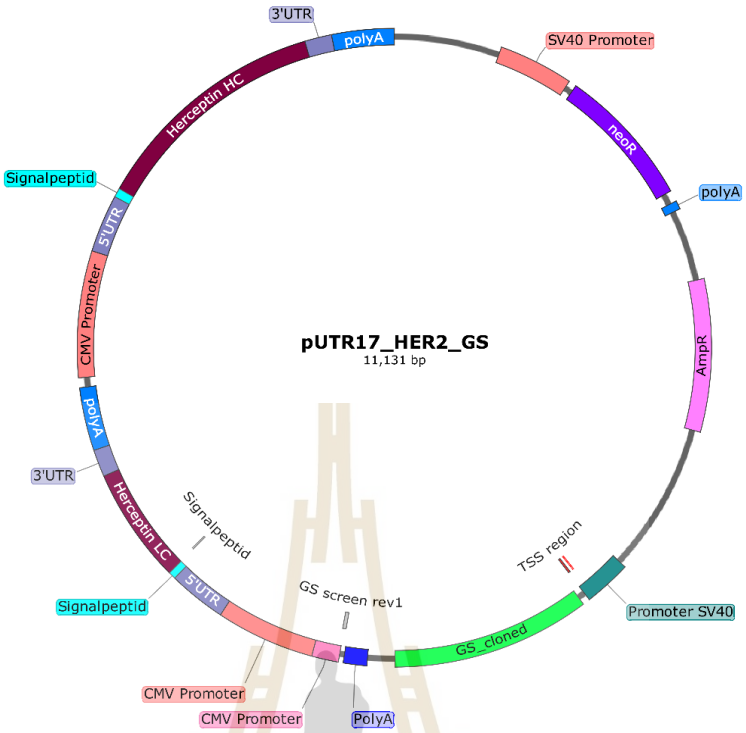

Figure 5.1 Map of pUTR17_HER2_GS expression vector. This vector contains heavy chain (HC) and light chain (LC) of Herceptin (Trastuzumab) which both genes were under the control of the CMV promoter and fused with SP. The vector also carries the GS gene, which under the control of the SV40 promoter, for the selection and maintenance of the GS-knockout CHO cells.

5.3.9 Titer and cell-specific productivity (q_p)

The Ab titre of the transfectants was determined from cell supernatant 3 days post transfection by the Octet RED96e (ForteBio, USA) with protein A probes using human IgG1 Trastuzumab as a standard. To assess the q_p (pg/cell/day) of cells, the viable cell density and Ab titer were evaluated and q_p was calculated as previously described (Meleady et al., 2011).

5.3.10 Intracellular staining

The Ab-expressing CHO cells were stained following previously published method (Pichler, Galosy, Mott, & Borth, 2011). The cells expressing the Ab gene were stained with Anti-Human IgG (γ-chain specific) Ab labelled with R-Phycoerythrin (Cat. No. P9170, Sigma-Aldrich, USA) and anti-Human kappa light chain Ab labelled with FITC (Cat. No. F3761, Sigma-Aldrich, USA). The fluorescent signal intensity was measured using a CytoFLEX S flow cytometer (Beckman Coulter, Germany) and the data were analysed using the CytExpert 2.4.0.28 software program (Beckman Coulter). The experiments were performed in duplicate.

5.3.11 DNA sequence

Plasmids were prepared using a plasmid purification kit as suggested by the manufacturer (MiniPrep; Qiagen, USA). Automated DNA sequencing was performed by (Eurofins, Austria) using U6 promoter primer. For finding the deleted regions, the PCR products were amplified by Phusion High-Fidelity DNA Polymerase (Thermo Fisher Scientific, USA) for all genes with deletion primers as indicated in Table 5.2 and cleaned up by Monarch® PCR & DNA Cleanup Kit (NEB, USA) following the manufacturer's instructions. The purified PCR products were sequenced by using deletion primers. The DNA sequences were analyzed with SnapGene version 4.2.6 (GSL Biotech).

5.4 Results and Discussion

5.4.1 Designation and Evaluation of the pair sgRNAs

Currently, the GS-CHO system is applied to efficiently identify high producing and stable clones in the cell line generation process for biopharmaceutical production by increasing the selection stringency. Selection of high producing cell lines

is based on the balance between GS gene expression and the MSX, which inhibits the activity of GS. In unmodified CHO cells, the endogenous GS gene expression interferes the selection stringency. Therefore, using GS-knockout cells can increased selection stringency by removal of endogenous CHO GS gene expression in CHO cells (Fan et al., 2012). However, since the current GS-CHO system applied to select the high producing clones is knockout only exon 5 or 6, which contain the key sequence critical for GS activity, by using zinc finger nuclease (ZFN) or transcription activator-like effector nucleases (TALEN) based-technology (Fan et al., 2012; Lin et al., 2019; Liu et al., 2010). They could express enough GS to support cell survival. In this case, large populations of low- to medium-producing cells can still survive in bulk-selected cultures even though when the transgenes integrated into inactive regions in the CHO genome.

As previously reported, full gene deletions with CRISPR systems and paired sgRNAs have several advantages compared to the frame-shift mutations with sgRNA (Schmieder et al., 2018). For example, the efficiency in generating biallelic knockouts and a coverable loss of function (LOF) modification of a gene is high. full gene deletion strategies are applicable in case of non-coding RNAs or regulatory DNA stretches and can be approached to study the function of genomic region.

The CHO GS genes were identified from previously published CHO genome and epigenome databases (Feichtinger et al., 2016). I found that the endogenous GS genes in CHO-K1 consist of three genes on chromosome 5 (GS5), 1 (GS1) and 6 (GS6) with high, low and non-expression, respectively. GS5 gene composes of 7 exons, exon 6 carrying the essential sequence for GS activity, and GS6 contains 6 exons while GS1 gene have only one exon (Figure 5.2). These genes were

confirmed with analysis of relative expression levels of mRNA in CHO-S and CHO-K1 by RT-qPCR with specific primers. The results showed that the mRNA expression levels of GS6 had no mRNA expression whereas GS5 and 1 expressed mRNA in both CHO cells (Figure 5.3). These results demonstrated that the mRNA expression of three genes are relation with CHO genome and epigenome databases (Feichtinger et al., 2016). Based on this database, I decided to full delete of all endogenous CHO GS genes. Three different pair of sgRNAs for each GS gene were designed to cover the genes and cloned into pY010(AsCpf1) with two BsmBI restriction sites (Figure 5.4).

Resulted in the overexpression plasmids containing a Cpf1 variant derived from *Acidaminococcus* sp. BV3L6 (AsCpf1), GFP and paired sgRNAs are under control of a U6 promoter for high level gene expression in CHO cells.

To check the efficiency of paired sgRNA activity, CHO-K1 cells were transfected with pY010(AsCpf1) plasmids containing different paired sgRNAs and subsequently transfected cell pools were evaluated by deletion PCR. The transfected cell pools with the paired GS5_sgRNA2, 3 (for GS5) GS5_ sgRNA1, 2, 3 (for GS6) GS1_ sgRNA1, 2 and 3 (for GS1) showed the positive band of PCR product while the transfected cell pools with the paired GS5_sgRNA1 (for GS5) had no band a similar result with using mock sample as negative control (Figure 5.5). These findings indicated that could delete the full GS genes. The paired GS5_sgRNA3, GS6_sgRNA1 and GS1_sgRNA2 were selected for further modification of CHO-S and CHO-K1 cell lines due to they showed high deletion PCR signal intensities and covered the biggest genomic deletions.

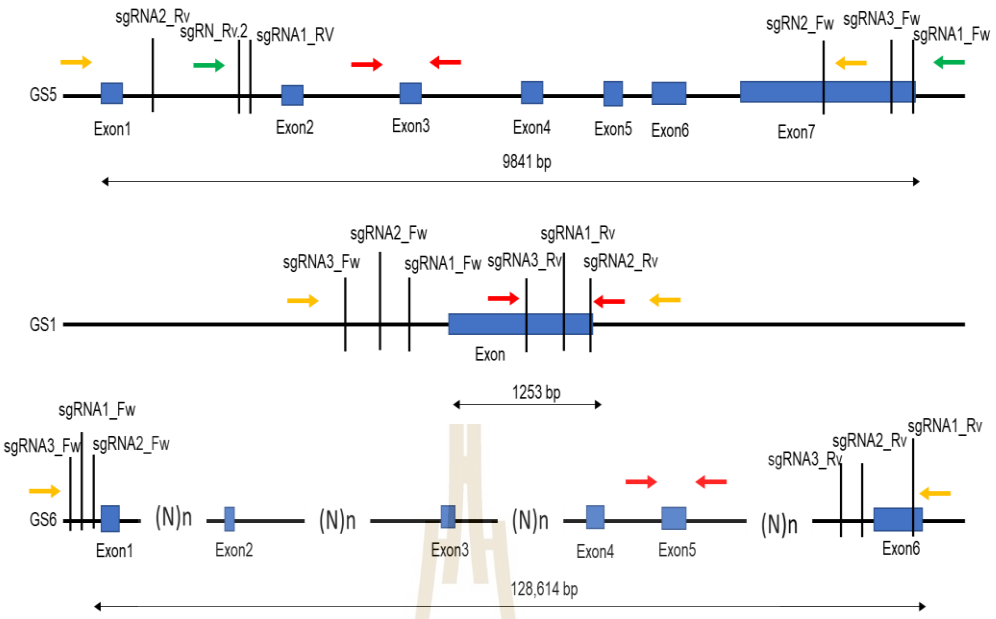

Figure 5.2 Schematic representation of the endogenous GS genes in CHO-K1 genome database and possible knockout strategies. The sgRNA positions are shown as vertical black lines. The sgRNA with the same number will be matched together such as sgRNA1.1 and sgRNA1.2 of GS5 gene are paired to create the GS5_sgRNA1. The yellow and green arrows indicate primers to detect the deletion PCR product and red arrows indicate primers to detect the non-deletion PCR product.

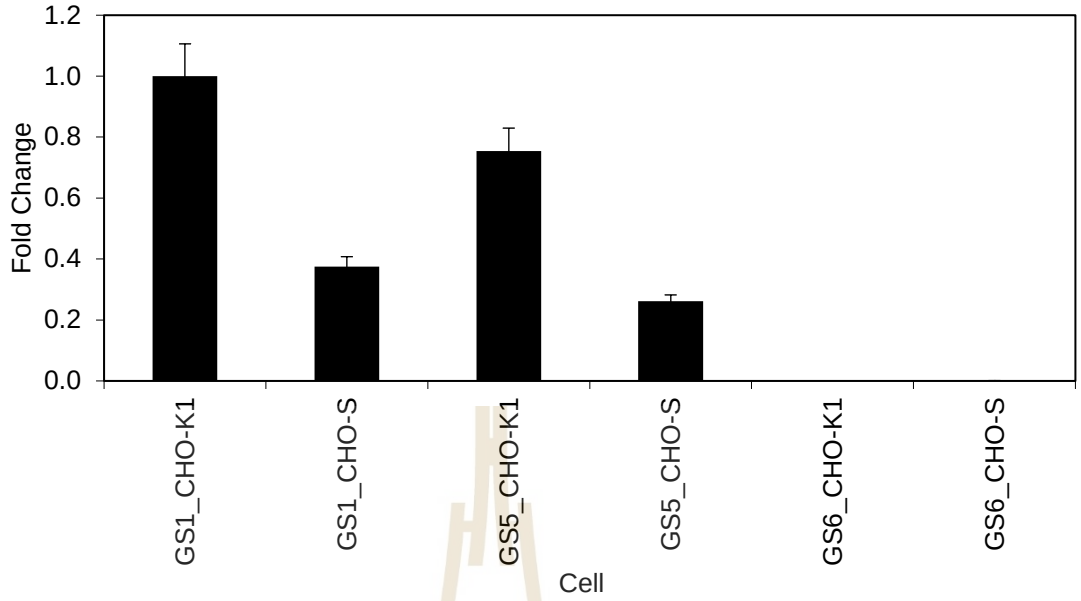

Figure 5.3 The relative mRNA expression of three GS genes in CHO-K1 and CHO-S normalized with GAPDH. Data represent mean ± SD from a quadruplicate representative example of one biological replicate.

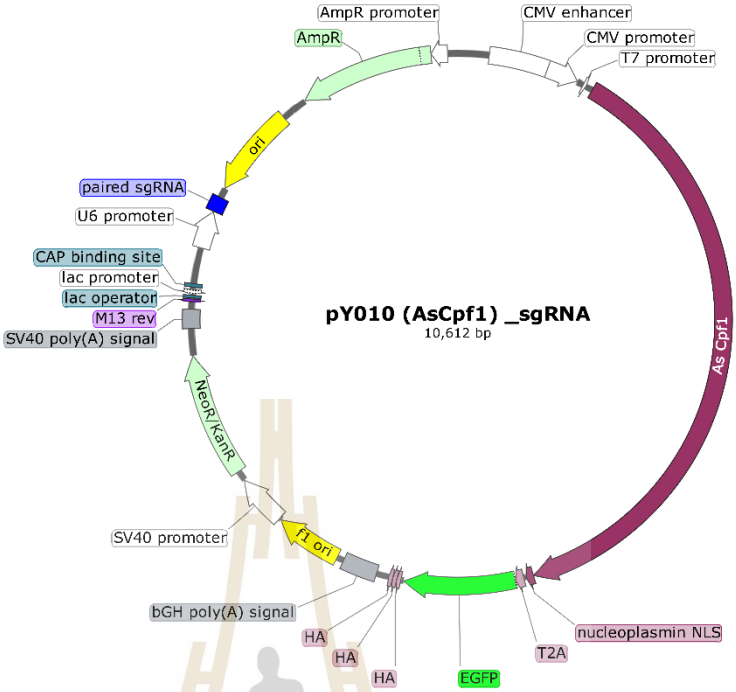

Figure 5.4 Map of pY101(AsCpf1)_sgRNA expression vector. This vector expresses the paired sgRNAs for GS gene deletions by CRISPR/Cpf1 system which these paired sgRNAs were under the control of the U6 promoter. The AsCpf1 and GFP genes, which liked with T2A liker, were under the control of the CMV promoter. The vector also carries the gene for ampicillin resistance (Kan^R) for the selection and maintenance of the plasmid.

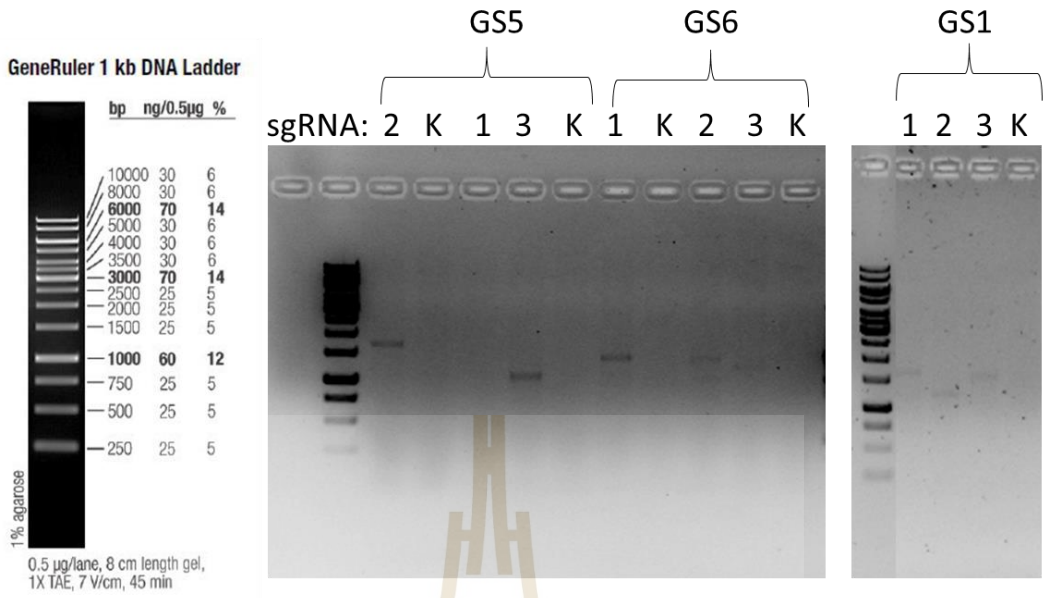

Figure 5.5 Evaluation of Efficiency of three GS gene deletions by co-transfection AsCpf1 and the paired sgRNAs. The vector carrying each paired sgRNA were transfected into CHO-K1. After transfection, the transfected cells were performed the deletion PCR with specific primers. The pool cells showed the deletion amplicon indicating the designed sgRNA pairs have potential gene deletion on CHO-K1(representative example of one biological replicate).

5.4.2 Generation of single and double GS-deficient cell lines

To knock out the three GS genes, CHO-S and CHO-K1 were transfected with selected three paired sgRNA plasmid combinations as noted above and subsequently the transfected cells were sorted to obtain single cells in cultivation medium supplemented with L-Gln. Figure 5.6A shows the outline of the workflow. A total of 144 (for CHO-S) and 96 (for CHO-K1) clones were first screened for deletion by non-deletion PCR for GS5 gene. Among these, 40 clones of CHO-S and 8 clones of CHO-K1 showed the absence of the deletion amplicon. Subsequently, they were

performed deletion PCR for GS5 gene, resulting in one clone of both CHO-S (P27E) and CHO-K1 (P27D) revealed the presence of the deletion amplicon. These results suggested that two candidate clones may identify as biallelic deletion clones having a band of the deletion PCR and no band of the non-deletion PCR. To further characterize the obtained clones and validate a successful full deletion, RNA was isolated and RT-qPCR was performed to confirm the absence of expression of GS5. RT-qPCR analysis showed no detectable GS5 expression (Figure 5.6B). Each clone was also evaluated by amplify deletion PCR product from gDNA and then PCR products were subjected to Sanger sequencing to identify the precise deletion. Sequencing results of CHO-S P27E and CHO-K1 P27D are shown in Figure 5.6C, demonstrating that they are biallelic with some different in deletion regions. In CHO-K1 P27D genome, it was inserted 2 bp into genome and cut at position 83 bp upstream of GS5_sgRNA3.2 whereas CHO-S P27E genome was deleted 8 bp and cut at position 4 bp upstream of GS5_sgRNA3.2. From first round of screening, I obtained only one GS5 knockout clone of each CHO cell. This issue may occur a large population of monoallelelic deletion and non-deletion clones in sorted cells. In this case can solve by sorting the cells using GFP expression or a deletion of each gene may transfect in three subsequent rounds for enhancing the efficiency of multi-gene deletions (Schmieder et al., 2018) or screening more clones from transfected cell pools but it is time consuming. It has been previously reported that gene deletion by CRISPR system revealed the majority of indel formation at the sgRNA recognition site and monoallelelic deletion clones (Bauer et al., 2015).

After GS5 deletion, I found that paired GS1_sgRNA2 and GS6_sgRNA1 can guide to induce the GS1 and 6 deletions in CHO-S P27E while they cannot guide to delete the GS1 and 6 deletions in CHO-K1 P27D. This event may be caused by

chromosomal rearrangement or chromosomal translocation from deletion of a larger fragment of the chromosome. To further delete the GS1 and GS6, the paired sgRNAs were rechecked the activity. This result showed that paired GS1_sgRNA1 and GS6_sgRNA1 can guide to induce the GS1 and 6 deletions in CHO-K1 P27D. Therefore, the appropriate paired sgRNAs were transfected into the cells, screened and identified for both GS genes by non-deletion and deletion PCRs, revealing no biallelic deletion clones lacking of GS1 and GS6 expressions. In this case, binding affinity of paired sgRNAs may be influenced by chromosomal rearrangement of GS5-deficient cells or sgRNA position and efficiency for each gene may also be affected genome deletion. Since the sequencing result only covered the paired sgRNAs targeting site, it is possible to have some mutations occurred outside this region which was not met from sequencing.

From the RT-qPCR analysis verified that CHO-S and CHO-K1 cells were indeed no expressed the GS6. Therefore, I decided to delete only GS5 and GS1 gene in both CHO-S and CHO-K1 cells. I try to remove the GS1 gene again by redesigning the new sgRNA pairs (GS_sgRNA4 and 5) for removal of GS1 expression. The paired GS_sgRNA4 and 5 are specific to internal and downstream of gene while old paired sgRNAs are specific to upstream and internal of gene (Figure 5.7A). The new ones were designed based on RNA-Seq data of CHO-K1 cells including both coding genes and long noncoding (lnc) transcripts and the chromatin states showing a high level of histone mark H3K27ac and H3K4me3, indicating active and highly express DNA region downstream (Feichtinger et al., 2016; Hernandez et al., 2019). The activity of the new paired sgRNAs was confirmed by the deletion PCR (Figure 5.7B). The paired GS_sgRNA5 was chosen to delete the GS1 gene. After transfection and sorting, the

single cells were screened by non-deletion and deletion PCRs. These findings suggested that seven candidate clones (5 clones for CHO-S P27E and 2 clones for CHO-K1 P27D) may identify as biallelic deletion clones. These candidate clones were further evaluated by RT-qPCR to confirm the lack of GS1 expression (Figure 5.8A). For the five candidate clones from CHO-S P27E, the GS1 expression decreased 0.20-0.61-fold compared to wild-type CHO-S cells. For two candidate clones from CHO-K1 P27D, the expression of GS1 reduced 0.43-0.68-fold compared to wild-type CHO-K1 cells. I also did the qPCR using gDNA as a template (Figure 5.8B). The results showed that decreasing in GS1 expression of 0.70-0.75 and 0.31-0.77-fold compared to their wild-type CHO cells was observed in candidate clones from CHO-S P27E and CHO-K1 P27D, respectively. CHO-S P2E5 and CHO-K1 P1F3 were chosen for further molecular characterization. Sequencing results of two clones are shown in Figure 5.8C, revealing that they are biallelic with full deletion region. I confirmed the GS5 knockout in CHO-S P27E and CHO-K1 P27D while GS5 and 1 knockout in CHO-S P2E5 and CHO-K1 P1F3. These results demonstrated that high efficiency of complete biallelic deletion in CHO cells by CRISPR/Cpf1 system with sgRNA pairs. In addition, I also found that the position of paired sgRNAs could affect the efficiency of GS1 deletion. Previous report has shown that CRISPR/Cpf1 system with sgRNA pairs can enhance the efficiency of full multi-gene deletions in CHO-K1 and the paired sgRNA position of each gene affect the efficiency of gene deletion and activity (Schmieder et al., 2018). However, our GS-knockout cells in this research are different from other GS-knockout cells which they knocked out only exon 5 or 6, which contain the key sequence critical for GS activity by using ZFN or TALEN based-technology (Fan et al., 2012; Lin et al., 2019)(Noh et al., 2018). Frameshift mutation strategies could probably cause the

protein misfolding that may not only cause a loss of function, but also occur unknown side effects and stress responses lead to cell impairment with multiple dysfunctional (Fan et al., 2012; Schmieder et al., 2018). Moreover, it is possible to have the existence of a pseudo GS gene in some CHO cells (Fan et al., 2012) relating to our finding that I found two expressed GS genes, GS5 and 1 with high and low expression, respectively, in CHO genome and epigenome databases (Feichtinger et al., 2016).

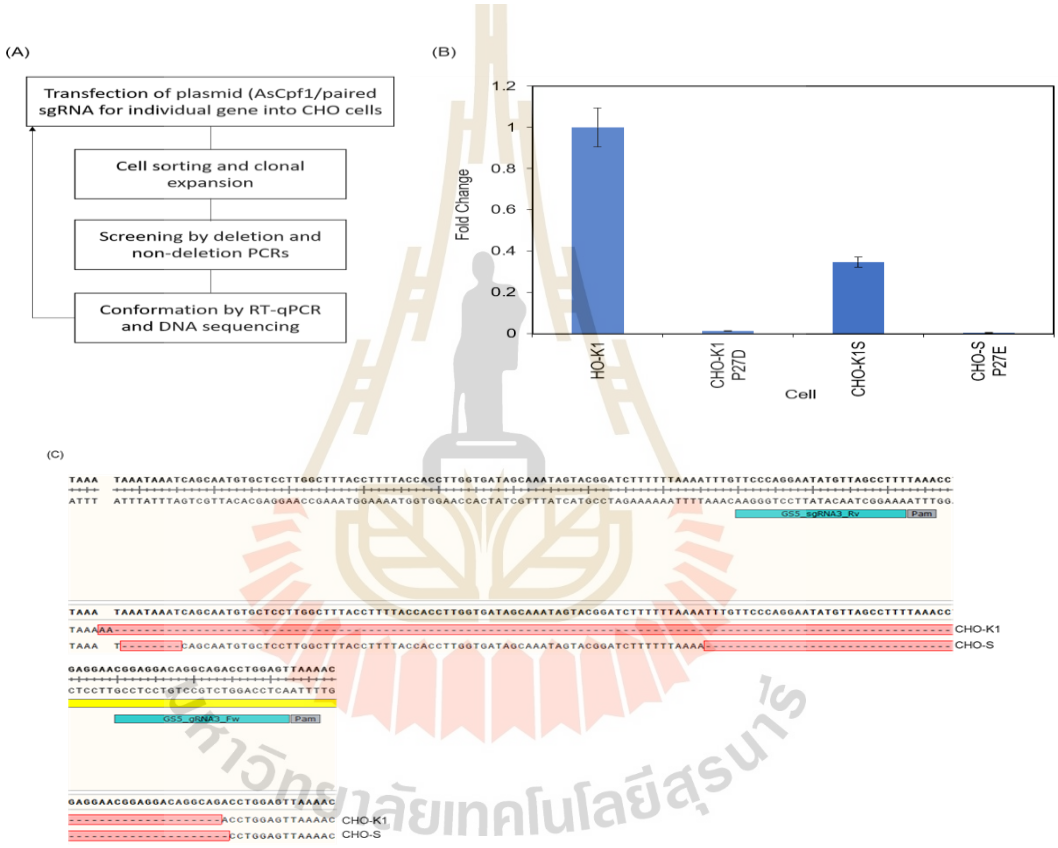

Figure 5.6 Generation of GS-knockout CHO-K1 and CHO-S cells. (A) An overview of construction of single and double GS-knockout CHO-K1 and CHO-S cells. (B) Expression level of GS5-knockout CHO-K1 and CHO-S cells relative to GAPDH expression in their wild-type CHO cells by RT-qPCR. (C) DNA sequence indicates th GS5 was deleted from CHO-K1 and CHO-S cells.

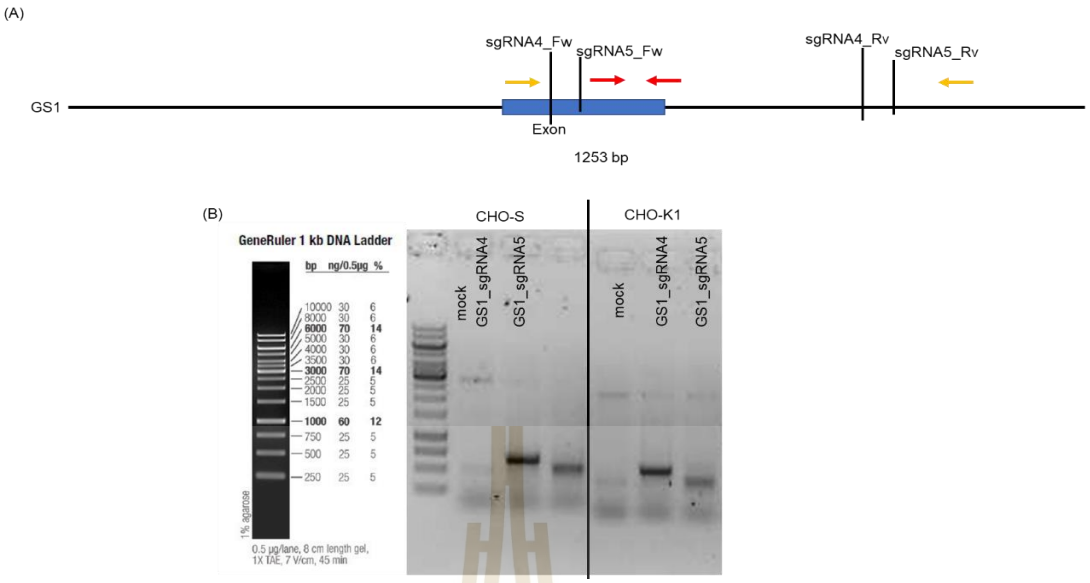

Figure 5.7 Generation of GS1-knockout CHO-K1 P27D and CHO-S P27E cells. (A) The new paired sgRNA positions are shown as vertical black lines. The yellow and green arrows indicate primers to detect the deletion PCR product and red arrows indicate primers to detect the non-deletion PCR product. (B) The deletion PCR of the paired GS_sgRNA4 and 5. The PCR results indicate two paired sgRNAs can delete the GS1 gene in pool cells.

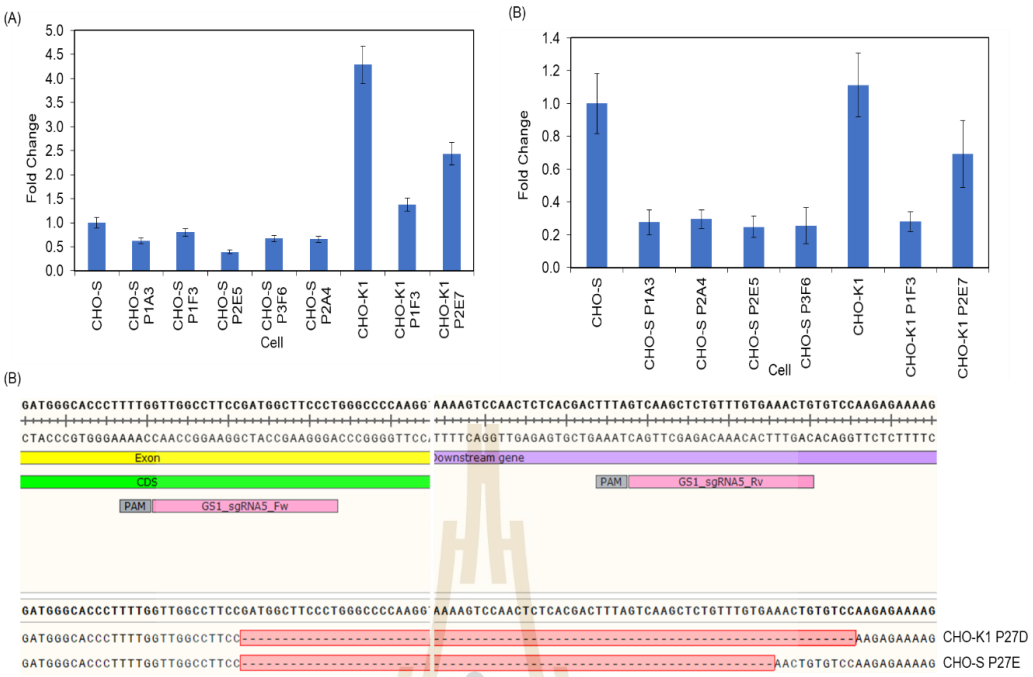

Figure 5.8 The confirmation of GS1-knockout CHO-K1 P27D and CHO-S P27E cells. The GS1 expression level in CHO-K1 P27D and CHO-S P27E cells relative to GAPDH expression in their wild-type CHO cells by RT-qPCR using mRNA (A) and gDNA (B) as a template. (C) DNA sequence confirms th GS5 was deleted from CHO-K1 P27D and CHO-S P27E cells.

5.4.3 Growth characteristics

The growth behavior of the engineered cells was assessed to confirm the disruption of GS enzyme activities. The CHO-S P27E and P2E5 cells had equal VCD, viability and cell diameter in medium presence of L-Gln throughout the experiment (Figure 5.9). The growth for CHO-S P27E and P2E5 cells was significantly slower compared with the wild-type CHO-S cell reaching average maximum VCD of 11.76 x 10^6 cells/mL on day 7. After day 5, a decrease of the viability and cell diameter for wild-type CHO-S cell was observed, due to the wild-type CHO-S faster growth than

the engineered cells which the cell density exceeds the capacity of the medium and the cells lose viability and reduce the size. In case of CHO-K1 cultured in normal medium, CHO-K1 P27D exhibited slightly slower growth before day 5 compared to CHO-K1 P1F3 and wild-type CHO-K1 cell, while the viability and cell size of CHO-K1 P27D cell were comparable with others CHO-K1 cells (Figure 5.9). These results demonstrated that the engineered CHO-S and CHO-K1 cells showed different on growth behavior in normal medium compared to their wild-type CHO cells.

In Gln-free medium, the engineered CHO-S and CHO-K1 cells did not grow when cultured in medium in the absence of L-Gln (Figure 5.10), which was consistent with the RT-qPCR analysis eliminating of GS catalytic activities. In contrast to wild-type CHO-S and CHO-K1 cells continued to grow in the medium without L-Gln due to they are able to synthesize the L-Gln from endogenous GS genes. The viability for GS knockout CHO-S and CHO-K1 cells significant decreased after day 4 (for CHO-K1 P1F3) or 5 (for the engineered CHO-S and CHO-K1 P27D) compared to their wild-type CHO cells. The cell size for the GS knockout CHO-S cells had no significant different but appreciably smaller when compared to wild-type CHO-S cells. The CHO-K1 P1F3 cells revealed the reduction of cell diameter overtime in Gln-free medium while cell diameter of CHO-K1 P27D and wild-type CHO-K1 cells showed no significant different. Taken together these data confirm the successful generation of GS knockout CHO cells, which showed strongly Gln-dependent growth, by CRISPR/Cpf1 system. Previous study has demonstrated that GS knockout CHO cells by using ZFN mRNA have no a negative impact in the behaviors with the exception of the presence of L-Gln in the culture medium for cell growth compare to the wild-type CHOK1SV cells (Fan et al., 2012). Our results indicated that full deletion strategy for

endogenous GS genes, which are crucial for endogenous L-Gln synthesis, may affect genetic and phenotypic of GS knockout CHO cells.

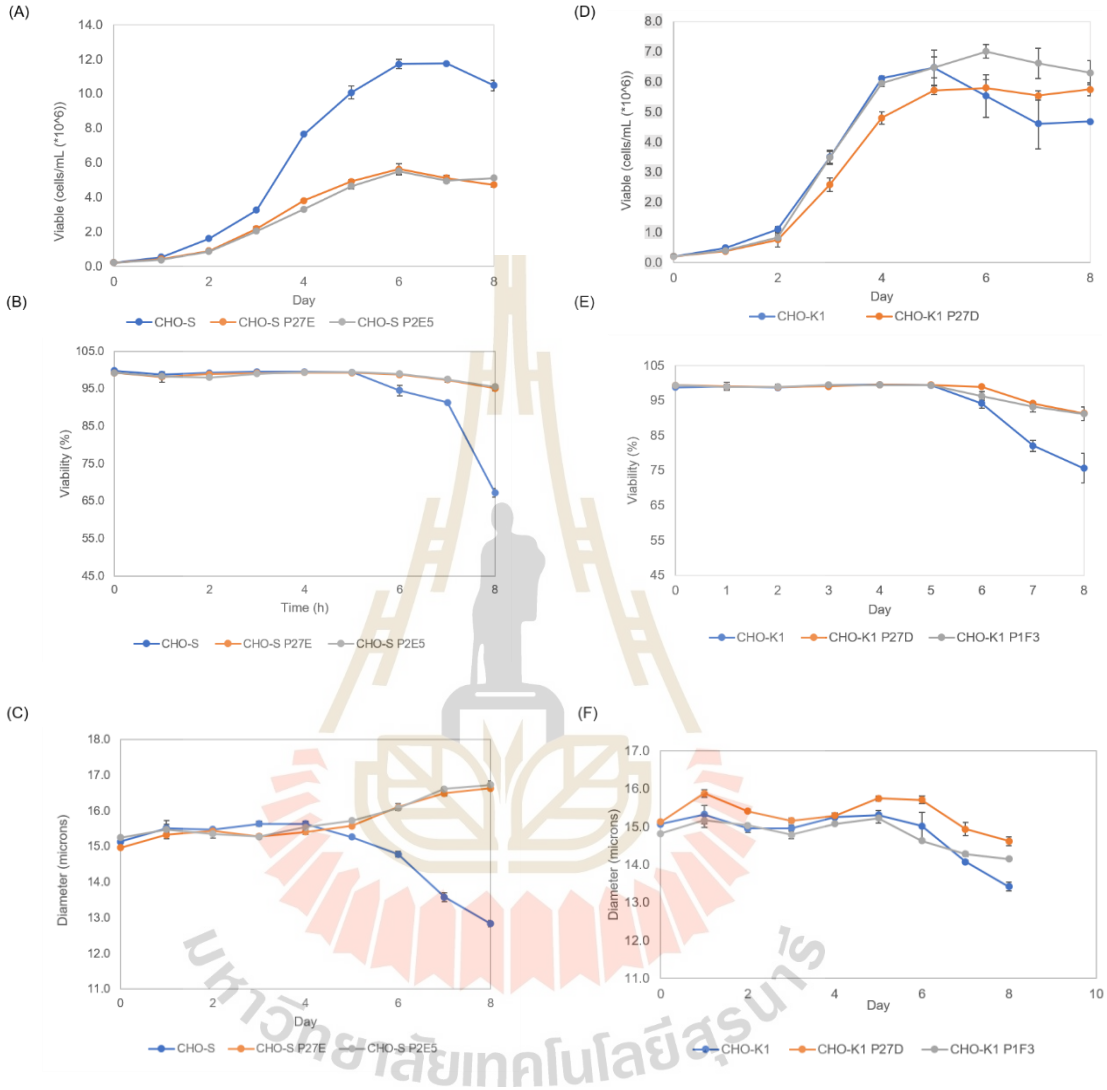

Figure 5.9 Growth behavior of GS-knockout CHO cell lines in medium supplemented with the L-Gln. VCD (A and D), viabilities (B and E) and cell size (C and F) of GS-knockout CHO cell lines**.** All values represent mean ± S.D. of triplicate.

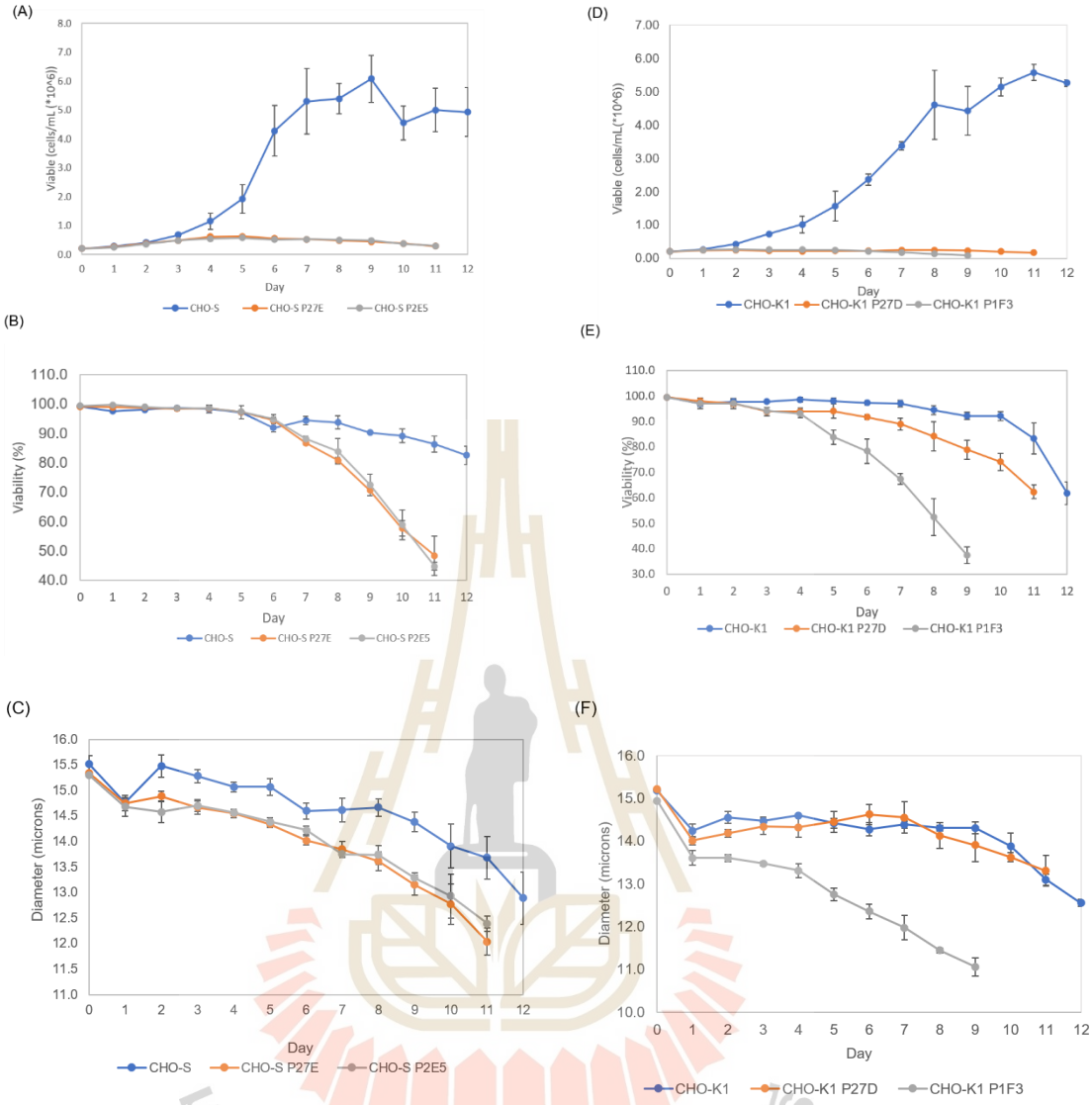

Figure 5.10 Growth behavior of GS-knockout CHO cell lines in Gln-free medium. VCD (A and D), viabilities (B and E) and cell size (C and F) of GS-knockout CHO cell lines**.** All values represent mean ± S.D. of triplicate.

5.4.4 Stable cell line generation

GS-knockout cells, removal of endogenous CHO GS gene expressions in CHO cells, allow increased stringent selection of high producing clones based on the balance between GS gene expression and MSX. In contrast, the wild-type CHO cells obstruct the selection stringency due to they can express the endogenous GS genes (Fan

et al., 2012; Noh et al., 2018). As reported previously, the selection stringency for the GS selection system can be improved by a single round of MSX selection with a low amount of 25 μM MSX on GS-knockout cells (Fan et al., 2012). Moreover, Noh and colleague demonstrated that the selection of the high producing clones could be succeeded in the absence of MSX. Therefore, the selection stringency of bulk culture in this research was done by using 25 μM MSX on single and double GS-knockout CHO-S and K1 cells compared to in the absence of MSX condition. In this experiment, I also did not use wild-type CHO-S and CHO-K1 cell as the control for bulk selection.

In order to compare the efficiency of selection stringency in bulk culture for single and double GS-knockout CHO-S and CHO-K1 cells, a vector containing Trastuzumab and *gs* genes was five transfected into single and double GS knockout CHO-S and CHO-K1 cells. At 24 hours post transfection, the bulk pools were selected in the Gln-free medium without MSX. VCD and viability profiles for all GS-knockout CHO-derived bulk pools are shown in Figure 5.11A-B. VCD and viability profiles for CHO-S P27E and P2E5-derived bulk pools were nearly identical expect VCD for CHO-S P2E5_3-derived bulk pool. The both GS-knockout CHO-S-derived bulk pools showed higher VCD than the GS-knockout CHO-K1-derived bulk pools. For GS-knockout CHO-K1 cells, the CHO-K1 P1F3-derived bulk pools showed a little lower VCD than the CHO-K1 P27D-derived bulk pools (Figure 5.11C-D). Surprisingly, bulk culture selection for all GS-knockout CHO-S and CHO-K1 cells had similar recovery (viability) profiles. A five-to-six day delay in bulk culture recovery time was observed for our GS-knockout CHO-S and CHO-K1 cells compared to a previous result, the wild-type SV40E promoter driven GS expression in GS-knockout cell when bulk culture were selected in medium in the absence of L-Gln ((Noh et al., 2018). This

result suggests that our engineered GS CHO cells may more stringent selection due to indication by the slower viability recovery at day 19 after selection in Gln-free medium. This experiment also consistent with growth curve of all GS-knockout CHO cells, viabilities reduced after day 5-6. Non- and lower-producing cells were eliminated in cell culture without MSX. In addition, intracellular staining of HC and LC of Trastuzumab showed that CHO-K1 P27D and P1F3 identified more expression strength of mAb than CHO-S P27E and P2E5 cells (Figure 5.12). To further determine a stepwise selection, the bulk pools were performed to a higher MSX concentration by subculturing them in culture medium in the presence of 25 µM MSX. All bulk culture pools showed no any growth inhibition at 25 µM MSX which the viability of the cells remained over 90% for all the bulk pools, consistent with earlier observations (Noh et al., 2018).

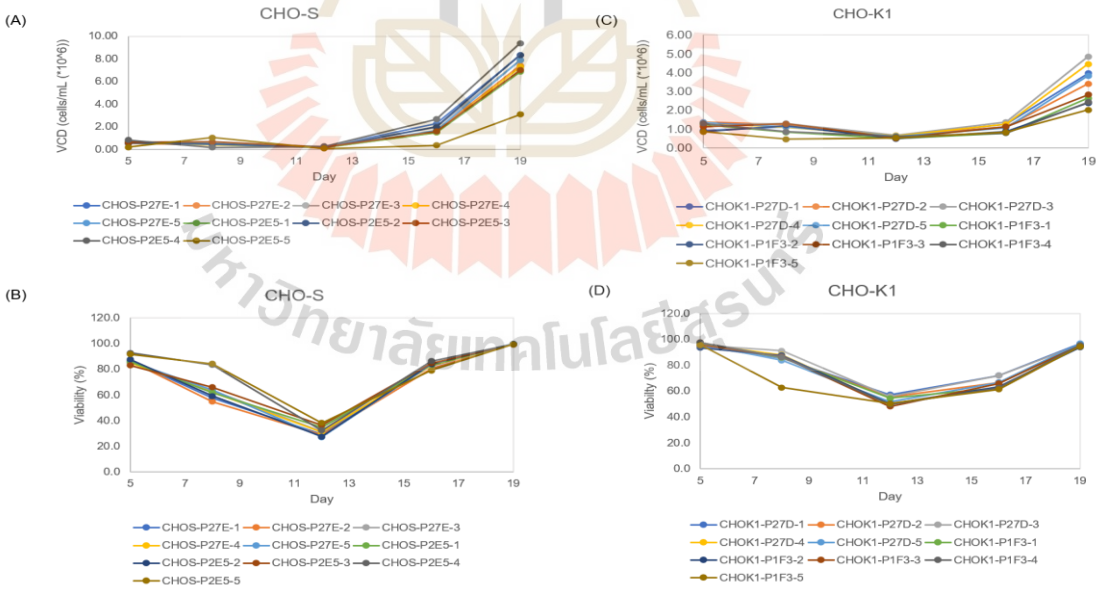

Figure 5.11 Bulk cultures selection of GS-knockout CHO cell lines in Gln-free medium without MSX. VCD (A and C), viability (B and B) profiles of GS-knockout CHO cell lines expressing Trastuzumab**.** All values represent mean ± S.D. of triplicate.

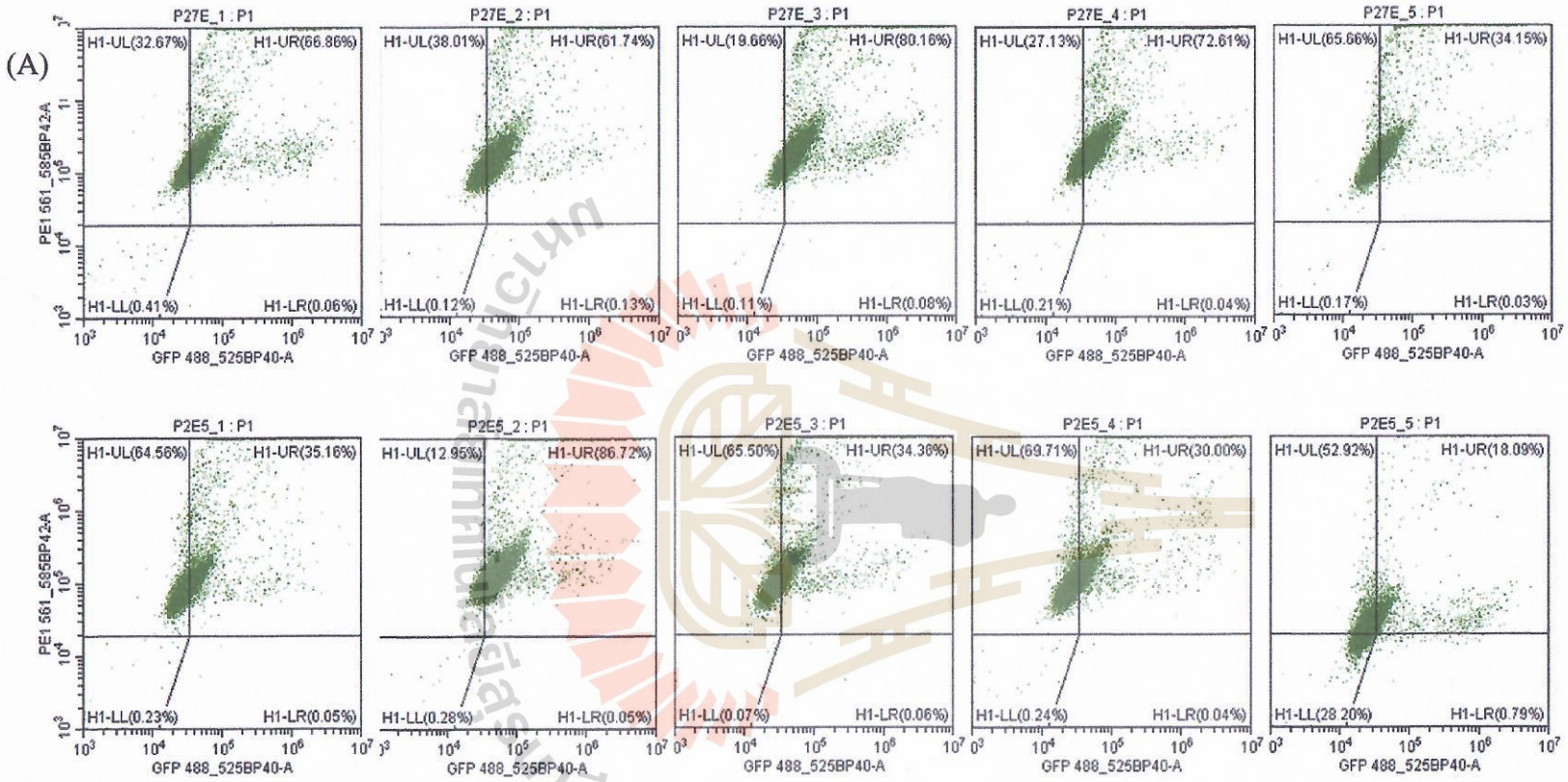

Figure 5.12 Intracellular staining against the Trastuzumab Ab in the bulk cultures selection of GS-knockout CHO cell lines in Gln-free medium without MSX. After bulk cultures recovery, the LC and HC of Ab were stained with Anti-Human Kappa Light Chain Ab labelled with FITC and Anti-Human IgG (γ-chain specific) Ab labelled with R-Phycoerythrin. The fluorescent signal intensity was measured using a CytoFLEX S flow cytometer.

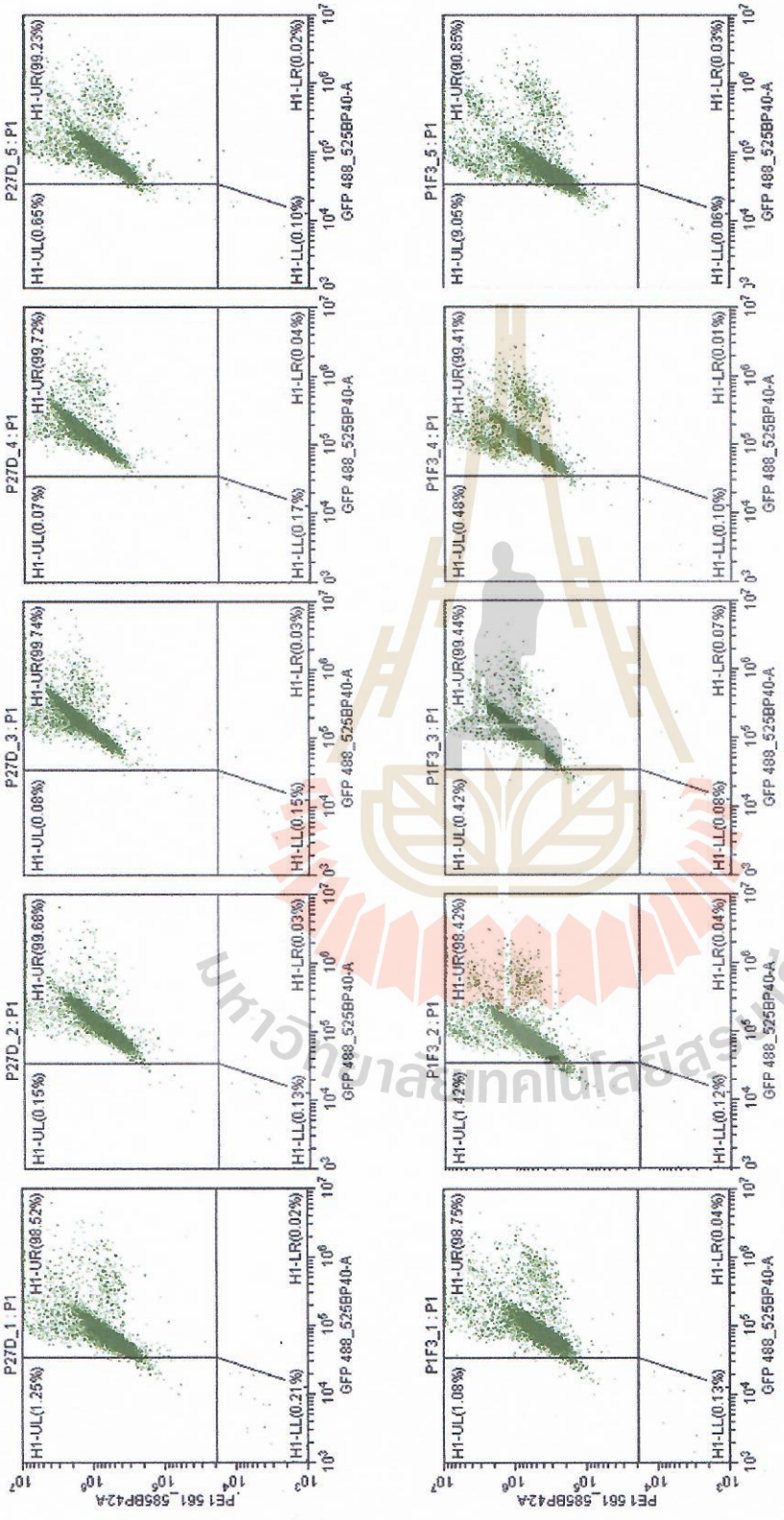

Figure 5.12 (continued).

After the pools recover from GS selection (viability >90 % in Figure 5.13), the bulk pools were further investigated to monitor the improvement in mAb productivity and compared the efficiency of expression host for a 7-day batch culture in the absence of MSX and the presence of 25 μM MSX conditions. The GS-knockout CHO-K1-derived bulk pools in the presence of MSX were higher mAb production and q_{mAb} than the GS-knockout CHO-S-derived bulk pools in the absence of MSX (Figure 5.14). The CHO-S-P2E5_3-derived bulk pool revealed significant greater improvement in mAb production on day 7 but the lower yield and q_{mAb} than the CHO-K1-P1F3_5-derived bulk pool. The CHO-S-P2E5_5-derived bulk pool exhibited too low the mAb production and the q_{mAb}. This bulk pool also had the lowest in the VCD when it recovered, which might have problem with transfection step. The mAb production and the q_{mAb} in most the bulk pools improved the mAb expression over 98% on day 7 in the absence of MSX compared to those of day 3 (Figure 5.15). This result suggests that high producing population cells may establish by using GS-knockout CHO cells in the absence of MSX, which drug-free system is desirable in pharmaceutical manufacturing to satisfy safety concerns and cost-effective process. The q_{mAb} of all GS-knockout CHO-derived bulk pools was significantly increased in the presence of 25 μM MSX (Figure 5.16.). The average q_{mAb} for bulk pools from CHO-S-P27E, CHO-S P2E5, CHO-K1 P27D and CHO-K1-P1F3 was 0.16, 0.18, 0.34 and 0.43 pg/cell/day, respectively, in the absence of MSX whereas they had the q_{mAb} of 0.38, 0.2, 0.93 and 1.29 pg/cell/day for bulk pools from CHO-S-P27E, CHO-S P2E5, CHO-K1 P27D and CHO-K1-P1F3, respectively at 25 μM MSX. Consistent with previous result (Fan et al., 2012), the bulk culture productivity of GS-knockout CHO cells was significant improved by a large reduction of low and non-producers after MSX selection stringency compared with the CHOK1SV cell. Our results indicate that

CHO-K1 P1F3 is the most suitable host, when compared with other GS-knockout CHO cells. This study also showed that GS-based system is successful for the bulk culture pool generation by a single round of 25 µM MSX selection.

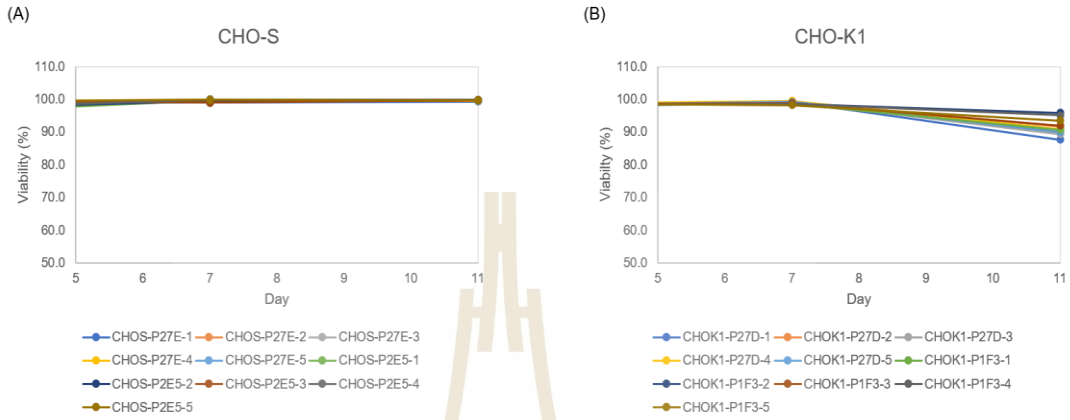

Figure 5.13 The viability profiles of GS-knockout CHO-S (A) and CHO-K1 (B) cell lines expressing Trastuzumab.

Due to the COVID-19 crisis in Austria during my research time, I cannot work in the laboratory. Therefore, all bulk pools were frozen in -80 ºC for 3 months. After that, these samples were thawed to repeat a 7-day batch culture in the presence of 25 µM MSX condition. Surprisingly, I found that most of GS-knockout CHO-S-derived cell pools showed a significant increase with mAb production and q_{mAb}, higher than GS-knockout CHO-K1-derived cell pools in some pools, while GS-knockout CHO-K1-derived cell pools exhibited a significant decrease with mAb production and q_{mAb} after thawing (Figure 5.16). The average q_{mAb} for bulk pools on day 7 from CHO-S-P27E, CHO-S P2E5, CHO-K1 P27D and CHO-K1-P1F3 was 0.62, 0.6, 0.19 and 0.33 pg/cell/day, respectively. In this case, the GS-knockout CHO-S P27E exhibited the highest for average yield and q_{mAb}. This result is different with the result from before freezing which may cause by the freezing/thawing of the cells made them unstable and a subpopulation of non-producers emerged.

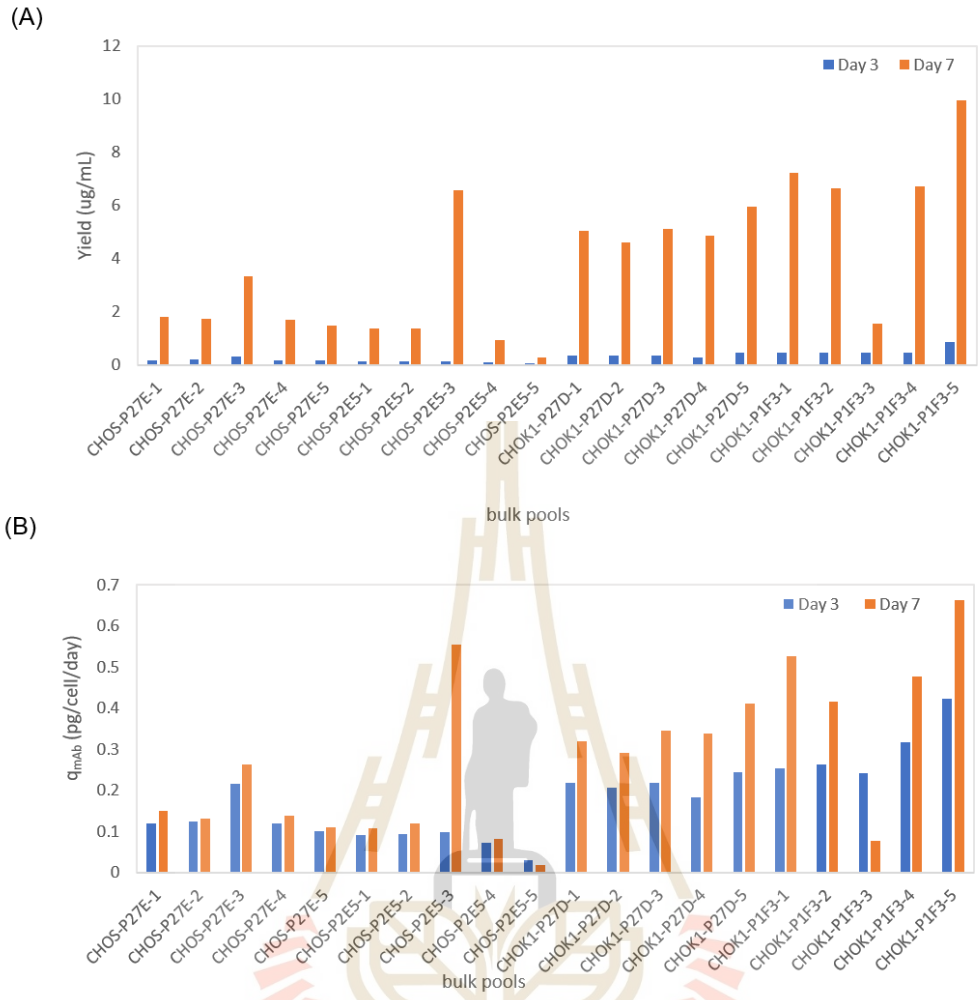

Figure 5.14 The efficiency of expression host for a 7-day batch culture in the absence of MSX. The yield and the q_{mAb} of bulk cultures were determined on day 3 and 7.

(A)

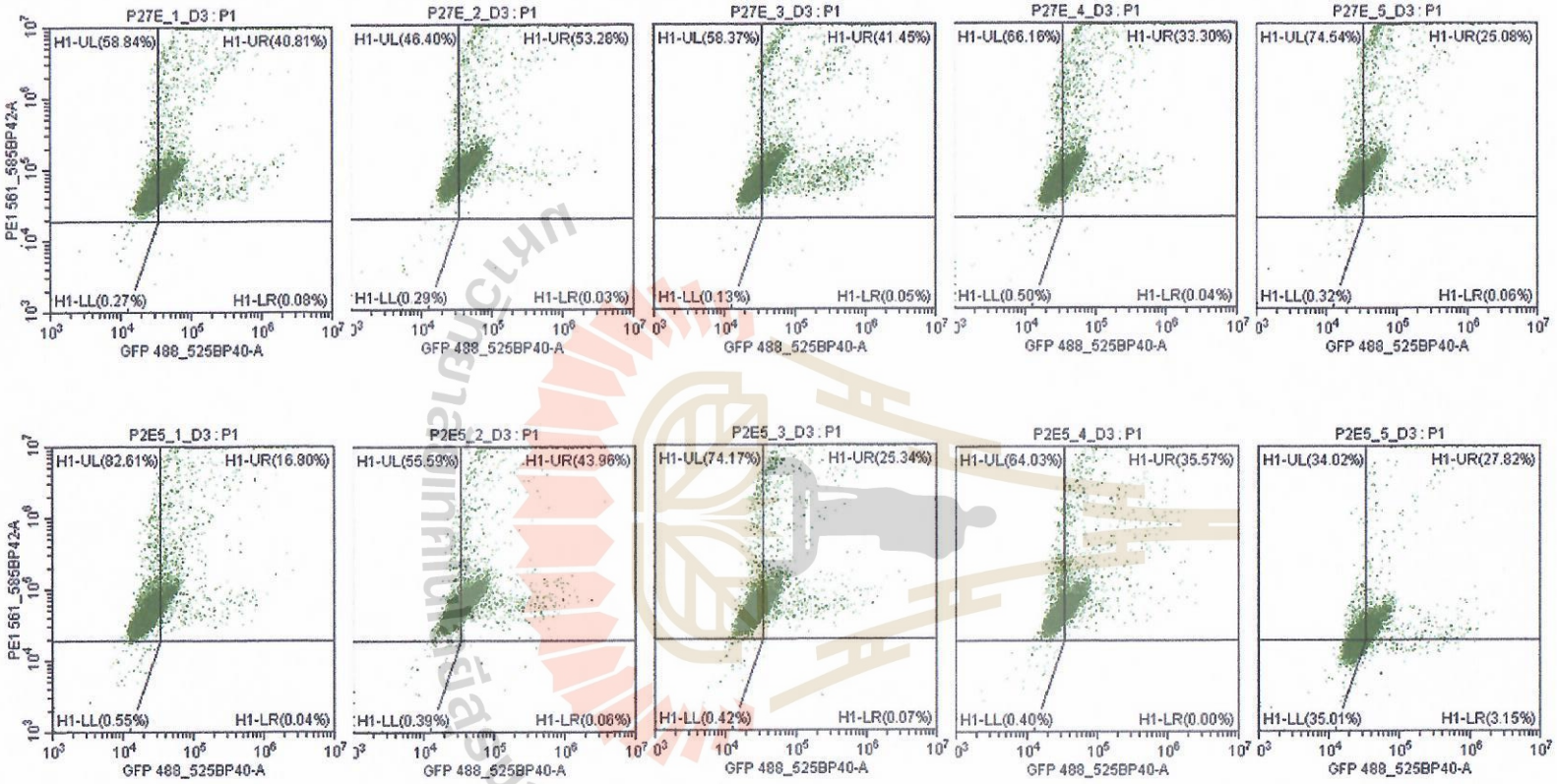

Figure 5.15 Intracellular staining against the Trastuzumab Ab in the bulk cultures selection of GS-knockout CHO cell lines in Gln-free medium without MSX on day 3 (A for GS-knockout CHO-S cells, B for GS-knockout CHO-K1 cells) and day 7 (C for GS-knockout CHO-S cells, D for GS-knockout CHO-K1 cell).

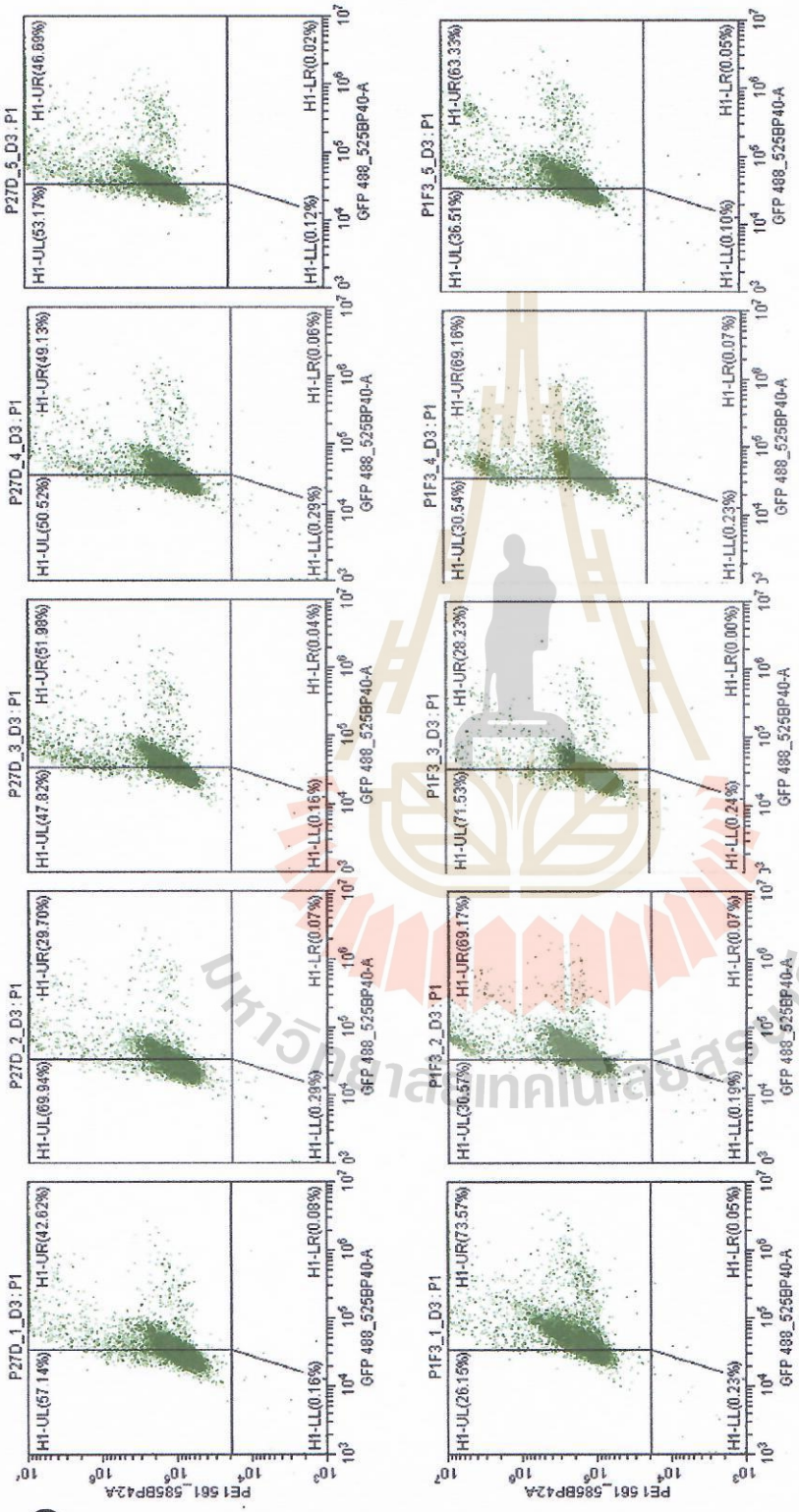

Figure 5.15 (continued).

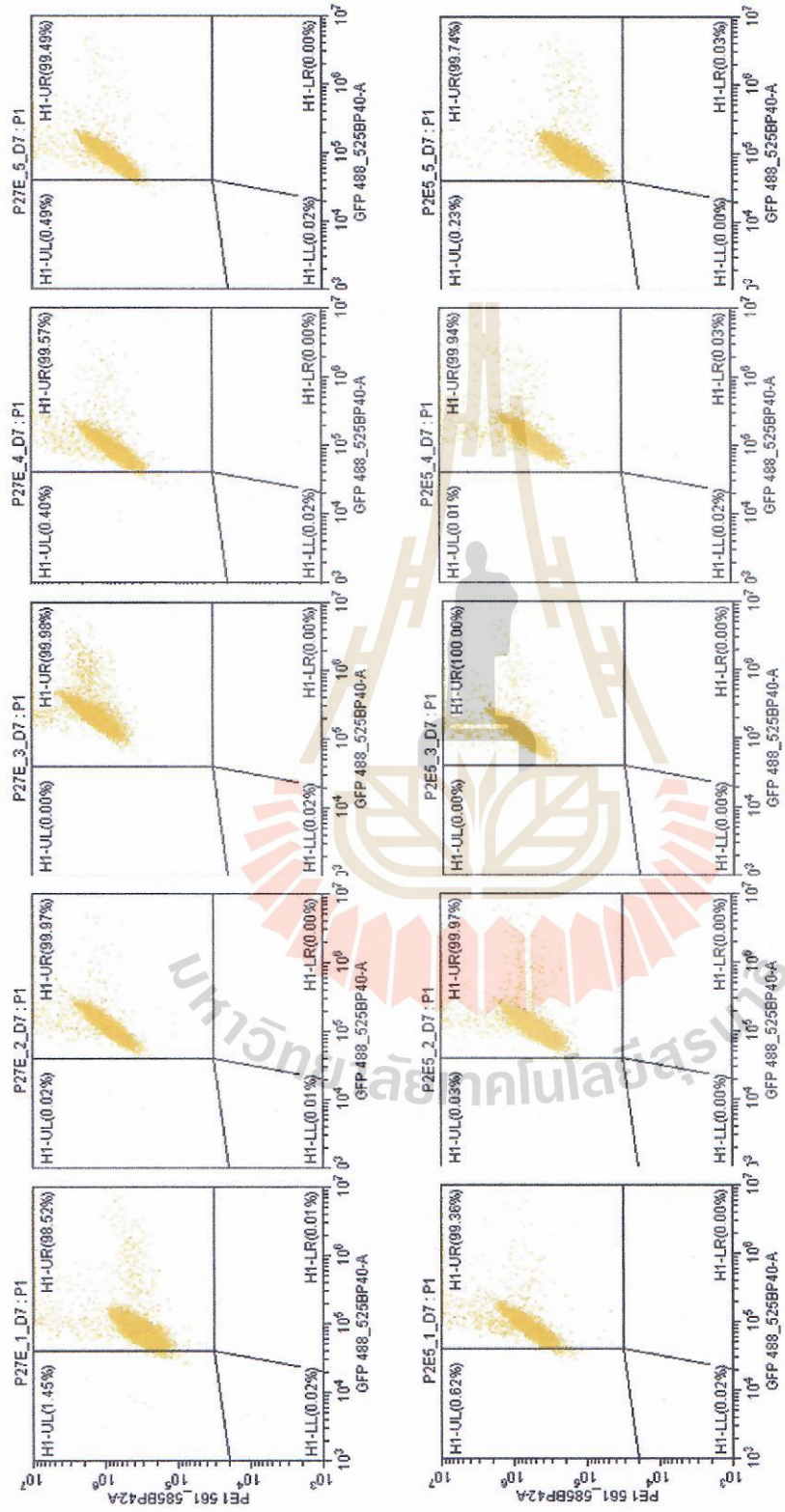

Figure 5.15 (continued).

(D)

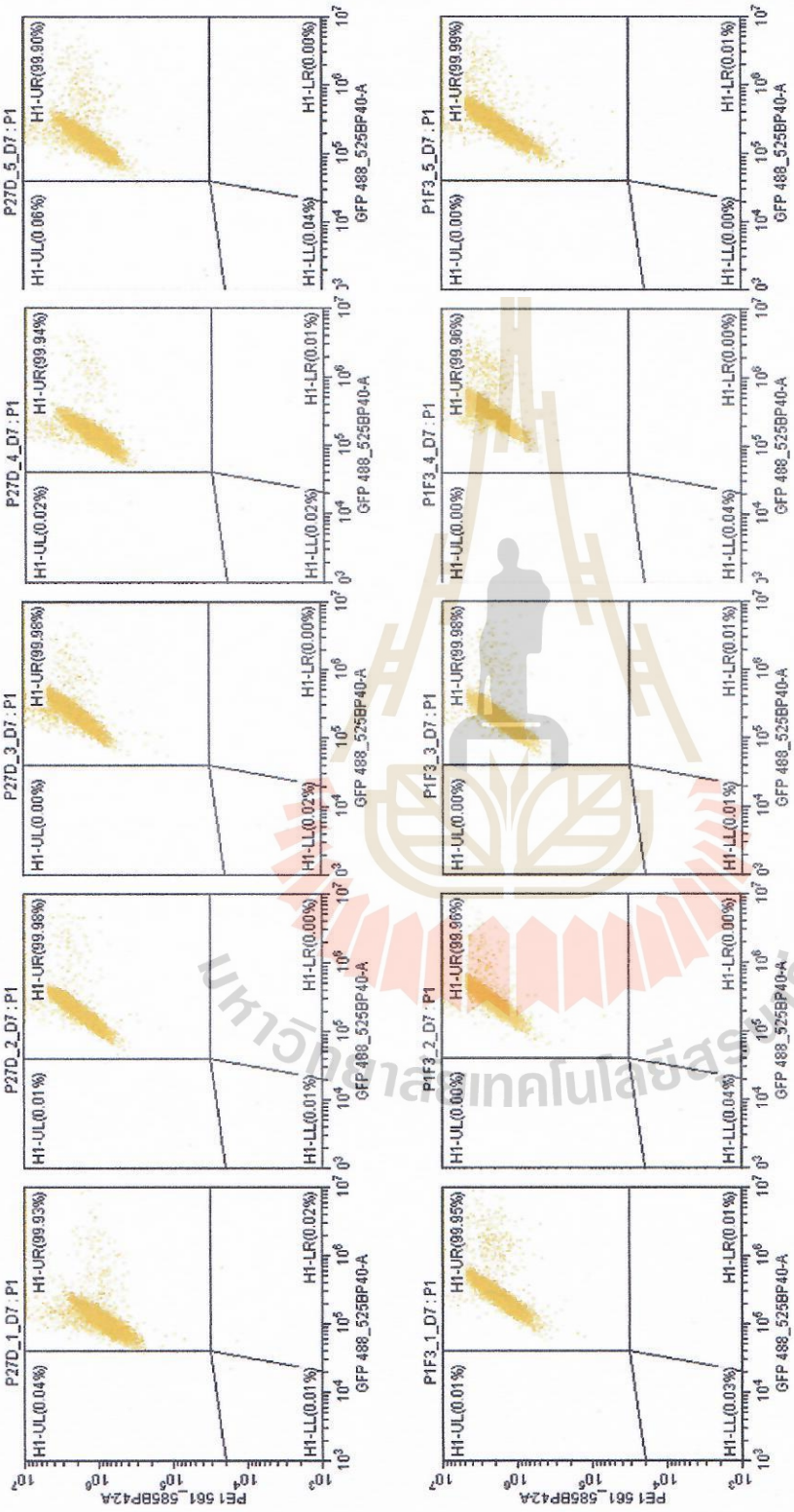

Figure 5.15 (continued).

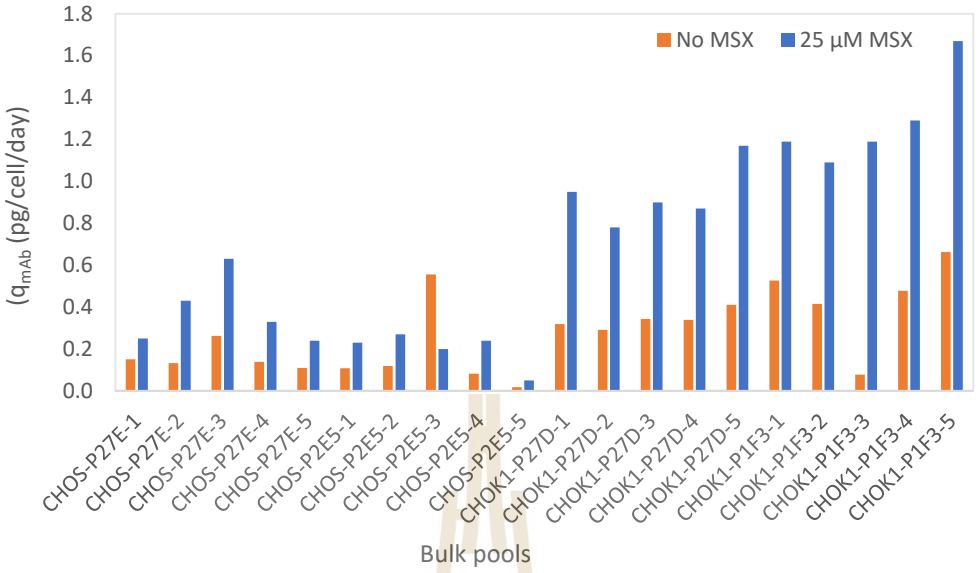

Figure 5.16 Comparison of the q_{mAb} of all GS-knockout CHO-derived bulk pools for a 7-day batch culture in the absence of MSX and in the presence of 25 µM MSX. The q_{mAb} of bulk cultures were calculated on day 7.

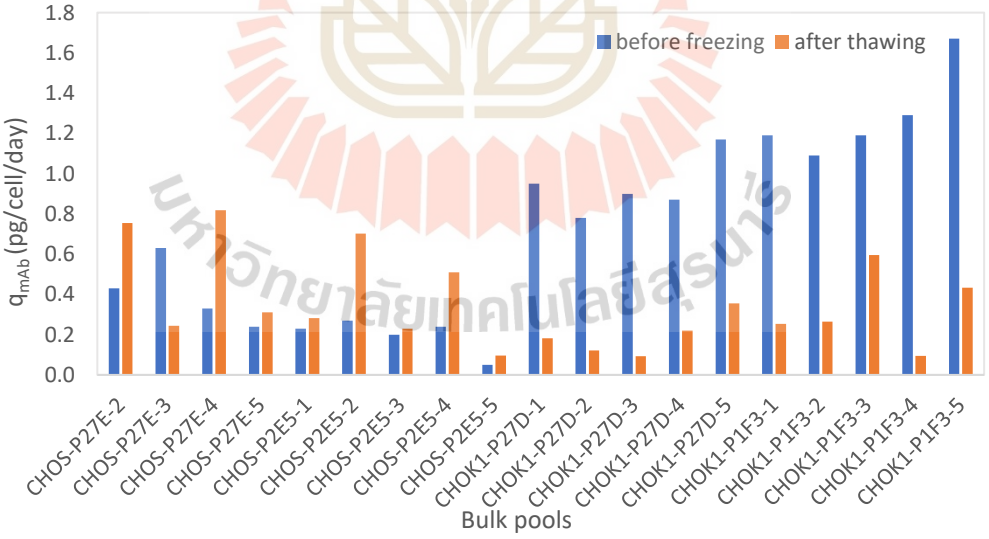

Figure 5.17 Comparison of the q_{mAb} of all GS-knockout CHO-derived bulk pools (before freezing and after thawing) for a 7-day batch culture in the presence of 25 µM MSX. The q_{mAb} of bulk cultures were calculated on day 7.

5.5 Conclusion

In conclusion, an efficient GS-knockout CHO host expression system suitable for cell line generation process by selection stringency that facilitates the identification of high producing clones has been developed. Moreover, this system has potential to be established and selected the high producing clones to reduce ammonia accumulation and save time.

5.6 References

Bauer, D. E., Canver, M. C., & Orkin, S. H. (2015). Generation of genomic deletions in mammalian cell lines via CRISPR/Cas9. *Journal of Visualized Experiments*(95), e52118.

Bebbington, C. R., Renner, G., Thomson, S., King, D., Abrams, D., & Yarranton, G. T. (1992). High-level expression of a recombinant antibody from myeloma cells using a glutamine synthetase gene as an amplifiable selectable marker. *Nature Biotechnology, 10*(2), 169-175.

Brown, M. E., Renner, G., Field, R. P., & Hassell, T. (1992). Process development for the production of recombinant antibodies using the glutamine synthetase (GS) system. *Cytotechnology, 9*(1-3), 231-236.

Bydlinski, N., Maresch, D., Schmieder, V., Klanert, G., Strasser, R., & Borth, N. (2018). The contributions of individual galactosyltransferases to protein specific N-glycan processing in Chinese Hamster Ovary cells. *Journal of Biotechnology, 282*, 101-110.

Chusainow, J., Yang, Y. S., Yeo, J. H. M., Toh, P. C., Asvadi, P., Wong, N. S. C., & Yap, M. G. S. (2009). A study of monoclonal antibody-producing CHO cell lines: What makes a stable high producer? *Biotechnology and Bioengineering,*

102(4), 1182-1196.

Cockett, M. I., Bebbington, C. R., & Yarranton, G. T. (1990). High level expression of tissue inhibitor of metalloproteinases in Chinese hamster ovary cells using glutamine synthetase gene amplification. *Biotechnology 8*(7), 662-667.

Dorai, H., Corisdeo, S., Ellis, D., Kinney, C., Chomo, M., Hawley-Nelson, P., Moore, G., Betenbaugh, M. J., & Ganguly, S. (2012). Early prediction of instability of Chinese hamster ovary cell lines expressing recombinant antibodies and antibody-fusion proteins. *Biotechnology and Bioengineering, 109*(4), 1016-1030.

Ecker, D. M., Jones, S. D., & Levine, H. L. (2015). The therapeutic monoclonal antibody market. *Monoclonal Antibodies, 7*(1), 9-14.

Fan, L., Kadura, I., Krebs, L. E., Hatfield, C. C., Shaw, M. M., & Frye, C. C. (2012). Improving the efficiency of CHO cell line generation using glutamine synthetase gene knockout cells. *Biotechnology and Bioengineering, 109*(4), 1007-1015.

Fan, L., Kadura, I., Krebs, L. E., Larson, J. L., Bowden, D. M., & Frye, C. C. (2013). Development of a highly-efficient CHO cell line generation system with engineered SV40E promoter. *Journal of Biotechnology, 168*(4), 652-658.

Feichtinger, J., Hernández, I., Fischer, C., Hanscho, M., Auer, N., Hackl, M., Jadhav, V., Baumann, M., Krempl, P. M., Schmidl, C., Farlik, M., Schuster, M., Merkel, A., Sommer, A., Heath, S., Rico, D., Bock, C., Thallinger, G. G., & Borth, N. (2016). Comprehensive genome and epigenome characterization of CHO cells in response to evolutionary pressures and over time. *Biotechnology and Bioengineering, 113*(10), 2241-2253.

Guo, D., Gao, A., Michels, D. A., Feeney, L., Eng, M., Chan, B., Laird, M. W., Zhang, B., Yu, X. C., Joly, J., Snedecor, B., & Shen, A. (2010). Mechanisms of unintended amino acid sequence changes in recombinant monoclonal antibodies expressed in Chinese Hamster Ovary (CHO) cells. *Biotechnology and Bioengineering, 107*(1), 163-171.

Handlogten, M. W., Lee-O'Brien, A., Roy, G., Levitskaya, S. V., Venkat, R., Singh, S., & Ahuja, S. (2018). Intracellular response to process optimization and impact on productivity and product aggregates for a high-titer CHO cell process. *Biotechnology and Bioengineering, 115*(1), 126-138.

Hernandez, I., Dhiman, H., Klanert, G., Jadhav, V., Auer, N., Hanscho, M., Baumann, M., Esteve-Codina, A., Dabad, M., Gómez, J., Alioto, T., Merkel, A., Raineri, E., Heath, S., Rico, D., & Borth, N. (2019). Epigenetic regulation of gene expression in Chinese Hamster Ovary cells in response to the changing environment of a batch culture. *Biotechnology and Bioengineering, 116*(3), 677-692.

Ho, S., Tong, Y., & Yang, Y. (2013). Generation of monoclonal antibody-producing mammalian cell lines. *Pharmaceutical Bioprocessing, 1*, 71-87.

Huang, Y.-M., Hu, W., Rustandi, E., Chang, K., Yusuf-Makagiansar, H., & Ryll, T. (2010). Maximizing productivity of CHO cell-based fed-batch culture using chemically defined media conditions and typical manufacturing equipment. *Biotechnology Progress, 26*(5), 1400-1410.

Jayapal, K., Wlaschin, K. F., Hu, W. S., & Yap, M. G. S. (2007). Recombinant protein therapeutics from CHO Cells - 20 years and counting. *Chemical Engineering Progress, 103*, 40-47.

Jun, S. C., Kim, M. S., Hong, H. J., & Lee, G. M. (2006). Limitations to the development of humanized antibody producing Chinese hamster ovary cells using glutamine synthetase-mediated gene amplification. *Biotechnology Progress, 22*(3), 770-780.

Kingston, R. E., Kaufman, R. J., Bebbington, C. R., & Rolfe, M. R. (2002). Amplification using CHO cell expression vectors. *Current Protocols in Molecular Biology, Chapter 16,* Unit 16.23.

Lacy, E., Roberts, S., Evans, E. P., Burtenshaw, M. D., & Costantini, F. D. (1983). A foreign β-globin gene in transgenic mice: Integration at abnormal chromosomal positions and expression in inappropriate tissues. *Cell, 34*(2), 343-358.

Langmead, B., Trapnell, C., Pop, M., & Salzberg, S. L. (2009). Ultrafast and memory-efficient alignment of short DNA sequences to the human genome. *Genome Biology, 10*(3), R25.

Lin, P.-C., Chan, K. F., Kiess, I. A., Tan, J., Shahreel, W., Wong, S.-Y., & Song, Z. (2019). Attenuated glutamine synthetase as a selection marker in CHO cells to efficiently isolate highly productive stable cells for the production of antibodies and other biologics. *Monoclonal Antibodies, 11*(5), 965-976.

Liu, P.-Q., Chan, E. M., Cost, G. J., Zhang, L., Wang, J., Miller, J. C., Guschin, D. Y., Reik, A., Holmes, M. C., Mott, J. E., Collingwood, T. N., & Gregory, P. D. (2010). Generation of a triple-gene knockout mammalian cell line using engineered zinc-finger nucleases. *Biotechnology and Bioengineering, 106*(1), 97-105.

Liu, W., Wei, H., Liang, S., Zhang, J., Sun, R., & Tian, Z. (2004). A balanced expression of two chains of heterodimer protein, the human interleukin-12,

improves high-level expression of the protein in CHO cells. *Biochemical and Biophysical Research Communications, 313*(2), 287-293.

Livak, K. J., & Schmittgen, T. D. (2001). Analysis of relative gene expression data using real-time quantitative PCR and the $2^{-\Delta\Delta CT}$ method. *Methods, 25*(4), 402-408.

Lu, R.-M., Hwang, Y.-C., Liu, I. J., Lee, C.-C., Tsai, H.-Z., Li, H.-J., & Wu, H.-C. (2020). Development of therapeutic antibodies for the treatment of diseases. *Journal of Biomedical Science, 27*(1), 1.

Matasci, M., Hacker, D. L., Baldi, L., & Wurm, F. M. (2008). Recombinant therapeutic protein production in cultivated mammalian cells: current status and future prospects. *Drug Discovery Today: Technologies, 5*(2), e37-e42.

Meister, A. (1980). 1 - Catalytic mechanism of glutamine synthetase; overview of glutamine metabolism. In J. Mora & R. Palacios (Eds.), *Glutamine: Metabolism, Enzymology, and Regulation* (pp. 1-40): Academic Press.

Meleady, P., Doolan, P., Henry, M., Barron, N., Keenan, J., O'Sullivan, F., Clarke, C., Gammell, P., Melville, M. W., Leonard, M., & Clynes, M. (2011). Sustained productivity in recombinant Chinese Hamster Ovary (CHO) cell lines: proteome analysis of the molecular basis for a process-related phenotype. *BMC Biotechnology, 11*(1), 78.

Nakamura, T., & Omasa, T. (2015). Optimization of cell line development in the GS-CHO expression system using a high-throughput, single cell-based clone selection system. *Journal of Bioscience and Bioengineering, 120*(3), 323-329.

Neermann, J., & Wagner, R. (1996). Comparative analysis of glucose and glutamine metabolism in transformed mammalian cell lines, insect and primary liver cells.

Journal of Cellular Physiology, 166(1), 152-169.

Nguyen, L. N., Baumann, M., Dhiman, H., Marx, N., Schmieder, V., Hussein, M., Eisenhut, P., Hernandez, I., Koehn, J., & Borth, N. (2019). Novel promoters derived from Chinese Hamster Ovary Cells via *in silico* and *in vitro* Analysis. *Biotechnology Journal, 14*(11), 1900125.

Noh, S. M., Shin, S., & Lee, G. M. (2018). Comprehensive characterization of glutamine synthetase-mediated selection for the establishment of recombinant CHO cells producing monoclonal antibodies. *Scientific Reports, 8*(1), 5361.

Pichler, J., Galosy, S., Mott, J., & Borth, N. (2011). Selection of CHO host cell subclones with increased specific antibody production rates by repeated cycles of transient transfection and cell sorting. *Biotechnology and Bioengineering, 108*(2), 386-394.

Rita Costa, A., Elisa Rodrigues, M., Henriques, M., Azeredo, J., & Oliveira, R. (2010). Guidelines to cell engineering for monoclonal antibody production. *European Journal of Pharmaceutics and Biopharmaceutics, 74*(2), 127-138.

Sanders, P. G., & Wilson, R. H. (1984). Amplification and cloning of the Chinese hamster glutamine synthetase gene. *The EMBO Journal, 3*(1), 65-71.

Schmieder, V., Bydlinski, N., Strasser, R., Baumann, M., Kildegaard, H. F., Jadhav, V., & Borth, N. (2018). Enhanced genome editing tools for multi-gene deletion knock-out approaches using paired CRISPR sgRNAs in CHO Cells. *Biotechnology Journal, 13*(3), e1700211.

Tripathi, N. K., & Shrivastava, A. (2019). Recent developments in bioprocessing of recombinant proteins: expression hosts and process development. *Frontiers in Bioengineering and Biotechnology, 7*(420).

Wurm, F. M. (2004). Production of recombinant protein therapeutics in cultivated mammalian cells. *Nature Biotechnology, 22*(11), 1393-1398.

Zhu, J. (2012). Mammalian cell protein expression for biopharmaceutical production. *Biotechnology Advances, 30*(5), 1158-1170.

CHAPTER VI

CONCLUSIONS

Therapeutic monoclonal antibodies (mAbs) are mainly produced in mammalian and microbial host cells, in addition to some other hosts including transgenic models, avian, insect, and transgenic animals. Prokaryotic systems are still primarily used for proteins that do not require complex glycosaccharides for their efficacy or stability. Biologics that need complex post translational modifications require mammalian hosts such as Chinese hamster ovary (CHO) cells, which are the predominant expression system for the production of therapeutic antibodies. They can secrete high levels of recombinant mAbs and provide a human-like glycosylation pattern with few concerns for immunogenic reactions. Therefore, the overall objective of this thesis is focusing on the development of efficient bacterial and animal expression systems for the production of human recombinant antibodies. This thesis is divided into three sub-objectives as follows.

Firstly, a suitable *Escherichia coli* (*E. coli*) expression system for the production of human recombinant single-chain variable fragment (scFv) and scFv-Emerald Green Fluorescent Protein (EmGFP) Abs was evaluated. Fluorescence-linked immunosorbent assay (FLISA) has become one of the most efficient analytical methods for immune analysis because it is a time-saving technique, with high sensitivity and reliability. This is because the secondary antibody and substrate for conjugated enzyme can be avoided.

In this research, scFv Abs against rabies virus, AFB1 and ZEN were engineered to fuse with the EmGFP and expressed in different *E. coli* expression hosts. Our results indicated that *E. coli* C3029 (B cell) is the best host, when compared with *E. coli* C3026 (K12) and BL21 (DE3). Three cytoplasmic fluobodies were characterized by ELISA and FLISA, which revealed that they retained both affinity binding of native antibodies and fluorescence activity of EmGFP. Furthermore, application of the purified yZA8B2-scFv-EmGFP for the detection of ZEN by competitive FLISA was demonstrated. This system has potential to be developed for both quantitative and qualitative analysis in various applications.

Secondly, I sought to compare the effects of different optimized codons and various SPs on the productivity of therapeutic antibody, expressed from monocistronic expression vectors from transiently transfected CHO cells. To compare the algorithm of codon optimization, Adalimumab was used as a model of the study. The LC and HC of human IgG1 of Adalimumab genes were codon-optimized and synthesized from GeneArt (GA, Adali_GA) and GenSript (GS, Adali_GS). While the yield and q_p of genes from GA were higher, the mRNA expression level of both HC and LC derived from both GA and GS showed no significant difference. Subsequently, various combinations of SPs fused to the codon-optimized HC and LC of Adalimumab and Trastuzumab were evaluated for secretory production efficiency. The results indicated that different antibody required different combinations of SP for optimal production, which are different from previous reports. In this study, I observed that the best SP combinations for HC and LC of Adalimumab are SpSH and SpB, while for Trastuzumab the SpB is the most suitable for both heavy and light chains. The binding

property of the produced antibodies was confirmed by ELISA against target antigens and the ratio of heavy and light chain was validated by flow cytometry.

Finally, the selection of high producing stable clones from a large population of low and non-productive clones from the transiently transfected bulk cultures, which is crucial step for recombinant antibody production from CHO cells, was explored. The GS-CHO system is an alternative approach to efficiently identify high producing and stable clones in the cell line generation process. This system is used to generate the highly producing population by using a combination of increasing selection stringency with MSX, a GS inhibitor, and a GS-knockout CHO cell line, where the endogenous CHO GS gene expression is removed. The hypothesis of this study was that since there are three GS genes in CHO cells, deleting only 1 GS gene may result in the activation of one of the other 2 GS genes, consequently reducing the selection stringency. Therefore, in this study, to further increase the selection stringency, two GS genes on chromosome 5 (GS5) and 1 (GS1) of CHO-S and CHO-K1, which express GS at high and low activity level, were deleted using CRISPR/Cpf1. The GS-knockout CHO cells were confirmed by RT-qPCR and DNA sequencing. The single and double GS-knockout CHO cells of CHO-S and CHO-K1 showed robust glutamine-dependent growth after eliminating GS activity. The bulk culture productivity of engineered CHO-S and CHO-K1 was significantly improved after a single round of 25 μM MSX selection, as non-transfected cells and cell populations of non and low producing cells were removed, even in medium not supplemented with MSX. Our results suggest that CHO-K1 P1F3 is the most suitable host to establish highly producing clones when compared with other GS-knockout CHO cell lines.

BIOGRAPHY

Mr. Witsanu Srila was born on August 24, 1984 in Nakhon Sawan Province, Thailand. He graduated with a Bachelor's Degree from Department of Biotechnology, Faculty of Engineering and Industrial Technology, Silpakorn University in 2007. He also received his Master's degree in Department of Biotechnology at the university in 2011. He had an opportunity to work in a research assistant at Molecular Biotechnology Laboratiry at School of Biotechnology, Institute of Agricultural technology, Suranaree University of Technology in 2012-2015. In 2015-2019, he had an opportunity to study Doctoral degree enrollment in School of Biotechnology, Institute of Agricultural technology, Suranaree University of Technology. She received the RGJ-PhD scholarship from The Thailand Research Fund (TRF) supporting on his study and research experience at at Institute of Animal Cell Technology and Systems Biology, Department of Biotechnology, Biotechnology, University of Natural Resources and Life Sciences, Vienna (BOKU), Austria for one and a half years. His work and research interests in development of the selection efficiency of recombinant CHO cells producing biopharmaceutical. He had presented some part of his research in the 13rd the Asian Congress for Biotechnology (ACB2017) "Bioinnovation and Bioeconomy", July 23-27,2017 at pullman Khon Kaen raja orchid hotel, Thailand (Poster presentation; Development of One-Step Detection of Aflatoxin B1 in Agricultural Products Using scFv-EmGFP format).